CHARACTERIZATION AND QUALITY ASSESSMENT OF BRINE SLUDGE BASED GEOPOLYMER BRICKS

A dissertation submitted in partial fulfilment of the requirements for the award of degree of

MASTER OF ENGINEERING

In

STRUCTURAL ENGINEERING

Submitted by

Souravpreet Singh

802124021

Under the Guidance of

Dr. PREM PAL BANSAL

(Professor and Head)

Dr. VIVEK GUPTA

(Assistant Professor)

THAPAR INSTITUTE
OF ENGINEERING & TECHNOLOGY
(Deemed to be University)

DEPARTMENT OF CIVIL ENGINEERING

THAPAR INSTITUTE OF ENGEERING AND TECHNOLOGY, PATIALA

(Deemed-to-be-University u/s 3 of the UGC Act, 1956)

(July 2023)

DECLARATION

I hereby declare that the thesis entitled **("Characterization and Quality Assessment of Brine Sludge based Geopolymer Bricks")** is an authentic record of my studies carried out as a requirement for the award of degree of **Master of Engineering in Structural Engineering** under the supervision of **Dr. Vivek Gupta**, Assistant Professor, and **Dr. Prem Pal Bansal**, Professor and Head, Department of Civil Engineering, Thapar Institute of Engineering and Technology, Patiala. The mater embodied in this report has not been submitted in part or full to any other institute or university for the award of any degree.

Souravpreet Singh

(Signature of student)

Souravpreet Singh

101882014

Date: 20-09-2023

Certified that the above statement made by the student is correct to the best of our knowledge and belief.

Dr. Prem Pal Bansal

(Head and Professor)

Civil Engineering Department

TIET, Patiala

Vivek gupta

Dr. Vivek Gupta

(Assistant Professor)

Civil Engineering Department

TIET, Patiala

ACKNOWLEGEMENT

Words are often less to reveal once deep regard for someone. With an understanding that work like this can never be the outcome of a single person, I take this opportunity to express my profound sense of gratitude and respect to all those who helped me through the duration of my work. My thesis could not have been completed without the help of many people who contributed directly or indirectly through their constructive criticism. It would not be fair on my part if I don't say a word of thanks to all those whose sincere suggestions made this period a real educative, enlightening, pleasurable and memorable one.

First of all, a special debt of gratitude is owed to my supervisor **Dr. Vivek Gupta, Assistant Professor, Department of Civil Engineering, Thapar Institute of Engineering and Technology, Patiala** for their gracious efforts and keen pursuits, which have remained a valuable asset for the successful completion of my work.

I would like to express my deepest gratitude to my mentor **Dr. Prem Pal Bansal, Head & Professor Department of Civil Engineering, Thapar Institute of Engineering and Technology, Patiala** for the extensive mentoring, support, and technical guidance he provided me with throughout my tenure of this research work.

I would also like to thank you **Jaspreet Singh (Lab Technician) and Amarjeet Singh (Lab Attendant), Department of Civil Engineering, Thapar Institute of Engineering and Technology, Patiala** for their immense support continuously.

I would also like to thank my parents and my friends for their constant encouragement & co-operation. Last but not least, I would like to thank God that my thesis got completed.

Sincerely,

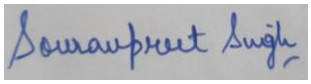

Souravpreet Singh

ABSTRACT

Burnt clay brick is still being used at large scale for masonry construction in building structures. The major shortcoming is the carbon emission during production of these burnt clay bricks. Now a days, cement based fly ash bricks are replacing conventional bricks as a sustainable alternative. However, in these bricks, cement as binder carries high carbon emission during its production and water required for curing of these bricks further creates a need to develop more sustainable masonry unit for building construction.

Waste utilization is an effective approach for enhancing the sustainability of construction products. In this study, brine sludge waste is used as an ingredient in fly ash bricks to enhance its sustainability. Brine sludge is a by-product of the chlor-alkali industries that is created during the electrolysis of brine to produce chlorine and caustic soda. Significant research and development of various cement-free geopolymeric materials that incorporate different wastes have taken place over the past ten years. Converting the waste into value-added materials presents an innovative and sustainable approach. This study primarily focuses on development of cement free bricks with high volume of brine sludge in a cost-effective manner which can be used over the conventional ones.

The research investigates the mechanical strength, durability, and mineralogy of brine sludge based geopolymer bricks. Various mixes are formulated with 70% brine sludge and 30% fly ash as a geopolymeric precursor and concentrations of alkaline activators have been varied for both volume based and weight based design mixes. The precursor to fine aggregate ration has been maximized to 1:3 and stone dust is used as a fine aggregate for cost effectiveness of the product. Firstly, flowable mortar has been formulated and then liquid content is reduced to get the low moist mortars for feasibility of compressed bricks.

Mixes have been optimized based on the compressive strength and bricks with optimized mixes have been tested for wet compressive strength, water absorption, efflorescence and mineralogy. The mineralogy of raw materials and the bricks have been studied using X-Ray Diffraction, Fourier transform Infrared spectroscopy and advanced characterization technique i.e. Raman Spectroscopy. The results demonstrate the feasibility of brine sludge as an ingredient into cement free geopolymer bricks while maintaining adequate structural integrity and durability. The optimized mix having material cost ~INR 10.0 complies the standard requirements of Class 7.5 bricks.

TABLE OF CONTENTS

LIST OF FIGURES

LIST OF TABLES

ABBREVIATIONS

CaO	Calcium oxide
MgO	Magnesium oxide
SrO	Strontium oxide
SiO_2	Silicon dioxide
Fe_2O_3	Ferric oxide
Al_2O_3	Aluminium oxide
Na_2O	Sodium oxide
XRD	X-ray diffraction
FTIR	Fourier Transform Infrared Spectroscopy
AC	Advance Composites
SEM	Scanning Electron Microscopy
IBSW	Industrial Brine Sludge Waste
CLSM	Controlled Low Strength Material
FA	Fly Ash
B_2O_3	Borax

1. INTRODUCTION

1.1 General-

The rapid growth of our society relies on industrialization, but it comes with a major problem – the generation of harmful waste. Industries, especially those involved in metal processing and petrochemicals, produce large amounts of waste worldwide. The environmental pollution issue has become more complex nowadays. However, this challenge presents a great opportunity for material scientists to take an interdisciplinary approach and turn this industrial waste into useful materials, reducing our dependence on non-renewable resources like bricks.

In the past decade, there has been significant research and development of cement-free geopolymeric materials. These geopolymeric materials offer a way to transform toxic industrial waste into valuable construction materials, making geopolymerization a promising solution for effective industrial waste management. Through this process, various waste materials can be converted into useful products.

By using the sludge from the Chloralkali industry for construction purposes, their operations can become more sustainable. This means we can find better ways to manage waste and make our industries more environmentally friendly.

1.2 What is brine?

Any solution with a very high concentration of salts, such as sodium chloride, is referred to as brine and can be produced artificially or naturally (such as in seawater, deep ocean pools, salt lakes, etc.). It may be created through the use of efficient industrial production techniques or as a by-product of other procedures. These "brine" streams, which are industrially produced, are usually highly concentrated salt solutions that, in some cases, contain more concentrated salts than natural brine solutions by weight. Additionally, different contaminants that vary depending on the source and different industrial processes used in its production can be found in brine.

1.3 What is brine sludge?

In India, there are 33 Chloralkali industries, and each year, about 2.0 lakh tonnes of sludge are produced. The use of sludge for construction tasks will make the operations of the Chloralkali industry more sustainable.

Figure 1.1: Chemfab Alkalis Limited (CCAL) Chlor-alkali Plant in India

One of the primary raw materials used in the production of Chloralkali is industrial grade salt. When brine is electrolyzed to produce chlorine and caustic soda, brine sludge is produced. Brine sludge is produced as a result of the removal of these impurities from the brine. We have separated the sludge and are using it to build the bunds in our own salt fields. Calcium carbonate (13–18%), magnesium hydroxide (1.5–11%), and insoluble residue (silica) (11.5-29%) make up the majority of the brine sludge.

Figure 1.2: Brine sludge as obtained from a chlor-alkali plant (Joshi et al. 2015)

The produced brine sludge must be disposed of properly or used to make other materials or products so as not to harm the environment or consume an excessive amount of the industries' land that could be used for other forms of production.

1.4 Different types of sludges-

There are different types of sludge which are generated from different industries. Some of them are listed below with process through which they are generated and their constituents.

- **Brine Sludge** - It a sludge which is generated in chlor-alkali industries by the electrolysis of Brine solution mostly it contains CaO, MgO, SrO, SiO_2, Fe_2O_3, Al_2O_3, Na_2O.
- **Lime Sludge** - It is a sludge which is produced from the lime calcining process. Calcium, silica, and aluminium make up the bulk of the ingredients in lime sludge. Less than 3% of the total composition is made up of iron, magnesium, and sulphur, while less than 0.01% of the composition is made up of zinc, chromium, selenium, lead, cadmium, barium, and silver as a whole.
- **Textile Sludge** - An inevitable by-product of the treatment of textile wastewater is textile sludge. Heavy metals like Fe, Cu, Cd, Zn, and Cr are present in high concentrations in the organic and inorganic complexes that make up textile sludge.
- **Drinking Water Sludge** - This is the sludge that is collected from tanks or drinking water treatment facilities. The majority of it is dumped in landfills as non-hazardous waste, so there aren't any complicated processes needed to treat the sludge. Additionally, it essentially lacks any pathogens, making it safe for disposal.

1.5 Environmental issues-

The industrial sector's biggest environmental issues and concerns revolve around how to properly dispose of brine sludge. In the chlor-alkali industry, brine sludge is conveniently available. It contains harmful substances that precipitate out of the brine over time and negatively impact the ecology as they drain out.

The nearby area needs a significant amount of land space for the industries. Brine sludge is disposed of by being dumped on the ground, and some businesses burn their industrial waste, which raises concerns primarily about air and land pollution.

So it's time to look for alternative methods of disposing of brine sludge that is safe for the environment and stabilize the leachable contaminants.

1.6 Utilization of the waste-

The ecological impact of adding brine sludge into construction material (bricks) can be a double-edged sword, depending on how it's managed and the specific context. On the positive side, incorporating brine sludge into brick production can serve as a sustainable means of recycling and reducing the environmental burden associated with waste disposal. By utilizing this waste material as a substitute for traditional raw materials like clay or shale, it may reduce the need for mining and excavation, helping to conserve natural resources and reduce habitat disruption. Moreover, the high salt content in brine sludge can act as a stabilizing agent, enhancing the structural integrity of bricks and potentially reducing the energy required for firing in kilns. However, the ecological impact may turn negative if not adequately managed. If the brine sludge contains contaminants or heavy metals, their presence in bricks could pose long-term environmental risks if the bricks deteriorate, potentially leaching these pollutants into the surroundings. Therefore, thorough assessment and treatment of brine sludge, along with proper monitoring during and after brick production, are essential to minimize any adverse ecological consequences and maximize the potential environmental benefits of this approach.

Geopolymerization aids in the stabilization and immobilization of toxic and dangerous materials. In light of the foregoing, brine sludge is used to create value-added materials because it naturally contains the complementary precursors needed to create novel geopolymeric materials. Industrial waste can be used to create a geopolymeric composite. According to sustainability indicators, using industrial waste to create geopolymer products has a significant positive impact on the environment.

By forming C-S-H gel or A-S-H gel in addition to N-S-H or N-A-S- H/C-A-S-H gel, the addition of brine sludge samples containing calcium carbonate, magnesium hydroxide, sodium chloride, and silica can improve the interfacial bonding of the geopolymeric matrix. The physical and mechanical characteristics of geopolymer materials are altered by the simultaneous presence of this variety of gels. Due to the development of a dense microstructure, compression resistance should be improved.

The higher compaction of geopolymer structures may be influenced by the high calcium content. On the other hand, chloride acts as a catalyst, speeding up the geopolymerization process and causing the gel to form. Additionally, toxic ions present in wastes may be immobilized by geopolymer materials.

There is one alternate or possible solution by using the brine sludge as a construction material (bricks), i.e., the brine sludge is used as a partial or full replacement of cement by mixing a certain amount brine sludge with the fly ash as well as aggregates for making geopolymer bricks, Brine sludge can also be employed in a geopolymeric matrix since it aids in immobilizing and stabilizing harmful and hazardous materials that are seeping into the water table.

Leachability investigations demonstrate that brine sludge undergoes geopolymerization to become a non-toxic substance. Making geopolymeric (cement-free) bricks from the sludge could be an appealing way to handle the problem of disposing of it.

The long-term durability effects of adding brine sludge to bricks can be a complex interplay of various factors. While brine sludge can enhance the immediate strength and durability of bricks due to its high salt content, there are potential risks to consider over the long term. The salts can act as a stabilizing agent, reducing the risk of cracking and improving resistance to freeze-thaw cycles, which is especially advantageous in colder climates. However, the hygroscopic nature of salt means that it can absorb moisture from the surrounding environment, leading to the gradual deterioration of the brick structure through a process called salt crystallization. This can weaken the bricks over time and even cause spalling, where the surface layers flake off. Additionally, if the brine sludge contains impurities or corrosive elements, such as sulfates or heavy metals, these can accelerate the degradation of the bricks, potentially compromising their long-term durability. Therefore, while brine sludge can offer short-term advantages in brick production, careful consideration and monitoring are essential to ensure that it doesn't compromise the bricks' integrity over their expected lifespan.

1.7 Research Gap of the study-

- Unlike fly ash, the utilization of brine sludge in cement-free geopolymeric matrix has not been studied.
- The Mix design is not clear whether its volume or weight based and find out the optimum mix.
- There is a partial replacement of cement with the brine sludge in bricks. Hence, the fully replacement of cement with the brine sludge as binder has not been explored yet.
- Majority of studies carried out mechanical studies while replacing the brine sludge in different cementious matrix.

- Durability studies are not s addressed which restricts he industrial scale implementation of the concluded results.
- Cost optimization of the bricks is not done yet in any of literature.

1.8 Aims and objectives of the study-

The primary aim of the study is to prepare a feasible geopolymer brick using brine sludge to reduce the negative impact of brine sludge on environment and promoting waste to wealth concept through utilization of brine sludge as a construction material.

The primary objectives to achieve above aim are as follows:

a. To compare the mechanical properties of volume based and weight based nominal mixes of brine sludge based geopolymer mortars, both for flowable mortars and low moist mortars suitable for bricks.
b. To optimize the recipe and manufacturing parameters of brine sludge based geopolymer brick mixes.
c. To access the mechanical and durability properties of the optimized brine sludge based geopolymer brick mixes as per requirement of IS: 12894.
d. To perform mineralogical characterization of raw materials and brick mixes to explore the geopolymer chemistry in brine sludge based geopolymer brick mixes.
e. To perform material cost comparison of the optimized mixes satisfying the codal requirement with existing products.

1.9 Layout of the thesis-

Chapter 1 provides an introduction to the analysis of the research work. The significance of the research, aims and objective of the investigation and the layout of the thesis.

Chapter 2 provides a literature review which provides in depth knowledge of the existing field of research.

Chapter 3 describes the materials and methodology of the work.

Chapter 4 summarizes the results and discussion on the experimental investigation.

Chapter 5 presents detailed summary of the work, conclusions and scope for further research.

The references are presented at the end of the thesis.

2. LITERATURE REVIEW

2.1 Physical and chemical properties-

Yadav et al. (2017): Numerous salts are present in the industrial chlor-alkali brine sludge. A reasonable amount of value that is cost-effective can be produced by separating components into their individual parts. Minimizing the negative effects on the environment brought on by the process' waste sludge. To separate the four main constituent salts of barium, calcium, magnesium, and sodium, it obtained the sludge from an industry. The procedure established is probably going to benefit the sector economically.

Garg and Pundir (2014): On the characteristics of cement-fly ash-sludge binders, the classification and recommendations of brine sludge are provided. The strength-building reaction products created during the hydration of the binder are what give the waste particles a physical summary and an interlocking framework. The use of brine sludge in brick production and the impact of sludge concentration on these products' engineering properties are also covered. The findings unmistakably demonstrated that brine sludge up to 35 and 25% can be used safely for producing bricks, respectively. According to the leachability studies, the metal ions and impurities in the sludge are largely fixed in the matrix and do not easily leach from it. A potential disposal method and way to lower the risk of pollution is the use of brine sludge in building materials.

Table 2.1: Physical and chemical properties (Garg and Pundir (2014))

Sr. no.	Properties	Brine Sludge	Fly Ash
Physical Properties			
1.	Color	Light grey	Grayish Black
2.	Physical state at room temperature	Semi - solid	Solid
3.	pH	12	10.5
4.	Bulk density, g/cc	2.52	2.35
Chemical composition %			
1.	SiO_2	9.16	62.51
2.	$Al_2O_3 + Fe_2O_3$	5.22	26.88
3.	CaO	9.32	2.20
4.	MgO	7.65	0.92
5.	BaO	40.03	-

6.	SO3	12.32	1.80
7.	Cl	5.30	-
8.	Na_2O	4.80	0.40
9.	K_2O	0.31	0.57
10.	Cr_2O_3	-	0.04
11.	ZnO	0.03	0.02
12.	CuO	0.05	0.01
13.	V_2O_5	0.01	-
14.	LOI	5.8	4.65

Amritphale et al. (2018): By creating non-toxic, geopolymeric (cement-free) materials for sustainable development, a different strategy to address environmental hazards of brine sludge and fly ash waste from chloral alkali industry has been considered. Fly ash and brine sludge, two industrial wastes, can be used in the process. There is disagreement over the use of brine sludge in the production of geopolymeric (cement-free) bricks and its impact on the engineering qualities of these goods. Presentations of the XRD, IR, and SEM studies have also been made. When made with brine sludge, geopolymeric mortar can have compressive strengths of up to 20 MPa. These findings unequivocally demonstrate that brine sludge can be used to create geopolymeric (cement-free) bricks. Leachability studies show that brine sludge undergoes geopolymerization to become a non-toxic material. An appealing solution to the problem of disposing of brine sludge would be to use it to create geopolymeric (cement-free) bricks instead of using non-renewable natural resources, which would otherwise be needed to produce the bricks.

Table 2.2: Chemical composition of brine sludge (Amritphale et al. 2018)

Oxides	Wt %
LOI	25.99
SiO_2	25.976
Al_2O_3	7.81
Fe_2O_3	1.327
Na_2O	10.05
K_2O	0.2579
CaO	13.995
MgO	6.24
SO_3	1.3345
ZnO	0.0037
Cr_2O_3	0..0029

CuO	0.0026
TiO_3	0.2129
Chlorides (Cl)	13.81

Joshi et al. (2014): Hazardous waste known as brine sludge is produced during the chlor-alkali process used to produce NaOH and Cl_2. The disposal of the brine sludge into a secure TSDF site raises the cost of monitoring for chlor-alkali industries. The sludge contains about 40% barium sulphate (BaSO4), which has a high economic value, according to analysis. In this paper, we suggest a straightforward chemical separation method for recovering BaSO4 from brine sludge. The BaSO4 derived in this way was determined to be 93% pure and is suitable for use in a number of industrial applications.

Table 2.3: Chemical composition of brine sludge (Joshi et al. 2014)

Constituent	% (w/w)
$BaSO_4$	42.21
$BaCO_3$	4.11
$CaCO_3$	16.50
$Mg(OH)_2$	3.90
NaCl	12.69
Moisture	18.80

Jhan et al. (2019): Materials with controlled low strength (CLSM) have been used. Brine sludge was used to replace the composition in CLSM for resource application and was produced by the chlor-alkali industry. Only the fine aggregates or all of the aggregates were replaced by the brine sludge mix composition. The compressive strength test was approved due to the appropriate composition being observed.

Table 2.4: The chemical composition and physical properties of brine sludge (Jhan et al. 2019)

Sr. no.	Properties	Brine Sludge
Physical Properties		
1.	Color	Light grey
2.	Specific gravity	2.63

3.	Natural water content %	36.21
4.	pH	10.55
Chemical composition %		
1.	CaO	58.95
2.	MgO	37.41
3.	SrO	0.92
4.	SiO_2	1.44
5.	Fe_2O_3	0.78
6.	Al_2O_3	0.36
7.	Na_2O	0.14

Yadav et al. (2020): With an annual production of 23.37 million vehicles in 2014–15, the Indian automotive industry has emerged as a "dawn segment" of the Indian economy. In addition to constructed landfills, other dumping techniques contaminate groundwater and have other negative financial effects. In the current investigation, an effort has been made to use the car ETP slime (dry), which is delivered from Goodbye MOTARS, PUNE, in the creation of development materials. A mechanical waste product of the chloral antacid industry is salt water muck. The produced saline solution ooze waste is disposed of in landfills and contains hazardous substances like chromium, zinc, copper, and vanadium as well as barium Sulfate, calcium carbonate, magnesium hydroxide, sodium chloride, and earth. Therefore, it is urgent to convert hazardous saline solution waste into its non-lethal structure.

This innovation aims to fully utilize the salt water ooze to create functionalized saline solution muck that can be used across a wide range of applications.

Table 2.5: Physical Parameters of brine sludge and fly ash (Yadav et al. 2020)

S.no.	**Properties**	**Brine sludge**	**Fly ash**
1.	Colour	Light Grey	Greyish Black
2.	Physical state at room temperature	Semi-solid	Solid
3.	pH	12	10.5
4.	Bulk Intensity, g/cc	2.52	2.35

Table 2.6: Chemical properties, % of brine sludge and fly ash (Yadav et al. 2020)

S.no.	Properties	Brine sludge	Fly ash
1.	SiO_2	9.16	62.51
2.	$Al_2O_3 + Fe_2O_3$	5.22	26.88
3.	CaO	9.32	2.20
4.	MgO	7.65	0.92
5.	BaO	40.03	-
6.	SO3	12.32	1.80
7.	Cl	5.30	-
8.	Na_2O	4.80	0.40
9.	K_2O	0.31	0.57
10.	Cr_2O_3	-	0.04
11.	ZnO	0.03	0.02
12.	CuO	0.05	0.01
13.	V_2O_5	0.01	-
14.	LOI	5.8	4.65

2.2 Composition of the bricks-

By combining different amounts (Table 2.7) of brine sludge, fly ash, and cement with a vibration-compaction technique (vibration time 15 sec), the bricks measuring 190 × 90 × 90 mm were cast at a consistency of 20%. The bricks were tested for compressive strength, water absorption (over 24 hours), and bulk density after being cured for 28 days in high humidity. The specimen's bulk density in kg/m3 was calculated by dividing its weight by all of its dimensions.

Table 2.7: Composition of bricks (Garg and Pundir (2014))

Designation	Composition of bricks (% by wt.)		
	Sludge	Fly Ash	Cement
R1	20	70	10
R2	25	65	10
R3	30	60	10

To create the alkaline activator solution, sodium hydroxide pallets (NaOH) and solid sodium metasilicate (Na_2O_3Si) are purchased. Alkaline activator solution had the following chemical

make-up: 9.4% Na_2O, 30.1% SiO_2, and 60.5% H_2O; the SiO_2/Na_2O weight ratio was 3.20:3.30; the specific gravity was 1.4 at 20°C; and the viscosity was 400 cP at 20°C.

Table 2.8: Mix composition of geopolymeric (cement-free) brine sludge bricks (GBSBC) (Amritphale et al. 2018)

Sr. no.	Mix Coding	Composition of bricks by weight (g)			
		Brine Sludge	Fly Ash	SMS	NaOH
1	GBSBC 1	20	522.25	50	100
2	GBSBC 2	25	522.25	50	100
3	GBSBC 3	30	522.25	50	100

The results were satisfied by the replacement of fine aggregates. Having to replace all of the aggregates meant that the initial strength levels at 1 day were insufficient. At 28 days, the compressive strength ranged from 1.709 to 21.37 kgf/cm^2.Overall, the mixture that took the place of the fine aggregates met all of the CLSM specifications. The consumption of brine sludge could be at its highest when coarse aggregate composition falls to 250 kg/m^3.

Table 2.9: Mix composition of group A (Jhan et al. 2019)

Group no.	Mix no.	Cement (kg/m^3)	Water (kg/m^3)	Coarse aggregate (kg/m^3)	Brine Sludge (kg/m^3)
A	A1	204	417	383	716
	A2	204	560	250	742

The composition in this mixture didn't use coarse aggregates to increase the replacement of the brine sludge. On the other hand, brine sludge took the place of all the aggregates in this mixture. In addition, the amount of cement in the mixture varied between B1 and B2. The additional water content adjustment followed the same steps as the creation of mixture A. In group B, the mix composition was displayed in Table 2.10.

Table 2.10: Mix composition of group B (Jhan et al. 2019)

Group no.	Mix no.	Cement (kg/m^3)	Water (kg/m^3)	Coarse aggregate (kg/m^3)	Brine Sludge (kg/m^3)
B	B1	204	571	0	955
	B2	153	611	0	866

The composition of the blocks are given in the table 2.11.

Table 2.11: Proportion of sample (Yadav et al. 2020)

Sr. no.	Sludge	Cement	Sand	Fly Ash	Lime	$CaCl_2$
M - 1 %	10	40	17	30	2	1
M - 2 %	20	40	17	20	2	1
M - 3 %	30	40	17	10	2	1

2.3 Compressive strength, Water absorption and Bulk density of the bricks-

Fig. 2.1 provides an illustration of the characteristics of cement-fly ash-brine sludge bricks (size: 190 × 90 × 90 mm) containing 20, 25, and 30% brine sludge designated as R1, R2, and R3. The findings demonstrate that as the concentration of brine sludge increased, bricks' compressive strength (C.S.) decreased and their water absorption (W.A.) increased.

It does not meet the minimum strength requirement for class 5 bricks specified in IS 12894 because mix R3's compressive strength is significantly lower than that of mixes R1 and R2. Bricks with a higher proportion of brine sludge showed a slight increase in bulk density (B.D.). The drying shrinkage of the R1, R2, and R3 designated bricks tested using the IS 4139 method was less than the maximum allowed value of 0.15 percent.

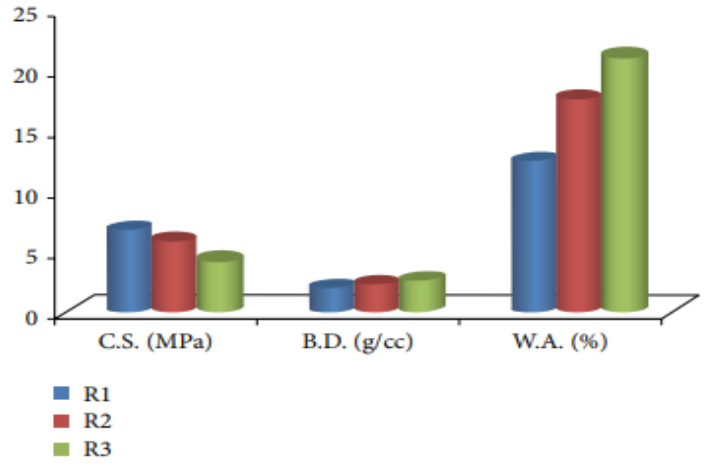

Figure 2.1: Properties of bricks (Garg and Pundir (2014))

The bricks' characteristics were in accordance with Indian standards. According to the findings, up to 25 and 35 percent of brine sludge can be used to make bricks, respectively.

The results below demonstrate that as the concentration of brine sludge in the geopolymeric matrix increased, the compressive strength of bricks decreased and their water absorption increased. Compared to GBBR 1 mix and GBBR 2 mix, GBBR 3 mix has a significantly lower compressive strength. Additionally, it does not meet the class 5 brick's minimum strength requirement outlined in IS 12894. Increased proportions of brine sludge led to a slight improvement in the bulk density (BD) of bricks, as shown in Figure 2.2. According to the method described in IS 4139 (1989), the drying shrinkage of the GBSBC1, GBSBC 2, and GBSBC3 designated bricks tested fell within the maximum allowed value of 0.15%.

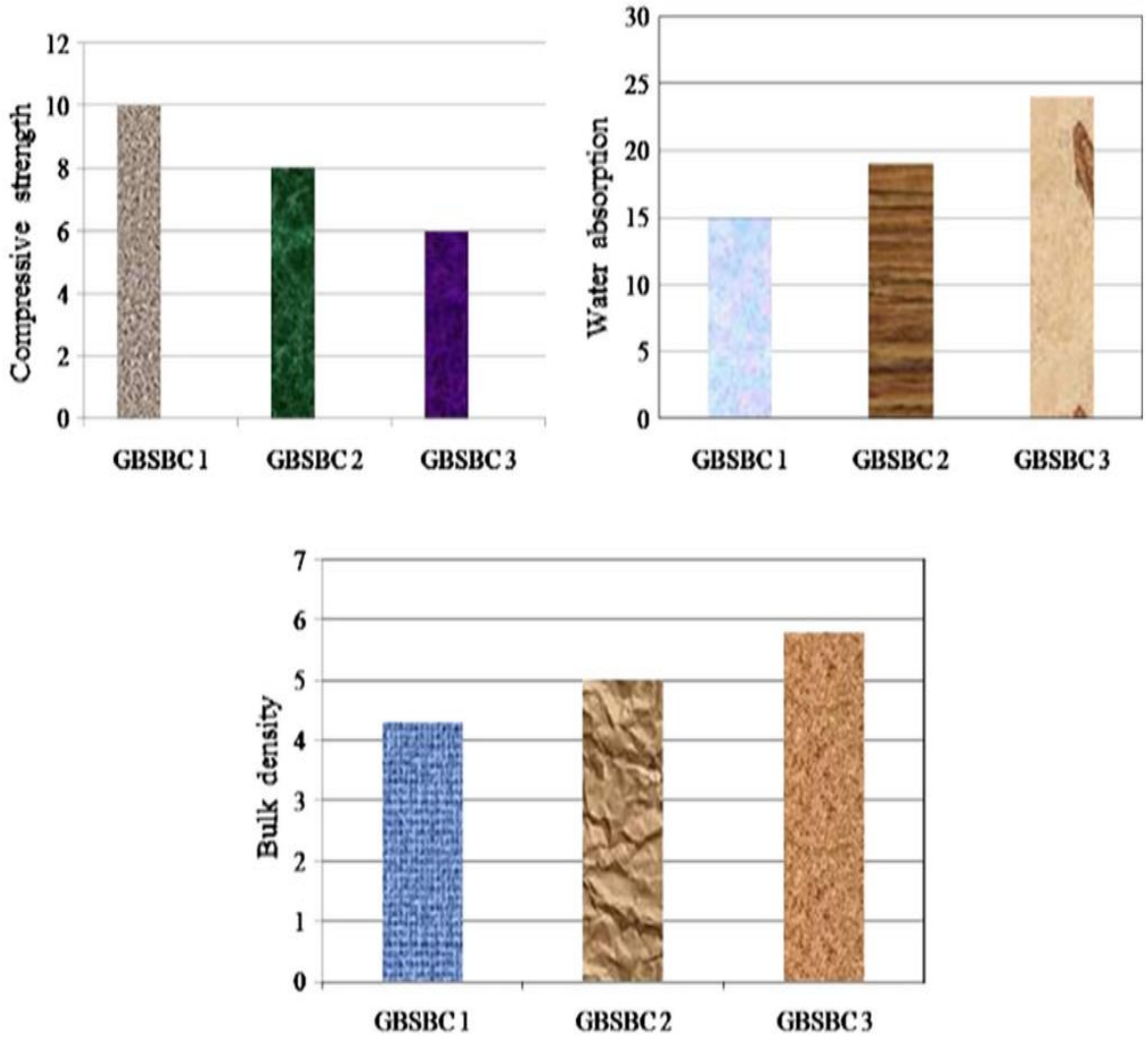

Figure 2.2: Compressive strength (CS), water absorption (WA) and bulk density (BD) geopolymeric (cement-free) brine sludge bricks (GBSBC) (Amritphale et al. 2018)

The results of the compressive strength at 1, 7, and 28 days in this study were displayed in Table 2.12. Compressive strength in group A ranged between 10.89 and 21.37 kgf/cm^2 after 28 days. A1 produced the highest 28-day compressive strength as well. At 28 days, group B's compressive strength was 1.709 and 6.744 kgf/cm^2.

Table 2.12: Compressive strength of CLSM at 1, 7 and 28 days (Jhan et al. 2019)

Group no.	Mix no.	Compressive strength (kgf/m^2)		
		1 day	7 days	28 days
A	A1	9.024	18.316	21.372
	A2	6.028	9.417	10.885
B	B1	2.14	5.494	6.744
	B2	0.749	1.23	1.709

The coarse aggregates might prevent additional loading. The average compressive strength decreased in step with the reduction in coarse aggregate volume. Cylindrical specimens in group A that contained coarse aggregates had a much higher strength than group B. Additionally, as people aged, the progression of compressive strength improved in both group A and group B. In Fig. 2.3, the compressive strength curve is shown.

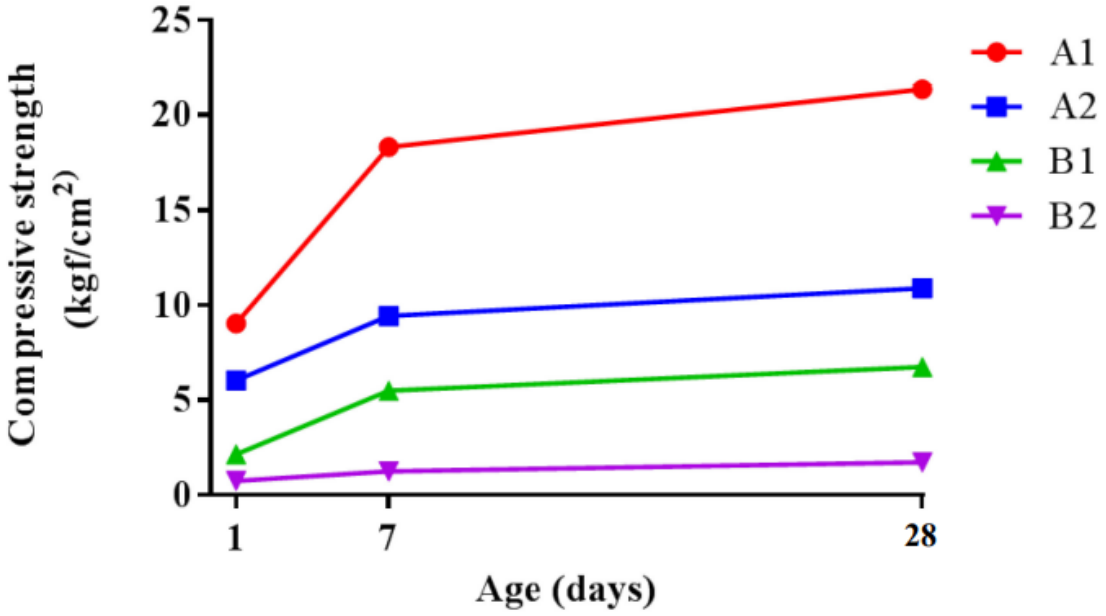

Figure 2.3: The compressive strength development (Jhan et al. 2019)

When comparing the CLSM properties, the top mix composition of the brine sludge is A2, which can meet all of the CLSM standards and also recycle the most brine sludge.

Figures 2.4 and 2.5 display the blocks' tested compressive properties. Slime does not expand as much as other constituents did to increase the compressive strength of blocks. However, despite this, the rate at which slime is expanding has resulted in a decline in compressive quality. However, since slop is better than soil at filling voids, it may also do so, causing the void space to decrease and the blocks to become denser. The compressive quality of blocks should now be expanded by the muck's filler activity. The sum of these two impacts should be clearly visible quality changes. When rate slop included is less than 5%, filler activity is more prevalent. Simply by forcing the coarse sand particles in the dirt apart, further ooze expansion consumes the available space. As a result, there will be less grinding between sand grains, which is a key factor in the blocks' ability to compress. Accordingly, a decline in compressive quality at higher ooze rates is common.

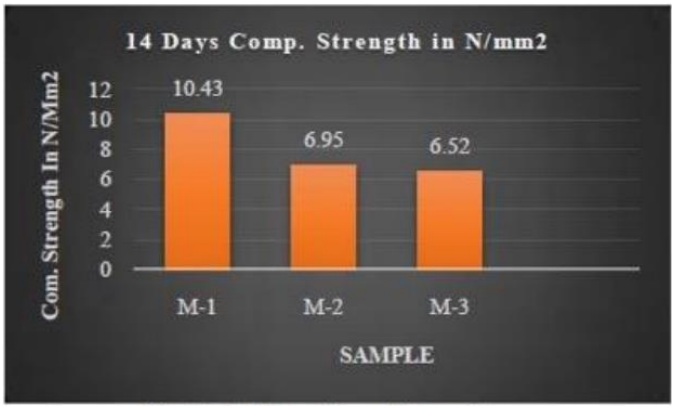

Figure 2.4: 14 days compressive strength (Yadav et al. 2020)

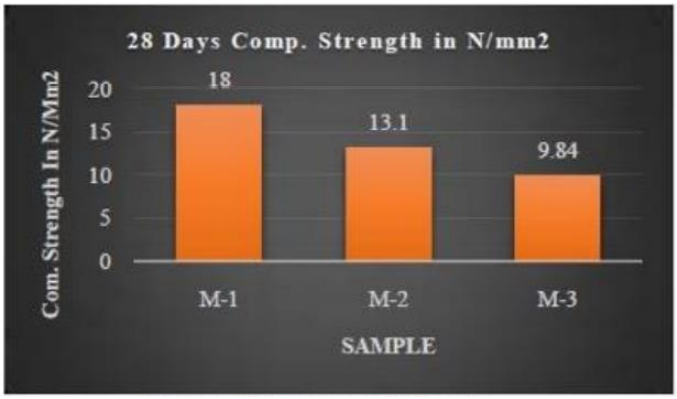

Figure 2.5: 28 days compressive strength (Yadav et al. 2020)

Figure 2.6 shows the effect of slop on the absorption of water. This demonstrates that blend water adsorption is within the acceptable range. Anyhow, less than 20% of a person's weight should be consumed as water.

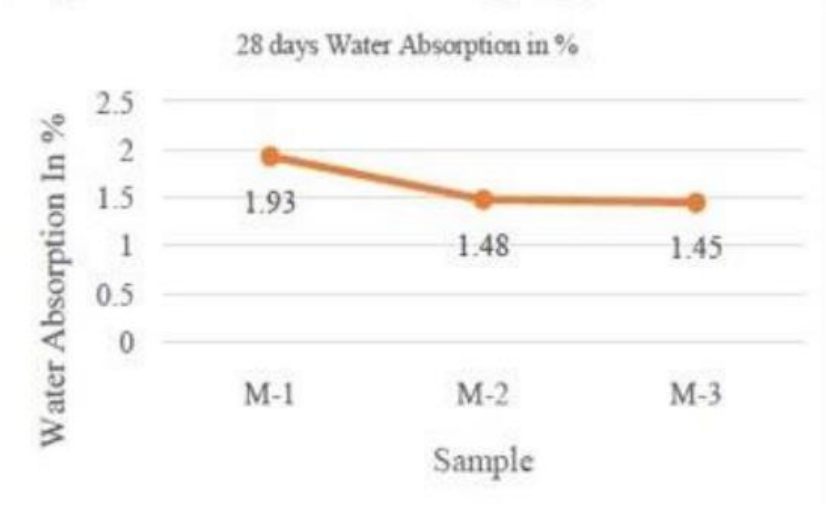

Figure 2.6: 28 days water absorption (Yadav et al. 2020)

2.4 X-ray Diffraction (XRD Analysis)-

The X-ray diffraction technique (XRD) was used to analyze the mineralogy, and the results are shown in Fig. 2.7.

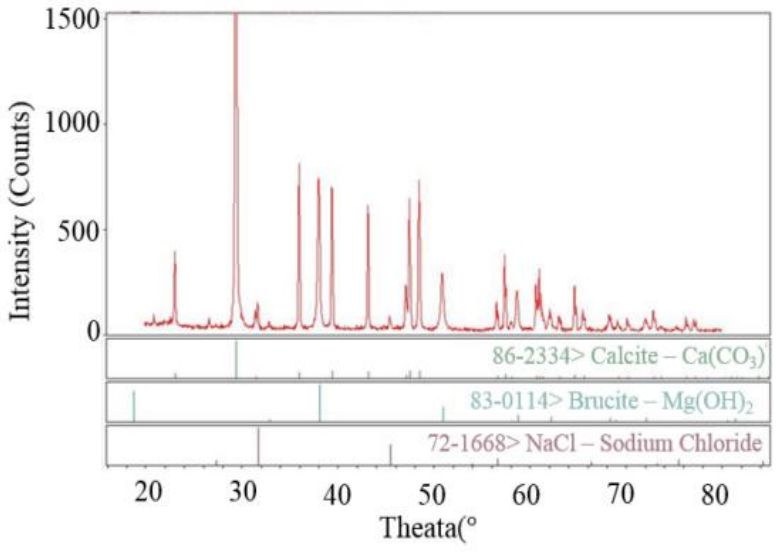

Figure 2.7: XRD of brine sludge sample (Chen et. al 2019)

Viviani et al. (2021): Multiple chemical compounds make up brine sludge, which could have an adverse effect on the environment. It was investigated whether brine sludge wastes could be used to create materials with added value. Using X-ray diffraction (XRD), two brine sludge

samples were characterized. The samples contained elements like Ca, Si, Na, Mg, Al, Cl, and Fe. The XRD results demonstrated the crystalline nature of the constituents and showed that quartz, calcium carbonate, sodium chloride, and magnesium hydroxide were the major constituents in the brine sludge samples.

Figures 2.8 and 2.9, respectively, show the X-ray diffraction spectra (XRD) of two distinct samples of brine sludge from two different origins. Despite coming from different sources, the samples' diffractograms are remarkably similar. The samples' predominance of crystalline structure is indicated by the XRD patterns' composition of sharp multiple peaks.

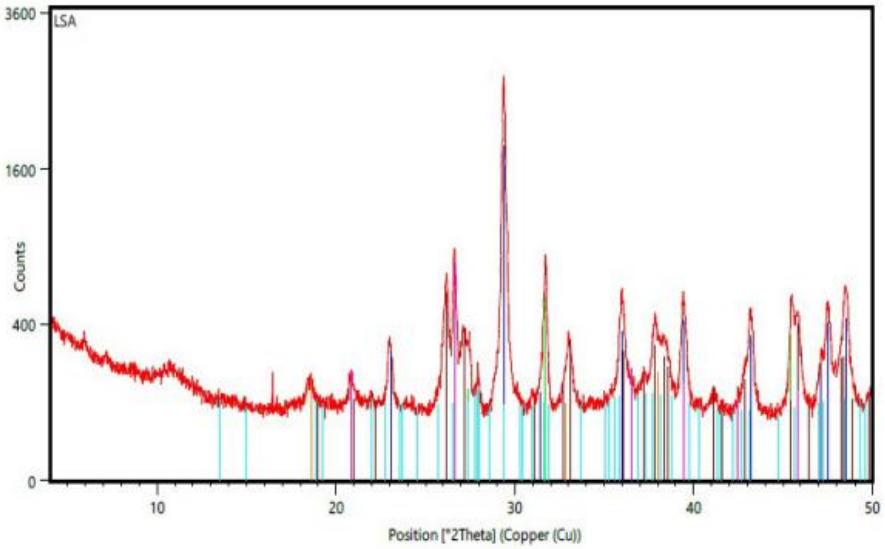

Figure 2.8: XRD pattern of brine sludge sample 1 (Viviani et al. 2021)

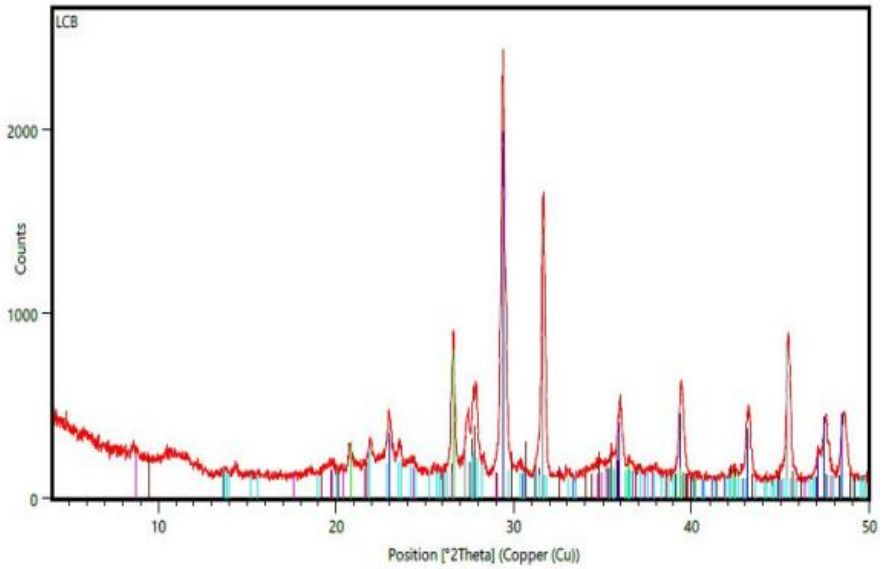

Figure 2.9: XRD pattern of brine sludge sample 2 (Viviani et al. 2021)

2.5 Fourier Transform Infrared Spectroscopy (FTIR Analysis)-

Different functional groups like carbonate, siloxane, and hydroxide were detected using FTIR. An alternative potential use for sustainable building material products is the incorporation of brine sludge in geopolymeric materials

The relevant vibration bands of the brine sludge samples were identified in the 400–4000 cm^{1} range and are displayed in Figs. 2.10 (a) and 2.11 (b), respectively, for BSSA and BSCB. The wave numbers and vibrational assignments of the absorption maxima in the material's spectra are listed in Table 2.13.

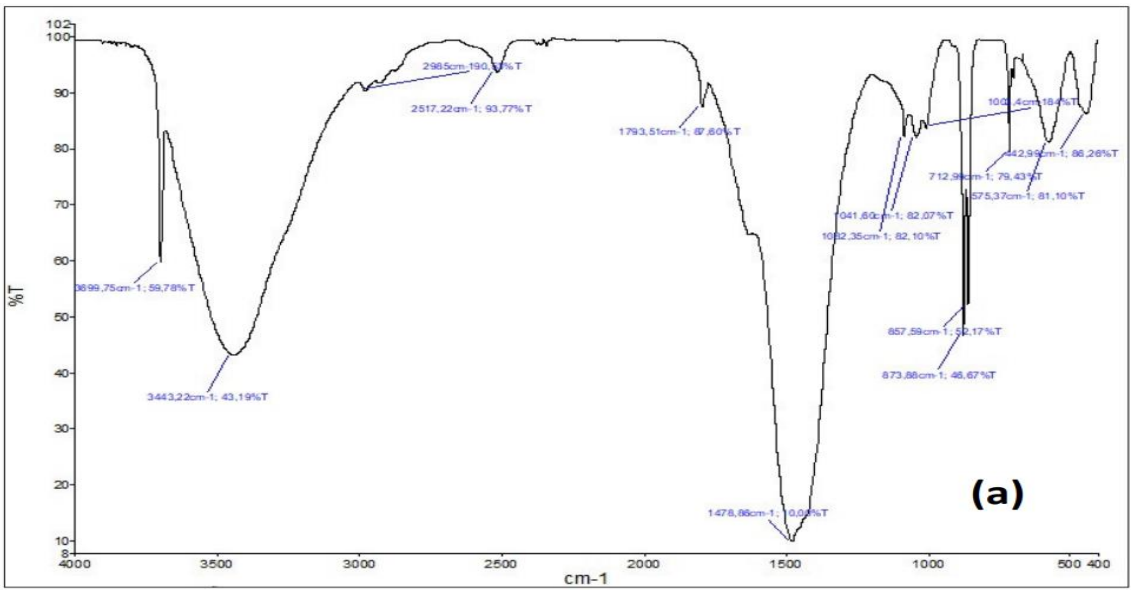

Figure 2.10: FTIR spectrum of brine sludge sample 1 (Viviani et al. 2021)

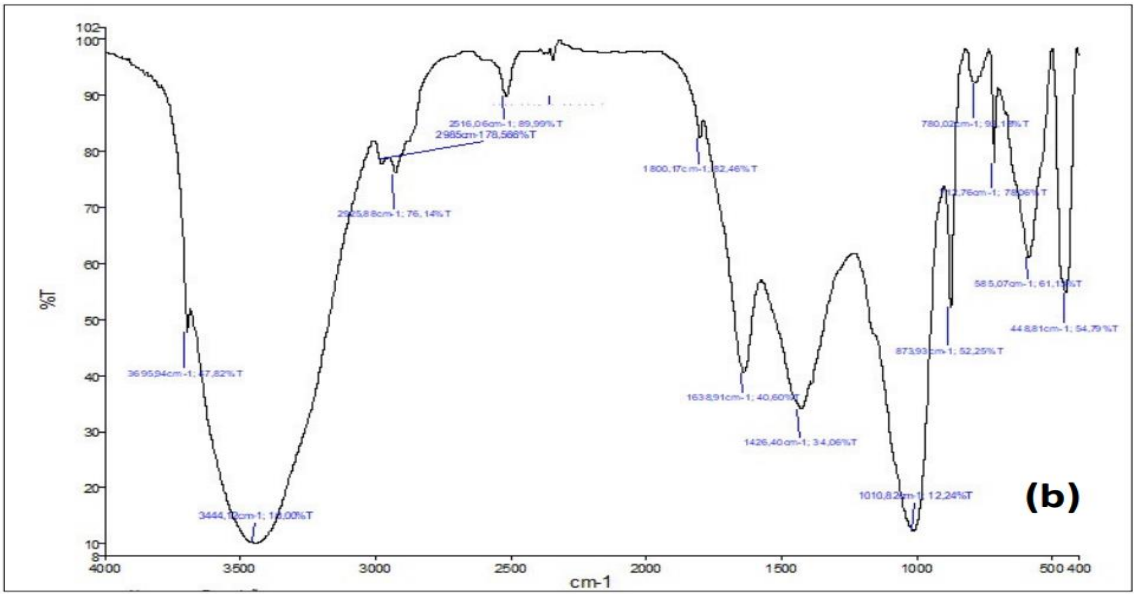

Figure 2.11: FTIR spectrum of brine sludge sample 2 (Viviani et al. 2021)

Brine sludge samples commonly contain calcium carbonate, and the FTIR spectrum is excellent for identifying the various phases of this compound. Identifying the absorption bands allows one to distinguish between the different calcium carbonate crystal phases.

The calcite and aragonite vibration frequencies were those of two crystalline calcium carbonate phases. The carbonate ion's symmetric stretch occurs at approximately 1080 cm^{-1} (v1), followed by the out-of-plane bending absorption at approximately 870 cm^{-1} (v2), the asymmetric stretch at approximately 1400 cm-^{1} (v3), and the in-plane bending at approximately 700 cm^{-1} (v4). Each of calcium carbonate's phases has a few distinctive absorption bands. The aragonite-specific bands are at 1480 cm^{-1}, 1083 cm^{-1}, and 858 cm^{-1} in length. Two distinct absorption bands that correspond to the stretching and deformation modes of OH (region 3670-3440 cm^{-1}) and the bending vibration mode of H2O (region 1640 cm^{-1}) respectively are used to detect the presence of H2O.The presence of the distinctive frequency of the hydroxyl group (OH-) stretching vibration of magnesium hydroxide is also indicated by a broad absorption band at 3670 cm^{-1}.

The minor peak at 2900 cm^{-1} is associated to a saturated C-H vibration from a KBr crystal impurity, and the minor peaks at 2500 and 2300 cm^{-1} were brought about by the adsorption of atmospheric CO_2.

The characteristic absorption bands at 448, 780, 1010-1040, and 1640 cm^{-1} were used to determine the presence of quartz. The best band for determining silica among these is the absorption at about 800 cm^{-1}, which is caused by Si-O-Si symmetrical stretching vibration. The formation of the Si-O-Al bond is indicated by the absorption bands at 585 and 575 cm^{-1}.

Table 2.13: IR bands of brine sludge samples (wavenumber cm^{-1}) (Viviani et al. 2021)

Wavenumber (cm^{-1})		
BSCB	BSSA	Assignments
3695.94	3699.75	stretching and deformation of adsorbed water molecule asymmetric stretching vibrations of OH groups from $Mg(OH)_2$
3444.12	3443.22	stretching and deformation of adsorbed water molecule

2925.88	-	saturated C-H vibration from some impurity in the KBr Crystal
2516.06	2517.22	atmospheric CO_2
2344.05	-	atmospheric CO_2
1800.17	1793.51	symmetric vibration (v1+v4) CO_3
1638.91	-	Si-O-Si asymmetric stretching and bending vibrations of water molecule
1426.4	1478.86	symmetric vibration v3 (CO_3)
-	1082.35	symmetric vibration v1(CO_3)
1010.82	1041.6	symmetric stretching of Si-O-Si
873.93	873.88	asymmetric vibration v2 (CO_3)
-	857.59	out-of-plane bending vibration v4(CO_3)
780.02	-	symmetric stretching of Si-O-Si
712.76	712.99	symmetric vibration v4(CO_3)
585.07	575.37	Si-O-Al bond
448.81	442.99	symmetric stretching of Si-O-Si and asymmetric bending of Si-O

The chemical make-up of the two brine sludge samples included Ca, Si, Na, Mg, Al, Cl, and Fe. For both samples, calcium made up the majority of the composition.

Mwenge et al. (2021): Biodiesel is a fuel that is produced through a transesterification process using a homogeneous catalyst, which pollutes the environment and cannot be recycled. To enable the trans-esterification of used cooking oil into biodiesel using the chloro-alkali industrial brine sludge waste as a heterogeneous catalyst. At the following reaction parameters: methanol to oil mass ratio (30 wt%), reaction time (1 hr), reaction temperature (60 °C), and catalyst to oil mass ratio (2.52 wt%), the highest yield value of biodiesel is obtained at 95.51 wt%. IBSW can be used as a heterogeneous catalyst up to four times without the biodiesel yield

changing noticeably. The FTIR and SEM results show that IBSW was modified both before and after the transesterification process.

The FTIR spectra of the industrial brine sludge waste samples after the first and fourth transesterification reactions are shown in Figures 2.12 and 2.13, respectively. Calcite (CaO), which has distinctive peaks at 3600, 1760, 1430, 121, and 712 cm^{-1}, is present. The peaks indicate that calcium in the form of calcilite is the primary chemical component of brine sludge waste. It's possible that the presence of Na2O, K2O, and MgO is what causes the low intensity peaks between 100 and 800 cm^{-1}. Peak intensity has slightly decreased, indicating that calcined IBSW can still be used after the fourth transesterification run.

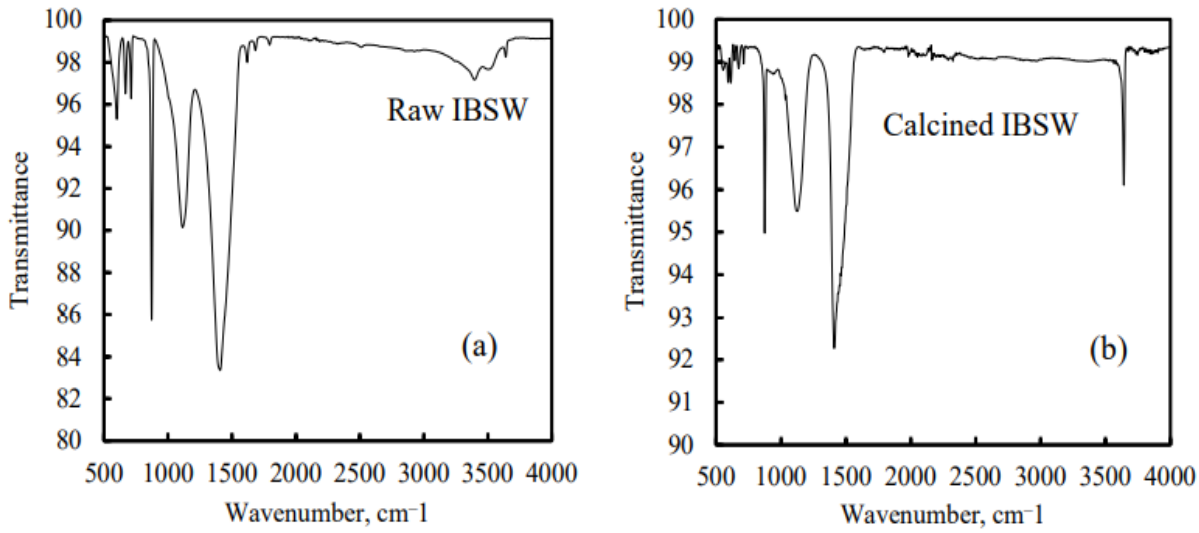

Figure 2.12: FTIR results: (a) raw IBSW; (b) Calcined IBSW (Mwenge et al. 2021)

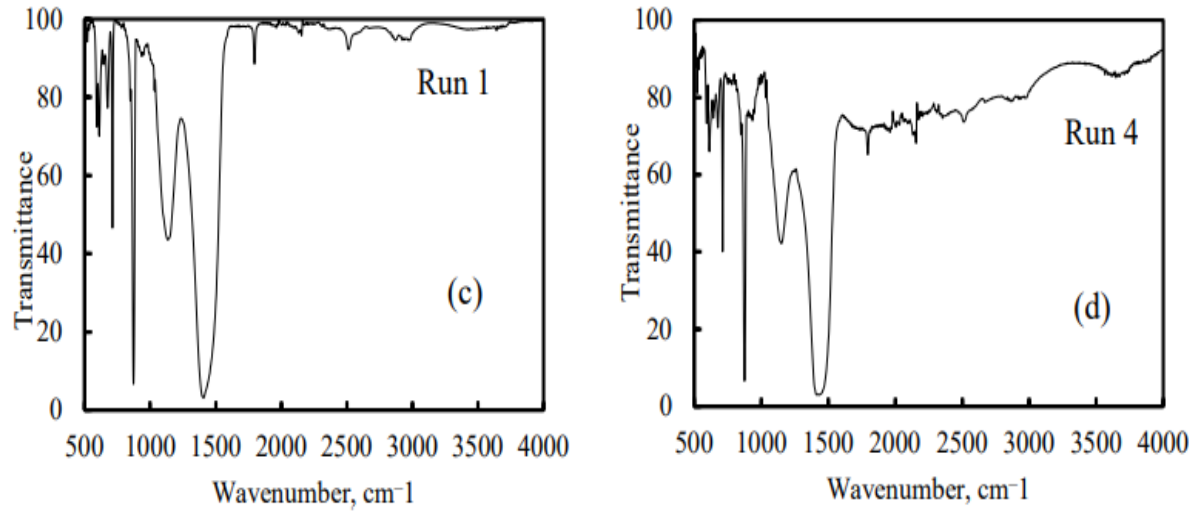

Figure 2.13: FTIR results: (c) Run 3; (d) Run 4 (Mwenge et al. 2021)

2.6 Scanning Electron Microscopy (SEM Analysis)-

Fig. 2.14 shows the SEM findings. Before transesterification, the morphological structure of the IBSW is non-deformed and more regular, as shown in Fig. 2.14 (a). In comparison to the calcined IBSW, the post-transesterification morphology was more deformed, rough, and irregular, as shown in Fig. 2.14 (b).

The first transesterification reaction run results in a negligible change in the morphological structure, as shown in Fig. 2.14 (c). A gellish morphology was seen after the catalyst IBSW was used up to four times, as shown in Fig. 3.14 (c). This demonstrated that the oil and glycerol were deposited on the IBSW catalyst's surface.

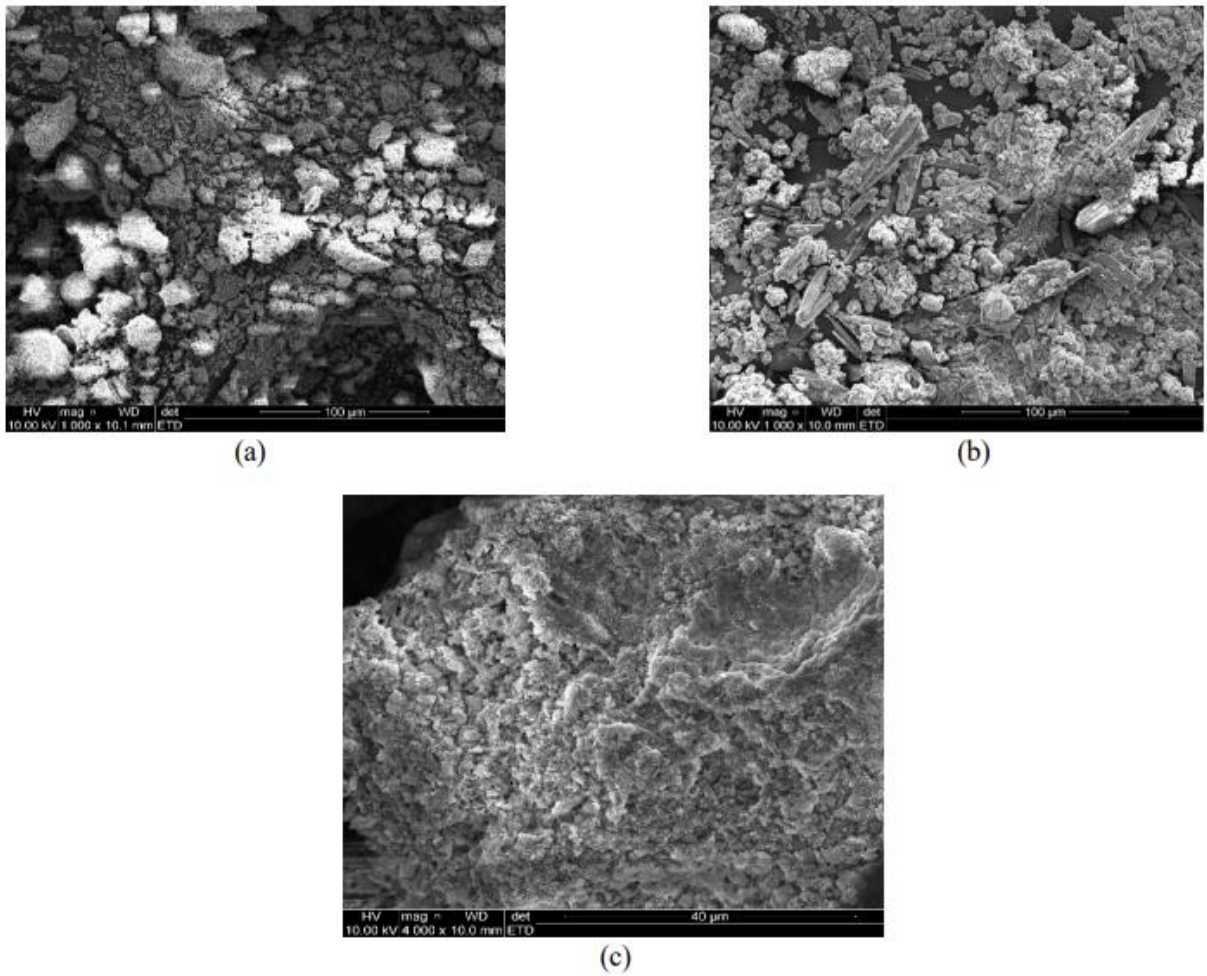

Figure 2.14: SEM results for calcined IBSW (a), after 1 run (b) and after 4 runs (c)

(Mwenge et al. 2021)

Transesterification is the chemical process by which triglycerides and alcohol are transformed into alkyl esters with the aid of a catalyst. Methanol and ethanol are the most frequently used alcohols in this process because of their affordability and accessibility.

Masilela et al. (2018): The research published in this journal demonstrated that an industrial brine sludge waste (IBSW) can be used as a sorbent in the wet flue gas desulfurization process. The dissolution kinetics of IBSW is defined by taking into account the effects of temperature, pH, stirring speed, solid-to-liquid ratio (m/v), particle size, and acid concentration. It was discovered that the solid-to-liquid ratio (m/v), particle size, and pH all had an effect on the rate at which IBSW dissolved, while acid concentration, temperature, and stirring speed had the opposite effect. It was discovered that the activation energy was 7.195 kJ/mol, indicating that the rate-limiting step was product layer diffusion.

Figure 2.15 demonstrates that the morphological structure of IBSW is more regular and undamaged prior to dissolution. Leaching took place, as evidenced by the particles' increased deformation, roughness, and irregularity following dissolution (60 min). These characteristics are not present in the raw industrial waste brine sludge.

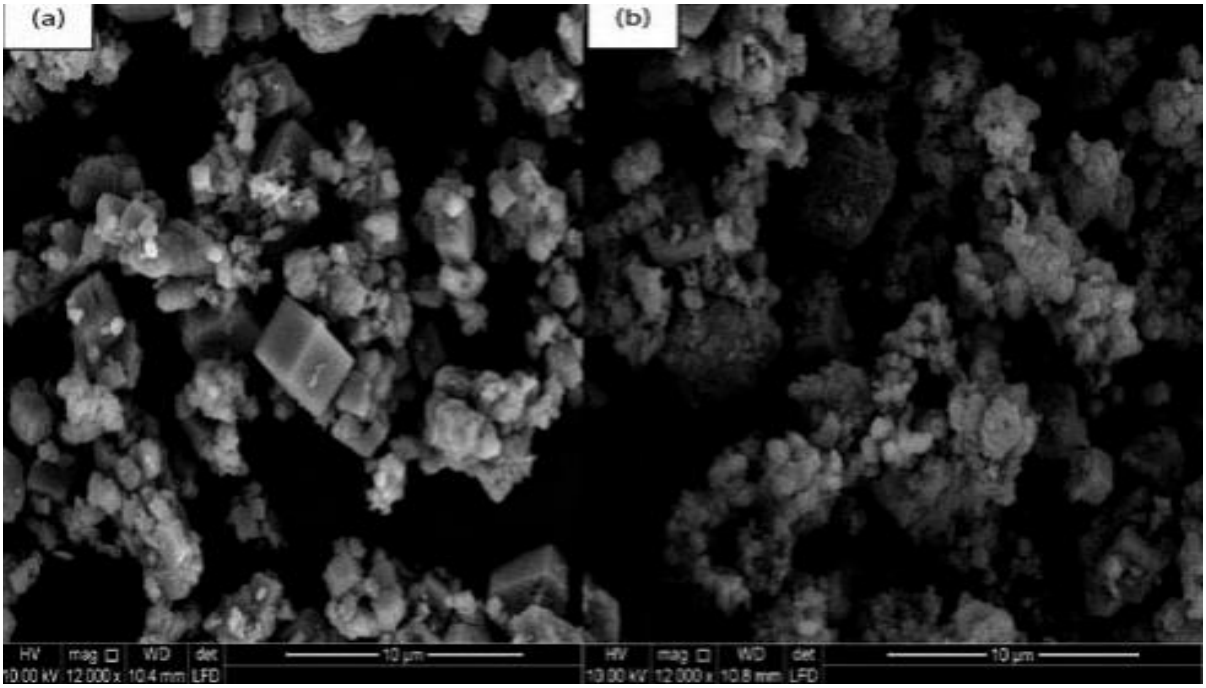

Figure 2.15: SEM images of IBSW (a) before dissolution and (b) at dissolution (60 min) (Masilela et al. 2018)

2.7 Leachability studies-

Khan et al. (2018): The geopolymerized product underwent the toxic characteristic leaching procedure (TCLP) test to assess the immobilization and stabilization of metal ions. Using the TCLP method, the leaching test was carried out on 28-day-cured paver block samples. The leachates were examined in triplicate, and Table 2.14 reports the average metal ion values for

geopolymerized brine sludge (cement-free) paver blocks (GBSP) and raw brine sludge. The outcomes were evaluated in comparison to the limits for pollutant discharge at inland surface waters specified in Indian standard IS 10500. The results clearly demonstrated that metal ions are chemically bound and retained into the geopolymeric material structure because the concentration of leached metals is below the detection limit of the limits specified in the India standard.

Due to the presence of alkaline ions, toxic metal ions form chemical bonds with the geopolymerized matrix that is made up of Silonol (Si-OH species) and Alonol (Al-OH species) during the process of geopolymerization. As a result, the geopolymeric matrix's mineralogical and chemical phases of the toxic sludge are designed in such a way that the toxic ions become entangled and unreachable to significant and desirable levels.

Table 2.14: Leachability studies of raw brine sludge and geopolymerized brine sludge (cement-free) paver blocks (Khan et al. 2018)

Sr. no.	Name of metal ions	Concentration of metal ions (mg/L)		IS 10500-2012 discharge limit of metal ions at inland surface water (mg/L)
		Raw brine sludge	Geopolymerized brine sludge (cement - free) paver blocks	
1.	Chromium	290	2.7	3.1
2.	Copper	260	2.50	3.0
3.	Vanadium	100	0.17	0.2
4.	Zinc	370	4.70	5.0

The leachability studies confirm that the metals and impurities in the brine sludge are significantly chemically fixed in the hardened geopolymeric product and well below the permissible limit.

Anshul et al. (2016): The toxic characteristic leaching procedure (TCLP) test is used to assess how well metal ions that are present in the hydrated product have been immobilised and stabilised. Using the ASTM extraction D3987-85 method, the leaching test for 28-day cured paver block samples was carried out. The sample was ground to a fine powder with particle sizes that could pass through a number 6 sieve (0.333 cm) but not a number 16 sieve (0.119

cm). The pH of the solution was then maintained at 5.0 0.2 by adding 1 N of acetic acid after 10 g of the sample had been added to 160 mL of water. The samples were shaken continuously for 24 hours at a rate of 170 RPM. Then a 0.45 m membrane filter paper was used to filter a 10 mL sample. By measuring the concentration of the metals using inductively coupled plasma optical emission spectroscopy (ICP-OES, model: Prodigy XP), the amount of metals that were leached was calculated.

The leachates were examined in triplicate, and Table 2.15 presents the average metal ion values. The outcomes were evaluated in comparison to the limits for pollutant discharge at inland surface waters specified in Indian standard IS 10500.

The reults clearly demonstrated that the metal ions under test are firmly bound and retained within the material structure and do not easily leach from there. Except for iron metal, the concentration of leached metals is considerably lower than the limits outlined in Indian standard.

Table 2.15: Leachability studies (Anshul et al. 2016)

Sr. no.	Metal ions	Metal ions concentration as per TCLP method (mg/kg)	Discharge limit of metal ions at inland surface water as IS 10500-2012 (mg/L)
1.	Vanadium	0.16	0.2
2.	Chromium	2.5	3.1
3.	Zinc	4.30	5.0
4.	Copper	2.32	3.0

The metals and impurities in the sludge are substantially fixed in the solidified product, according to the leachability studies.

3. MATERIALS AND METHODS

The brief descriptions of the different materials which are used in this study presented in this chapter. Various approaches are used to take into account the different material properties, sample preparations are made using various mix designs, and various tests are used to ascertain the various properties of the specimens.

3.1 Material properties-

This study made use of brine sludge, fly ash, sodium hydroxide, sodium silicate, standard sand, natural sand, stone dust, and distilled water. The sections below provide discussions of these materials' physical and chemical characteristics.

3.1.1 Brine sludge-

Brine sludge is produced when brine is electrolyzed to produce chlorine and caustic soda. One of the primary raw materials used in the manufacturing of Chlor-alkali is industrial-grade salt, such as brine. Impurities in the salt include insoluble residues (silica), calcium, and magnesium. Brine sludge is produced as a result of the removal of these contaminants from the brine. The brine sludge has a specific gravity of 2.419 as per IS 2386 (Part 3) (Bureau of Indian Standards, 2016).

Figure 3.1: Brine sludge

3.1.2 Fly ash-

In this study, Class F fly ash is used throughout the inquiry. Fly- ash used was lump-free and had a greyish look. The fly ash has a specific gravity of 2 as per IS 2386 (Part 3) (Bureau of Indian Standards, 2016).

Figure 3.2: Fly ash

3.1.3 Sodium hydroxide and sodium silicate solution-

This investigation used sodium hydroxide pallets (hemispherical shapes) with diameters ranging from 5 to 7 mm. It also goes by the name caustic soda. The majority of NaOH pallets are crystalline solids with high water solubility. It reacts with the moisture in the air and produces heat when it is neutralised with acid or combined with water. The sodium silicate used in the investigation was in liquid form. With the help of distilled water, NaOH, and Na2SiO3, a geopolymer activating solution has been prepared.

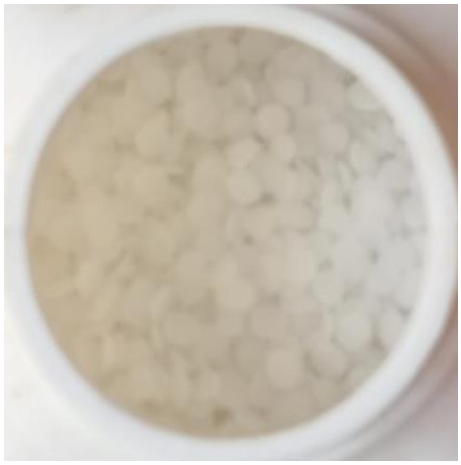

Figure 3.3: Sodium hydroxide pallets

Sodium Hydroxide (NaOH) solutions with molarities of 10 and 18 were created. The distilled water was used to dissolve 400 and 720 grams (Molarity × molecular weight) of NaOH pellets

to create a 1-liter solution. Two to three hours were given for the solution to cool. The following product's Chemical Abstracts Service register number is (CAS No. 1310-73-2).

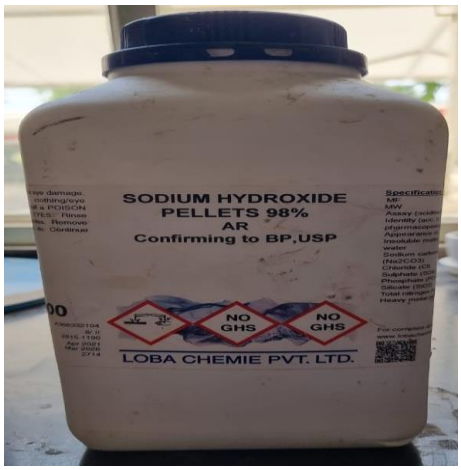

Figure 3.4: Sodium hydroxide

After cooling, the sodium silicate solution of same volume was added to the solution and was kept for 24 hours for activating and was then used in casting of specimens.

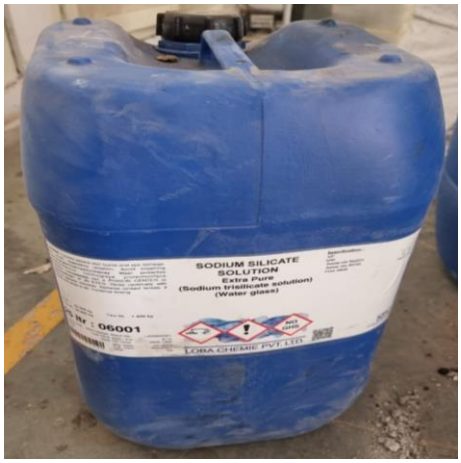

Figure 3.5: Sodium silicate

The chemical abstracts service registry number of the above product is (CAS No.1344-09-8).

3.1.4 Standard sand-

The Standard sand is quartz, Grey light or white in colour and must be free from silt content. The grain of sand particles must be angular, and the shape of the grain particles must be in spherical in shape. There shall be elongated or flattened particles of grains only in the small or minute quantity.

The chemical characteristics of the standard sand includes that it must be free from the organic impurities. The present study used the Standard Sand of all three grades conforming to Indian standard IS 650 (Bureau of Indian Standards, 2008).

The standard sand is 100% passing from 2 mm sieve and is 100% retaining on 90 micron sieve and particle size distribution of standard sand is shown in below Table 3.1. According to IS 2386 (Part 3) (Bureau of Indian Standards, 2016), the specific gravity ranged from 2.5 to 2.7.

Table 3.1: Particle Size Distribution (IS: 650)

Sr. no.	Particle Size	Percent used
1.	Less than 2 mm and larger than 1 mm	33.333
2.	Less than 1 mm and larger than 500 microns	33.333
3.	Less than 500 microns and larger than 90 microns	33.333

Figure 3.6: Three grades of sand

3.1.5 Natural sand-

Unlike other types of the sand which are produced by crushing rock, river sand is a naturally occurring sand that is shaped through weathering or erosion processes. Although the gradation of natural sand can vary, it is typically coarse sand. In this investigation, the river sand complies with IS 383 (Bureau of Indian Standards, 2016). Grading Zone II.

Figure 3.7: Natural Sand

3.1.6 Stone dust-

The types of stone dust that are easily available depend on the stones that are crushed and are a direct result of stone crushing. Naturally, each of these several types has different characteristics and appearances. In this investigation, the stone dust complies with IS 383 (Bureau of Indian Standards, 2016) Grading Zone II. According to IS 2386 (Part 3) (Bureau of Indian Standards, 2016) the specific gravity of stone dust is 2.5.

Figure 3.8: Stone dust

3.1.7 Distilled water-

Water is a key component of concrete/mortar because it actively participates in the chemical interaction between cement and water. Water's quantity and quality must be carefully managed because it helps to make the cement gel, which gives structures their strength. In general, potable water is thought to be sufficient. Distilled water is employed in this study to prepare various molarity solutions and aid in casting the different geopolymer mortar specimens. Using the pH tutor (EUTECH instruments), 6.88 was found to be the distilled water's pH.

Figure 3.9: Distilled water bottles

3.2 Mix design proportions-

3.2.1 For cubes-

In contrast to cement mortar, geopolymer mortar lacks any established mix design methods. The geopolymer mortar specimens were designed and prepared with various trial mixes. The ratio of (fly-ash, brine sludge), (standard sand, natural sand and stone dust) and solution was kept at 1:3: x (where x = varying ratio of activating solution). The replacement percentages of brine sludge with fly-ash were varied from 30% to 100%.

A brine sludge sample was studied and were replaced with fly-ash. The specimens of different mixture with a variable amount of the brine sludge and fly ash were then casted.

The replacement of brine sludge and fly ash with cement was done by equivalent volume substitution. Equivalent volume substitution was done by considering the Specific gravity of Brine Sludge and the Specific Gravity of Fly-ash. The geopolymer mortar specimens contain Brine Sludge: Fly-ash: Standard Sand, Natural Sand, and Stone Dust: Activating solution in the proportion.

The activating solution for the preparation of geopolymer mortar specimens was prepared by sodium hydroxide pallets, sodium silicate, and distilled water. NaOH was prepared at a concentration of 10 moles. 400 grams of NaOH pellets (molarity × molecular weight) were dissolved in 1 litre of distilled water to create the solution.

Calculations for preparing the solution:-

10M Solution:-

NaOH Molarity = 39.997 g/ml

1M = 40 g

10M = 40 × 10 = 400 g

4 × 10 = 40 g in 100 ml

40 × 10 = 1000 ml

Therefore, 400g = 1 litre

The solution was kept for cooling for 2 to 3 hours. After cooling, a double-weight sodium silicate solution was added to the mixture, which was then allowed to sit for 24 hours before being used to cast specimens.

Figure 3.10: Activating solution (10M)

Mix calculations-

- *By weight ratio (1:3:0.5)*

Brine sludge + fly ash = 1, Standard sand = 3, Activating solution = 0.5

Fly ash = $\frac{1}{4.5}$ × 2000 = 500 kg

Standard sand = $\frac{3}{4.5}$ × 2000 = 1500 kg

Solution = 250 kg

The proportion of brine sludge and fly ash is 0.7 and 0.3 in the mix.

Brine sludge proportion:-

= 0.7 × 500 × $\frac{\text{specific gravity of brine sludge}}{\text{specific gravity of fly ash}} = \frac{2.4}{2.1}$ = 400 g

Fly ash proportion:-

= 0.3 × 500 = 150 g

- *By volumetric ratio (1:3:0.5)*

Brine sludge + fly ash = 1, Standard sand = 3, Activating solution = 0.5

Fly ash = $\frac{1}{4.5}$ × 1m^3 = 0.22 m^3, wt. of fly ash = 2056.1 × 0.22 = 452.342 kg

Standard sand = $\frac{3}{4.5}$ × 1m^3 = 0.667 m^3, wt. of standard sand = 2617 × 0.667 = 1745.53 kg

Activating solution = $\frac{0.5}{4.5}$ × 1m^3 = 0.11 m^3, wt. of activating sol. = 0.11 × 1345 = 149.295 kg

The proportion of brine sludge and fly ash is 0.7 and 0.3 in the mix.

Brine sludge proportion:-

= 0.7 × 452.342 × $\frac{\text{specific gravity of brine sludge (2.4)}}{\text{specific gravity of fly ash (2.1)}}$ = 361.8736 g

Fly ash proportion:-

= 0.3 × 452.342 = 135.7 g

For cube 50 × 50 × 50 mm

wt. of fly ash = $(0.05)^3$ × 452.342 = 0.05654 kg = 56.54 g

wt. of standard sand = $(0.05)^3$ × 1742.53 = 0.2181 kg = 218.1 g

wt. of fly ash = $(0.05)^3$ × 149.295 = 0.01866 kg = 18.66 g

Mix composition-

The various trial mixes of different ratios were performed for selecting the ratio of the mix which gives desired strength to the samples. There is a variation in type of fine aggregate and partial replacement of fly ash in the mix.

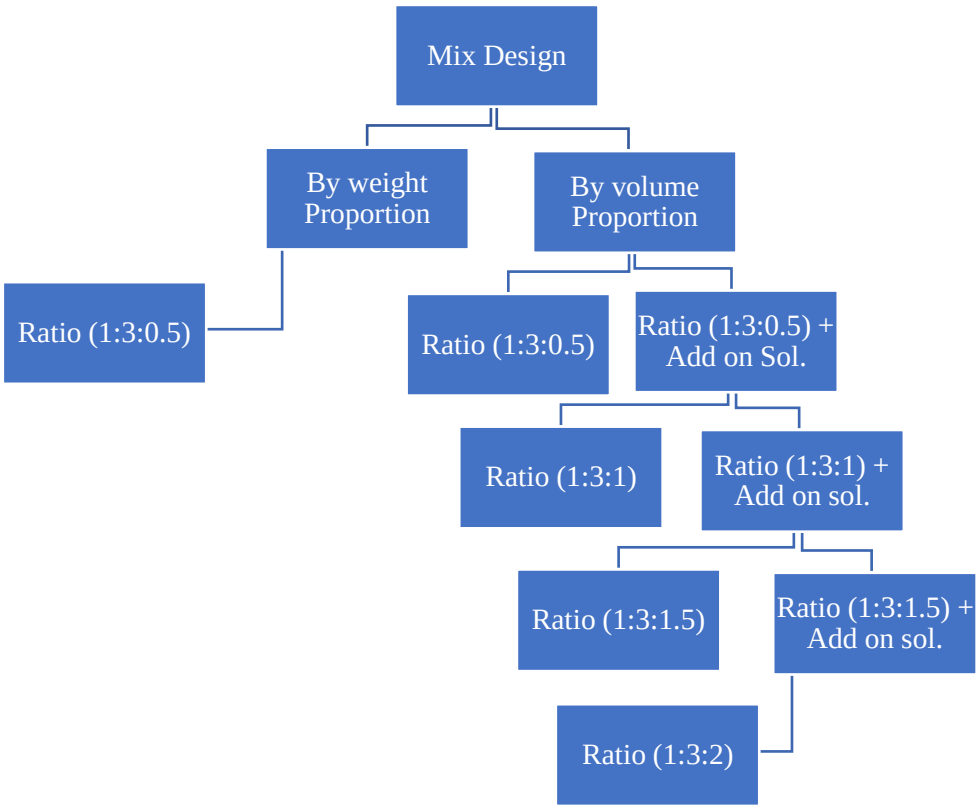

Figure 3.11: Design methodology of mix with different ratios

- Mix – 1

By weight proportion including 10 percent wastage

Ratio = 1:3:0.5 (Brine Sludge and Fly Ash: Standard Sand, Natural Sand, Stone Dust: Solution)

Table 3.2: By weight proportion of brine sludge based geopolymer mortar mix with different fine aggregates

Mixture		Fly Ash	Brine Sludge	Aggregate			Solution		Molarity of NaOH	Solution Content (%)
				Standard Sand	Natural Sand	Stone Dust	NaOH	Na_2SiO_3		
CW1	Ratio	1	0	3	-	-	0.17	0.33	10M	12.5
	Weight (kg)	500	0	1500	-	-	83.33	166.66		
CW2	Ratio	0.3	0.7	3	-	-	0.17	0.33	10M	12.19
	Weight (kg)	150	400	1500	-	-	83.33	166.66		
CW3	Ratio	0.3	0.7	-	3	-	0.17	0.33		

	Weight (kg)	150	400	-	1500	-	83.33	166.66	10M	12.19
CW4	Ratio	0.3	0.7	-	-	3	0.17	0.33	10M	12.4
	Weight (kg)	150	400	-	-	1465	83.33	166.66		

- Mix – 2

By volume proportion including 10 percent wastage.

Ratio = 1:3:0.5 (Brine Sludge and Fly Ash: Standard Sand, Natural Sand, Stone Dust: Solution)

Table 3.3: By volume proportion of brine sludge based geopolymer mortar mix with different fine aggregates

Mixture		Fly Ash	Brine Sludge	Aggregate			Solution		Molarity of NaOH	Solution Content (%)
				Standard Sand	Natural Sand	Stone Dust	NaOH	Na_2SiO_3		
CV1	Ratio	1	0	3	-	-	0.17	0.33	10M	6.1
	Weight (kg)	501.68	0	1919.13	-	-	49.765	99.53		
CV2	Ratio	0.3	0.7	3	-	-	0.17	0.33	10M	6.04
	Weight (kg)	150.50	401.34	1919.13	-	-	49.765	99.53		
CV3	Ratio	0.3	0.7	-	3	-	0.17	0.33	10M	6.04
	Weight (kg)	150.50	401.34	-	1919.13	-	49.765	99.53		
CV4	Ratio	0.3	0.7	-	-	3	0.17	0.33	10M	6.15
	Weight (kg)	150.05	400	-	-	1874.8	49.765	99.53		

- Mix – 3

In this mix, the ratio of the activating solution increased to 1 from 0.5 due to very less % moisture.

By volume proportion including 10 percent wastage.

Ratio = 1:3:0.5 to 1 (Brine Sludge and Fly Ash: Standard Sand, Natural Sand, Stone Dust: Solution)

Table 3.4: By volume proportion of brine sludge based geopolymer mortar mix with different fine aggregates and add on solution

Mixture		Fly Ash	Brine Sludge	Aggregate			Solution			Molarity of NaOH	Solution Content (%)
				Standard Sand	Natural Sand	Stone Dust	NaOH	Na_2SiO_3	Add on sol.		
CV1	Ratio	1	0	3	-	-	0.17	0.33	0.5	10M	13.5
	Weight (kg)	501.68	0	1919.13	-	-	49.765	99.53	179.488		
CV2	Ratio	0.3	0.7	3	-	-	0.17	0.33	0.5	10M	13.3
	Weight (kg)	150.50	401.34	1919.13	-	-	49.765	99.53	179.488		
CV3	Ratio	0.3	0.7	-	3	-	0.17	0.33	0.5	10M	13.3
	Weight (kg)	150.50	401.34	-	1919.13	-	49.765	99.53	179.488		
CV4	Ratio	0.3	0.7	-	-	3	0.17	0.33	0.5	10M	13.5
	Weight (kg)	150.05	400	-	-	1874.84	49.765	99.53	179.488		

- Mix – 4

By volume proportion including 10 % wastage.

Ratio = 1:3:1(Brine Sludge and Fly Ash: Stone Dust: Solution)

Activating solution increased to 1 to 1.58.

Table 3.5: By volume proportion of brine sludge based geopolymer mortar mix with stone dust, with and without add on solution

Mixture		Fly Ash	Brine Sludge	Stone dust	Solution			Molarity of NaOH	Solution Content (%)
					NaOH	Na_2SiO_3	Add on sol.		
CV5	Ratio	0.3	0.7	3	0.33	0.67	-	10 M	13.5
	Weight (kg)	135.6	361.776	1687.14	98.63	197.27	-		
CV6	Ratio	0.3	0.7	3	0.33	0.67	0.58		21.4
	Weight (kg)	135.6	361.776	1687.14	98.63	197.27	171.62		

- Mix – 5

By volume proportion including 10 % wastage.

Ratio = 1:3:1.5 (Brine Sludge and Fly Ash: Stone Dust: Solution)

Activating solution increased to 1.5 to 1.64

Table 3.6: By volume proportion of brine sludge based geopolymer mortar mix with stone dust, with and without add on solution

Mixture		Fly Ash	Brine Sludge	Stone dust	Solution			Molarity of NaOH	Solution Content (%)
					NaOH	Na_2SiO_3	Add on sol.		
CV7	Ratio	0.3	0.7	3	0.5	1	-	10 M	20.3
	Weight (kg)	123.366	328.976	1533.96	134.5	269	-		
CV8	Ratio	0.3	0.7	3	0.5	1	0.14		22.2
	Weight (kg)	123.366	328.976	1533.96	134.5	269	37.656		

- Mix – 6

By volume proportion including 10 % wastage.

Ratio = 1:3:2 (Brine Sludge and Fly Ash: Stone Dust: Solution)

Table 3.7: By volume proportion of brine sludge based geopolymer mortar mix with stone dust with above mentioned ratio

Mixture		Fly Ash	Brine Sludge	Stone dust	Solution			Molarity of NaOH	Solution Content (%)
					NaOH	Na_2SiO_3	Add on sol.		
CV9	Ratio	0.3	0.7	3	0.67	1.33	-	10 M	27.08
	Weight (kg)	113.0853	301.56	1406.13	164.40	328.81	-		

3.2.2 For bricks-

Similarly, geopolymer mortar for making bricks has no standard mix design approaches. The geopolymer mortar specimens were designed and prepared with various trial mixes. The ratio of fly-ash, brine sludge, stone dust and solution was kept at 1:3: x (where x = varying ratio of activating solution). The replacement percentages of brine sludge with fly-ash were varied from 30% to 100%. A brine sludge sample was studied and were replaced with fly-ash. The specimens of different mixture with a variable amount of brine sludge and fly ash were then casted.

The replacement of the brine sludge and fly ash with cement was done by equivalent volume substitution and equivalent weight substitution.

Equivalent volume and weight substitution were done by considering the Specific gravity of Brine Sludge, Fly-ash and Stone dust. The preparation of geopolymer mortar for bricks containing Brine Sludge: Fly-ash: Stone Dust: Activating solution in the proportion.

The activating solution for the preparation of geopolymer mortar specimens was made by Sodium hydroxide pallets, Sodium silicate, and distilled water. 10 and 18 Molarities concentration of NaOH was prepared. 400 and 720 grams (Molarity × molecular weight) were dissolved in the 1 litre of distilled water to create the solution.

Calculations for preparing the solution:-

10M Solution:-

NaOH Molarity = 39.997 g/ml

1M = 40 g

10M = 40 × 10 = 400 g

4 × 10 = 40 g in 100 ml

40 × 10 = 1000 ml

Therefore, 400g = 1 litre

18M Solution:

NaOH Molarity = 39.997 g/ml

1M = 40 g

18M = 40 × 18 = 720 g

4 x18 = 72 g in 100 ml

72 x 10 = 1000 ml

Therefore, 720 g = 1 litre

NaOH pellets were dissolved in distilled water and make upto a total of 1- litre solution. The solution was kept for cooling for 2 to 3 hours. After cooling, the sodium silicate solution of double weight was added to solution and was kept for 24 hours and was then used in casting of specimens.

Figure 3.12: Activating solution (10M and 18M)

Mix calculations-

- *By volumetric ratio (1:3:1)*

Brine sludge + fly ash = 1, Standard sand = 3, Activating solution = 1

(Without wastage considered)

Fly ash = $\frac{1}{5}$ × 1m^3 = 0.2 m^3, wt. of fly ash = 2056.1 × 0.2 = 411.22 kg

Standard sand = $\frac{3}{5}$ × 1m^3 = 0.6 m^3, wt. of standard sand = 2617 × 0.6 = 1170.2 kg

Activating solution = $\frac{1}{5}$ × 1m^3 = 0.2 m^3, wt. of activating sol. = 0.2 × 1345 = 269 kg

The proportion of brine sludge and fly ash is 0.7 and 0.3 in the mix.

Brine sludge proportion:-

$$= 0.7 \times 1.418 \times \frac{\text{specific gravity of brine sludge (2.4)}}{\text{specific gravity of fly ash (2.1)}} = 1.1344 \text{ kg}$$

Fly ash proportion:-

$$= 0.3 \times 1.418 = 0.344 \text{ kg}$$

Stone dust proportion:-

$$= 4.037 \times \frac{\text{specific gravity of stone dust (2.54)}}{\text{specific gravity of standard sand (2.6)}} = 1.1344 \text{ kg}$$

For brick 230 × 100 × 75 mm

wt. of fly ash = $(3.45 \times 10^{-3}) \times 411.22 = 1.418$ kg

wt. of stone sand = $(3.45 \times 10^{-3}) \times 1170.2 = 4.037$ kg

wt. of fly ash = $(3.45 \times 10^{-3}) \times 269 = 0.928$ kg

Mix composition-

The various trial mixes of different ratios were performed for selecting the ratio of the mix which gives desired strength to the samples. The brick specimens were casted at ambient curing and oven drying at 70° C for 24 hours after thin film plastic wrapping of the bricks.

- Mix – 1 (By volume proportion)

Ratio = (1:3:1) (Brine Sludge and Fly Ash: Stone Dust: Solution)

Table 3.8: By volume proportion of geopolymer mortar mix for 10M and 18M bricks with oven drying

Mixture	Curing	Fly Ash (g)	Brine Sludge (g)	Stone dust (g)	Solution		Molarity	Solution Content (%)
					NaOH (g)	Na_2SiO_3 (g)		
Ratio		0.3	0.7	3	0.33	0.67		

B1	Oven drying at 70° C	234	624	2975	170	340	10M	13.3
B2	Oven drying at 70° C	234	624	2975	170	340	18M	13.3

- Mix – 2 (By volume proportion)

Ratio = (1:3:1) (Brine Sludge and Fly Ash: Stone Dust: Solution)

Table 3.9: By volume proportion of geopolymer mortar mix for 10M bricks with ambient curing

Mixture	Curing	Fly Ash (g)	Brine Sludge (g)	Stone dust (g)	Solution		Molarity	Solution Content (%)
					NaOH (g)	Na_2SiO_3 (g)		
Ratio		0.3	0.7	3	0.33	0.67		
B3	Ambient Curing	234	624	2975	170	340	10M	13.3

- Mix – 3 (By weight proportion)

Ratio = (1:2:0.67) (Brine Sludge and Fly Ash: Stone Dust: Solution)

Table 3.10: By weight proportion of geopolymer mortar mix for 10M bricks with ambient curing

Mixture	Curing	Fly Ash (g)	Brine Sludge (g)	Stone dust (g)	Solution		Molarity	Solution Content (%)
					NaOH (g)	Na_2SiO_3 (g)		
Ratio		0.3	0.7	2	0.225	0.45		
B4	Ambient Curing	310	723	2067	280	420	10M	22.58

- Mix – 4 (By weight proportion)

Ratio = (1:2:0.67) (Brine Sludge and Fly Ash: Stone Dust: Solution)

Table 3.11: By weight proportion of geopolymer mortar mix for 10M bricks with ambient curing

Mixture	Curing	Fly Ash (g)	Brine Sludge (g)	Stone dust (g)	Solution		Molarity	Solution Content (%)
					NaOH (g)	Na_2SiO_3 (g)		
Ratio		0.3	0.7	2	0.225	0.45		
B5	Ambient Curing	310	723	2067	233	467	10M	22.58

- Mix – 5 (By weight proportion)

Ratio = (1:2:0.67) (Brine Sludge and Fly Ash: Stone Dust: Solution)

Table 3.12: By weight proportion of geopolymer mortar mix for 10M bricks with ambient curing

Mixture	Curing	Fly Ash (g)	Brine Sludge (g)	Stone dust (g)	Solution		Molarity	Solution Content (%)
					NaOH (g)	Na_2SiO_3 (g)		
Ratio		0.3	0.7	2	0.225	0.45		
B6	Ambient Curing	310	723	2067	200	500	10M	22.58

- Mix – 6 (By weight proportion)

Ratio = (1:2:0.67) for B7 and B8 (Brine Sludge and Fly Ash: Stone Dust: Solution)

Ratio = (1:2:0.38) for B9 (Brine Sludge and Fly Ash: Stone Dust: Solution)

Table 3.13: By weight proportion of geopolymer mortar mix for 10M and 18M bricks with oven drying

Mixture	Curing	Fly Ash (g)	Brine Sludge (g)	Stone dust (g)	Solution		Molarity	Solution Content (%)
					NaOH (g)	Na_2SiO_3 (g)		

Ratio		0.3	0.7	2	0.225	0.45		
B7	Oven drying at 70° C	310	723	2067	233	467	10M	22.58
B8		310	723	2067	233	467	18M	22.58
Ratio	Oven drying at 70°C	0.3	0.7	2	0.127	0.254	10M	12.89
B9		310	723	2067	133	266.67		

3.3 Specimen preparation-

3.3.1 Brine sludge based mortar specimens (cement free)-

There is no use of any kind of cement to prepare the samples. The brine sludge-based mortar specimens were prepared using the mix proportion in section 3.2.1.The brine sludge based mortar specimens were casted to investigate the different mechanical properties. The cubical specimens of 50 mm × 50 mm × 50 mm casted for determining the compressive strength at 3 and 7 days. Different concentrations of activating solutions were considered in the research work.

To determine the compressive strength, mortar cubes were casted according to ASTM C109. For each set of a mixture, three or six specimens were casted. A total of three or six samples has been tested for compressive strength after oven drying for 24 hours at 70 degree Celsius.

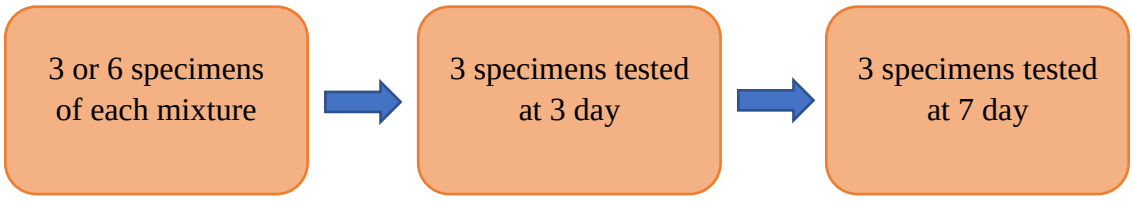

Figure 3.13: Compressive strength assessment chart of geopolymer mortar cubical specimens

An extra 10% of the material was considered for the preparation of cubical specimens so to avoid any complications in casting.

The procedure of preparation of cubical specimens was as follows:-

1. The raw materials were kept at room temperature. All the materials were weighed with great accuracy and precision according to the requirement of mix design. The three grades

of standard sand, natural sand, stone dust, brine sludge, fly ash, sodium hydroxide (NaOH), sodium silicate (Na_2SiO_3) and distilled water were the key ingredients of the cubical mortar specimens.

2. The cubical moulds were cleaned properly It was ensured that no lumps or traces of other mortar or any other material were stick on the mould. It was made ensure that the interior faces are smooth and clean.

Figure 3.14: Cubical moulds

3. A thin film of the oil was provided on the interior faces of the mould. After this, the screws were tightened in order to get the perfect dimensions of the cube moulds. And it was also ensured that no leakage of mortar paste occur.
4. Each set of mortar mix was mixed with hand mixing in the head pan. The first and foremost, the raw materials were added after weighing and the mixing was done in a dry state. After dry mixing, the solution was then added, and the hand mixing was done for 2-3 minutes.

Figure 3.15: Dry mix in head pan

5. Then the hand mixing was stopped, and adhered mortar along the walls of the head pan was removed with the help of trowel and then was collected at the bottom of the head pan and was placed in the middle and mix it well again.

Figure 3.16: Wet mix in head pan

6. After mixing, the process of casting was started. The cubical moulds were filled. The excess of the mortar was removed from the mould after filling. The vibration of the mould was done on a compaction machine for 1-2 minutes.

Figure 3.17: Casting of the cubical moulds

7. After the vibration, the mould were covered with a thin plastic film to avoid the solution to get evaporate and then kept for oven drying for a period of 24 hours at a temperature of 70 degree Celsius.

Figure 3.18: Mould wrapped with a thin film of plastic polythene

8. At last, the cubical samples were demoulded after 24 hours.

Figure 3.19: Demoulding of cubes

3.3.2 Brine sludge based geopolymer bricks-

The brine sludge mortar based mortar specimens were prepared using the mix proportion in section 3.2.2. The brine sludge based mortar bricks were casted to investigate the different mechanical properties. The bricks of 230 mm × 100 mm × 75 mm to determine the compressive strength at 7 days and 28 days. Different concentrations of activating solutions were considered in the research work.

To determine the compressive strength, the bricks were casted according to the trial mixes. For each set of a mixture, three or six specimens were casted. A total of three or six samples has been tested for compressive strength after oven drying for 24 hours at 70 degree Celsius.

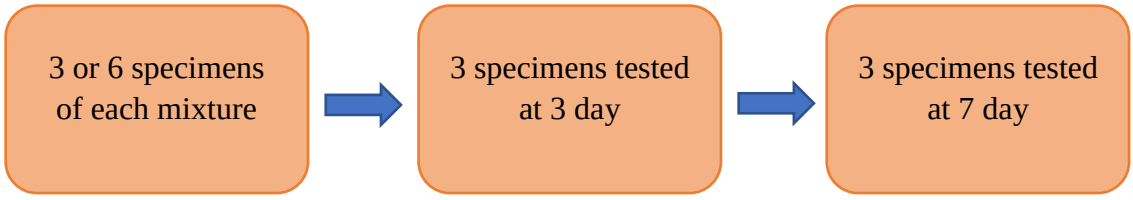

Figure 3.20: Compressive strength assessment chart of geopolymer bricks

An extra 10% of the material was considered for the preparation of bricks so to avoid any complications in casting.

The procedure of preparation of brick specimens was as follows:-

1. The raw materials were kept at room temperature. All the materials were weighed with great accuracy and precision according to the requirement of mix design. Brine sludge, fly ash, stone dust, sodium hydroxide (NaOH), sodium silicate (Na_2SiO_3) and distilled water were the key ingredients for the preparation of mortar for making bricks.
2. The brick casting machine was cleaned properly It was ensured that no lumps or traces of other mortar or any other material were stick inside the mould of the machine.
   It was made ensure that the interior faces are smooth and clean.

Figure 3.21: Brick casting machine

3. A thin film of the oil was provided on the interior faces of the mould of the machine after cleaning.
4. Each set of mortar mix was mixed with hand mixing in the head pan. The first and foremost, the raw materials were added after weighing according to the mix and the mixing was done in a dry state. After dry mixing, the solution was then added of calculated amount, and the hand mixing was done for 2-3 minutes.

Figure 3.22: Dry mix in head pan

5. Then the hand mixing was stopped, and adhered mortar along the walls of the head pan was removed with the help of trowel and then was collected at the bottom of the head pan and was placed in the middle and mix it well again.

Figure 3.23: Wet mix in head pan

6. After mixing, the process of casting was started. The mould of the brick casting machine was filled with the help of trowel. After pouring the entire mortar in the mould. The compaction was done by pressing the handle of casting machine until it gets to touch its extreme end.

Figure 3.24: Brick casting machine mould

7. After compaction, the cover of the mould opened up and then pressing the handle of the machine after unlocking.

Figure 3.25: Demoulding of brick

8. The brick was carried out and covered with a thin plastic film to avoid the activated solution to get evaporate and then kept for oven drying for a time period of 24 hours at a temperature of 70 degree Celsius.

Figure 3.26: Bricks wrapped with a thin film of plastic polythene (10M)

Figure 3.27: Bricks wrapped with a thin film of plastic polythene (18M)

9. At last, the plastic film was removed from the bricks. Finally, the geopolymer bricks were fabricated and ready for testing.

Figure 3.28: Casted bricks (10M)

Figure 3.29: Casted bricks (18M)

3.4 Tests conducted-

3.4.1 Determination of compressive strength-

3.4.1.1 For Cubical specimens-

The Compressive strength was determined for the mortar cubical specimens. The compressive strength of brine sludge-based geopolymer mortar specimens were demonstrated as per ASTM C109. Cubical samples of size 50mm × 50mm × 50mm were tested. The compressive strength of cement-based geopolymer mortar specimens tested for 7, 14 and 56 days.

Here in this study, the compressive strength of geopolymer based mortar specimens were tested for 7 and 14 days. Test was conducted in ACTM (Automatic Compression Testing Machine), which had total capacity of 5000 kN. At the time of testing of the specimens, the loading rate was 0.1 kN/sec.

Figure 3.30: Compression testing machine

The side face of the cubical sample was put in an upward direction under direct load from CTM. The reason for keeping the side face at the top is because the surface is smooth because at time of casting it was touched by the face of the moulds. And the top face of the specimen was kept at the front face. The following fig.3.30 shows the apparatus of the Compressive Testing Machine.

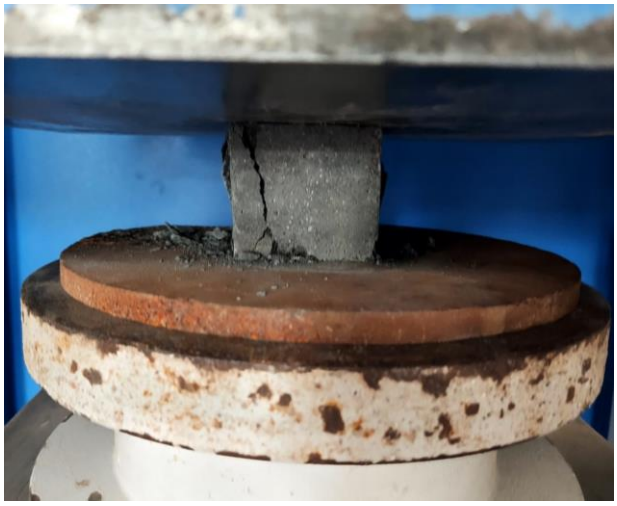

Figure 3.31: CTM for compressive strength test

The compressive strength of the specimens was calculated by the formula below:-

Compressive Strength (MPa) = Load in (N)/Area in (mm^2)

$$= \frac{P \times 1000}{50 \times 50} \text{ MPa}$$

P = Load at breakage in CTM

3.4.1.2 For Bricks-

Compressive strength was determined for the brick specimens. The compressive strength of brine sludge-based geopolymer brick specimens were demonstrated as per IS 3495 (Part 1) (Bureau of Indian Standards, 2002). Brick samples of size 230mm × 100mm × 75mm were tested. Here in this study, the compressive strength of geopolymer based brick specimens were tested for 7, 14 and 28 days.

Test was conducted in ACTM (Automatic Compression Testing Machine), which had total capacity of 5000 kN. At the time of testing of the specimens, the loading rate was 0.1 kN/sec.

The specimen is places with flat faces horizontal, and the mortar filled face i.e., frog, facing upwards between two metallic plates each of 5 mm thickness to ensure a uniform surface for application of axial load and carefully centred between plates of the testing machine.

Apply load axially at a uniform rate of 14 N/mm^2 (140 kgf/cm^2) per minute till failure occurs and note the maximum load at failure. The load at failure shall be the maximum load at which

the specimen fails to produce any further increase in the indicator reading on the testing machine.

The compressive strength was calculated by the formula below:-

Compressive Strength (MPa) = Maximum Load at failure in (N) /Area of the face in (mm^2)

$$= \frac{P \times 1000}{230 \times 100} \text{ MPa}$$

P = Load at breakage in CTM

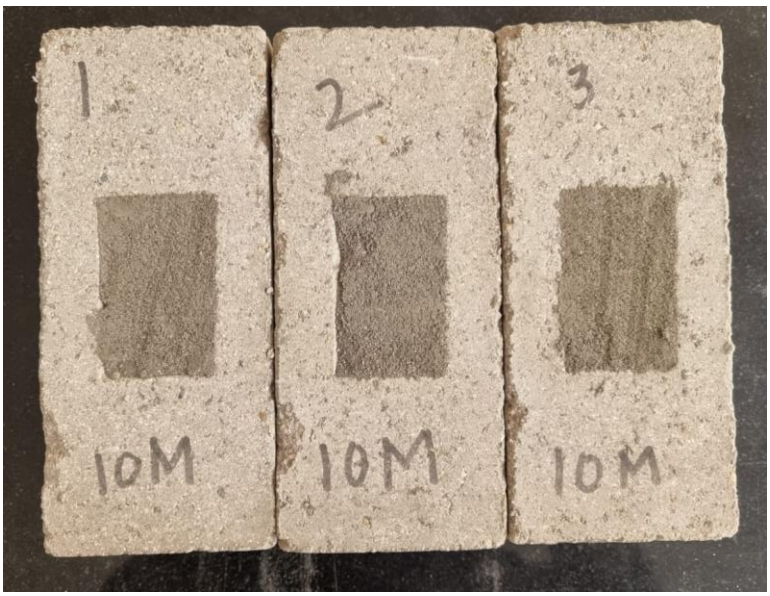

Figure 3.32: Bricks (10M) for compressive strength test

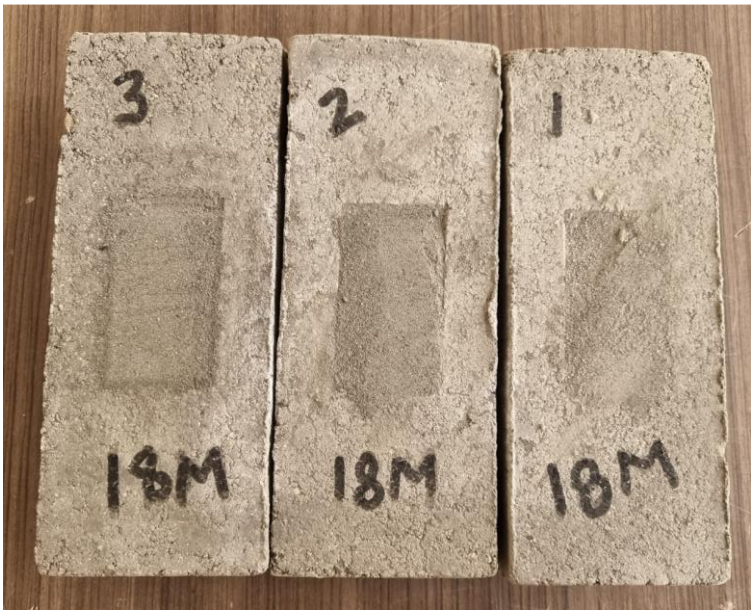

Figure 3.33: Bricks (18M) for compressive strength test

S1, S2, S3 of molarity 10M and 18M are the brick specimens which are used to determine the compressive strength after 28 days. Fig. 3.34 shows the brick placed in the CTM with the help of the spacer and metallic plates to ensure uniform loading.

Figure 3.34: Brick placed in CTM

The following fig 3.35 shows the failure of the bricks after applying the load with pace of 5.0.

Figure 3.35: Failure of the brick in CTM

3.4.2 Determination of wet compressive strength (for bricks)-

When tested in accordance with the procedures outlined in IS 12894 (Bureau of Indian Standards, 2011), the pulverized fuel ash-lime bricks' minimum average wet compressive strength must not be less than the value provided for each class.

The wet compressive strength of any individual brick shall not fall below the minimum average wet compressive strength specified for the corresponding class of bricks by more than 20 percent.

Table 3.14: Class Designation of the Pulverized Fuel Ash-Lime Bricks

Sr. No.	Class Designation	Average Wet Compressive Strength not Less Than (N/mm^2)
1.	30	30
2.	25	25
3.	20	20
4.	17.5	17.5
5.	15	15
6.	12.5	12.5
7.	10	10
8.	7.5	7.5
9.	5	5.0
10.	3.5	3.5

S10, S11, S12 of 18M and S11, S12, S13 of 10M are the brick specimens which are used for determining the wet compressive strength after 28 days. For 24 hours, the bricks were submerged in water.

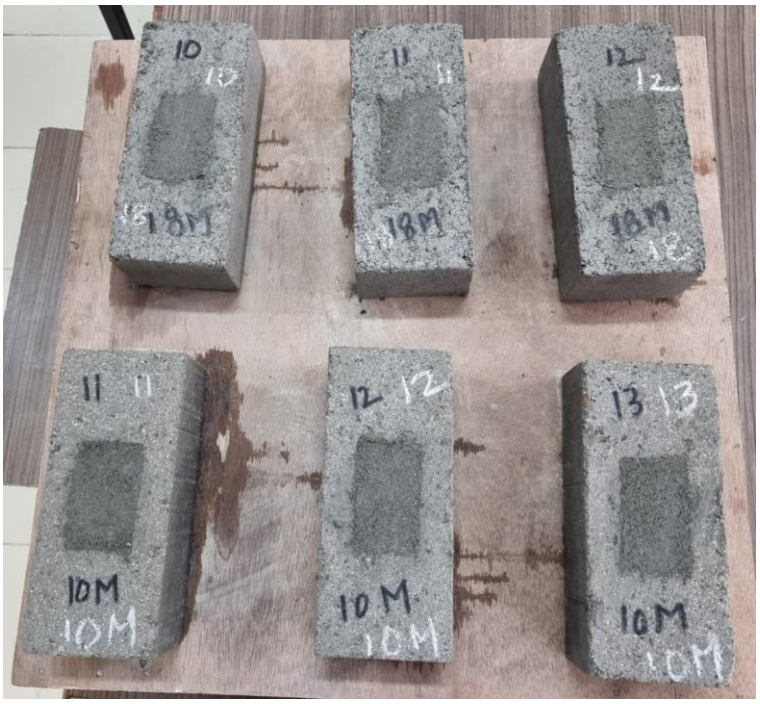

Figure 3.36: Bricks for wet compressive strength test

Fig 3.37 shows the brick placed in the CTM with the help of the spacer and metallic plates to ensure uniform loading.

Figure 3.37: Brick placed in CTM

3.4.3 Determination of water absorption (for bricks)-

The bricks were evaluated using the steps outlined in IS 3495 (Part 2) (Bureau of Indian Standards, 2002). Weigh the dry weight of the block (W1) before submerging. With the aid of the bucket, submerge the dried specimen for 24 hours at a temperature of 27 + 2° C in clean water. Remove the sample from the bucket after 24 hours, wipe out any remaining water using a moist cloth, and weigh the sample. Finishing the weighing 3 minutes after the specimen has been removed from water (W2).

The specimen must average a maximum water absorption of 15% by mass for classes higher than 12.5, and no more than 20% by mass overall.

The following formula can be used to calculate the mass of water that has been absorbed after 24 hours of immersion in cold water:

$$= \frac{W2 - W1}{W1} \times 100$$

Therefore,

W1 = Initial weight

W2 = Final weight after immersion

Brick specimens S4, S5, and S6 of molarities 10M and 18M are utilised to calculate the water absorption after 28 days. The dry weight of the brick samples is displayed in the following table.

For 10M Geopolymer bricks:-

Table 3.15: Initial weight of the 10M bricks

Sr.no.	Sample no.	Initial Weight (W1) (kg)
1.	S4	3.286
2.	S5	3.294
3.	S6	3.266

Figure 3.38: Bricks immersed in water (10M) for 24 hours

For 18M Geopolymer bricks:-

Table 3.16: Initial weight of the 18M bricks

Sr.no.	Sample no.	Initial Weight (W1) (kg)
1.	S4	3.598
2.	S5	3.600
3.	S6	3.544

Figure 3.39: Bricks immersed in water (18M) for 24 hours

3.4.4 Determination of efflorescence (for bricks)-

The bricks were tested in accordance with the guidelines given in IS 3495 (Part 3) (Bureau of Indian Standards, 2002). The specimen must only have 'slight' efflorescence for classes greater than 12.5 and 'moderate' efflorescence at most.

According to the following table, the liability for efflorescence must be stated as "nil," "slight," "moderate," "heavy," or "serious":-

Table 3.17: Liability for the efflorescence

S.no.	Efflorescence of Description	Percentage of White Patches covered on bricks (Extent of Deposits)
1.	Nil	There is no detectable efflorescence deposit.
2.	Slight	A thin layer of salt covers no more than 10% of the brick's exposed surface.
3.	Moderate	A heavier deposit than under "slight" and covering up to 50% of the brick surface's exposed area
4.	Heavy	Heavy salt build up has at least partially covered the visible brick surface.
5.	Serious	Salts are heavily deposited, and the exposed surfaces begin to flake and powder.

Put the bricks' (standing in pan) ends in the dish with a 25 mm depth of distilled water submerged in them. Place the entire setup in a warm (for instance, 20 to 30°C) well-ventilated room for however long it takes for the specimens to thoroughly absorb all the water in the dish and the extra water to evaporate. Place an equal amount of water in the dish and let it evaporate as previously, once the water has been absorbed and the bricks appear to be dry. After the second evaporation, checked the bricks for efflorescence and obtain the findings.

Figure 3.40: 10M bricks placed in the pan

For 10M Geopolymer bricks:-

The brick specimens S7, S8, and S9 of molarity 10M were used to calculate the efflorescence after 28 days. The following fig 3.40 showed the whole arrangement of the brick specimens for determining the efflorescence. This is the first trial.

Figure 3.41: Bricks submerged in distilled water (25mm)

Figure 3.42: Bricks submerged in distilled water after 2 hours

Figure 3.43: Bricks completed absorbed the distilled water after 1 day

Now, repeat the procedure again after the bricks fully absorbed the water for determining the efflorescence.

Figure 3.44: Bricks submerged in distilled water (25mm)

For 18M Geopolymer bricks:-

The brick specimens S7, S8, and S9 of molarity 18M are used to determine the efflorescence after 28 days. The following fig 3.44 shows the whole arrangement of the brick specimens for determining the efflorescence.

Figure 3.45: Bricks placed in the pan

Figure 3.46: Bricks submerged in distilled water (25mm)

Figure 3.47: Bricks submerged in distilled water after 2 days

3.4.5 X-Ray diffraction (XRD)-

In materials research, X-ray diffraction analysis (XRD) is the method used to ascertain the substance's crystallographic structure. A material must be exposed to incident X-rays in order to use XRD to determine the intensity and scattering angles of the X-rays that are released from it.

Figure 3.48: XRD apparatus

X-rays are electromagnetic radiation waves, while crystals are regular collections of atoms. Since their electrons interact with the incident X-rays, crystal atoms typically deflect these rays. The electron is the scatterer in this phenomenon known as elastic scattering. A regular array of scatterers generates a predictable pattern of spherical waves. According to Bragg's law, these waves add constructively in a small number of very specific directions but interfere destructively in the majority of directions, cancelling each other out.

$$2d\sin\theta = n\lambda$$

The distance between diffracting planes, n, and the beam wavelength are all integers. Additionally, D is the separation between diffracting planes. Reflections, which appear as spots on the diffraction pattern, stand in for the precise directions. X-ray diffraction patterns are created when electromagnetic waves collide with a predictable arrangement of scatterers.

Because of how frequently their wavelength and the separation between crystal planes, d, are of the same order of magnitude, X-rays are used to create the diffraction pattern.

3.4.6 Fourier transform infrared spectroscopy (FTIR)-

Transforming Fourier FTIR analysis and FTIR spectroscopy are other names for infrared spectroscopy, which is used to distinguish between organic, polymeric, and occasionally inorganic materials. Using infrared light, the FTIR analysis method scans test materials and looks at chemical properties.

Identification of materials based on their diffraction pattern is one of the main applications of XRD analysis. In addition to phase identification, XRD reveals how internal stresses and defects cause structures to deviate from ideal ones.

Figure 3.49: FTIR Scanning Microscope

The absorbed bands seen in the spectrum are degenerative and only marginally distinct. Other chemical and matrix elements (as well as the way the incident energy is delivered) might cause the specific "peak" of energy at a specific wavenumber to wander about.

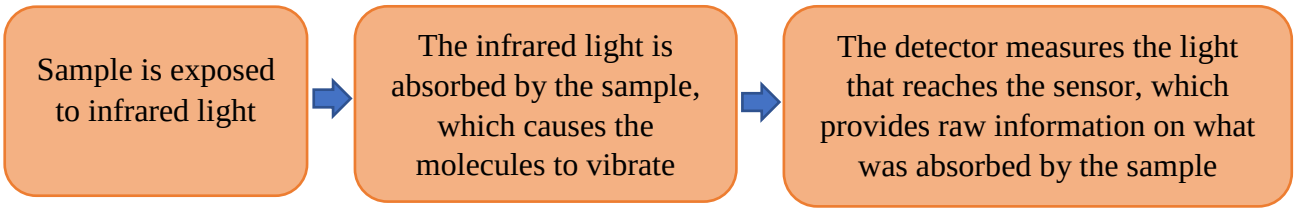

Figure 3.50: FTIR assessment chart of material

Procedure:-

The procedure for the FT-IR Analysis are as follows:-

1. The source: An aperture controls the energy output as an IR energy beam is emitted from the luminous black-body source.
2. The interferometer: The IR beam enters the interferometer, where "Spectral encoding" takes place, as was previously mentioned. The interferometer precisely calibrates the wavelengths using a reference laser.
3. The sample: After entering the sample compartment, the IR beam strikes the sample and either bounces off its surface or passes through it. The sample absorbs specific energy frequencies that are uniquely recognizable as the sample.
4. The detector: The beam is ultimately measured after going through the detector.
5. The computer: After the FFT computation and digitalization of the signal, the user is presented with the completed infrared spectrum.

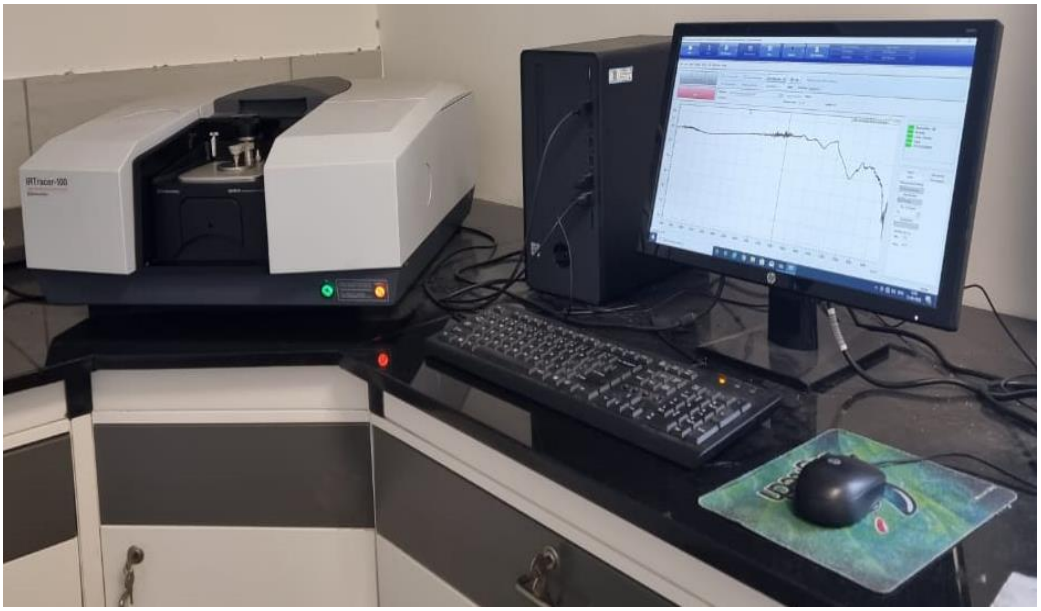

Figure 3.51: FTIR apparatus

The results are obtained as transmittance versus wavenumber (cm^{-1}). The shape, position, and intensity of peaks are utilized for interpretation. The functional groups of material dictate the pattern of the absorption bands. The results can be presented either in absorbance or transmission (on Y- axis) depending on sample preparation.

3.4.7 Raman spectroscopy-

Raman spectroscopy is a non-destructive technique for chemical analysis that provides comprehensive information on molecular interactions, phase and polymorphy, crystallinity, and chemical structure. It is based on how light interacts with a substance's chemical bonds.

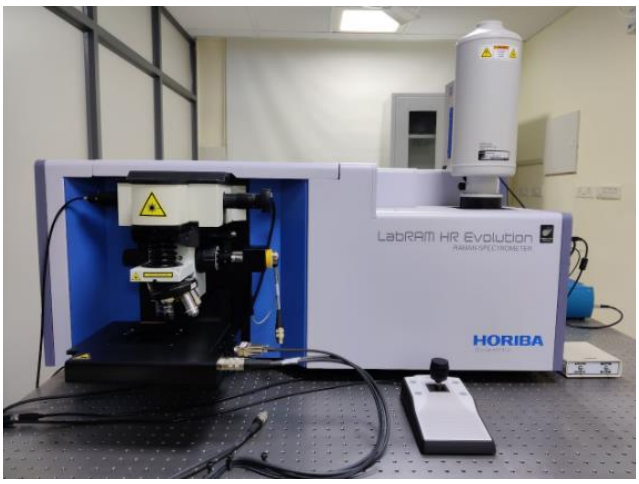

Figure 3.52: Raman spectroscopy machine

A molecule scatters incident light from a potent laser light source using the Raman method of light scattering. When the majority of the scattered light has the same wavelength (or colour) as the laser source and provides no useful information, this situation is referred to as Rayleigh scatter. The tiny amount of light (typically 0.0000001%) that is scattered at different wavelengths (or colours), depending on the chemical makeup of the analyte, is known as Raman scatter.

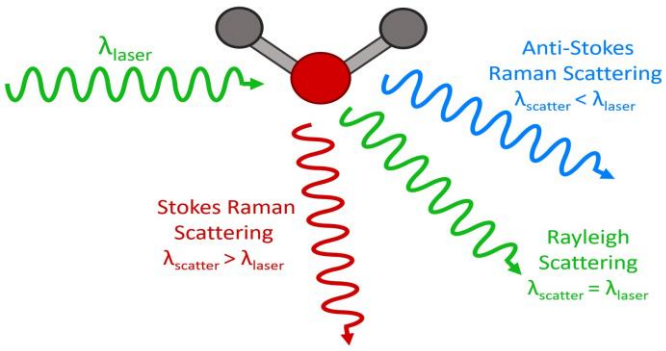

Figure 3.53: Principle of Raman spectroscopy

A Raman spectrum has a number of peaks that show the strength and location of the wavelength of the Raman scattered light. Each peak corresponds to a specific molecular bond vibration, such as the breathing mode of the benzene ring, polymer chain vibrations, lattice modes, etc., as well as single bonds like C-C, C=C, N-O, and C-H.

4. RESULTS AND DISCUSSIONS

A thorough investigation of the experimental program was conducted in this work, replacing cement with brine sludge along with fly ash, stone dust, natural sand, and standard sand, and activating solutions of various molarities. In this study, different concentrations of the activating solution is taken into account for the preparation of the cubical specimens both in weight and volume based mixes. For brick casting, different concentrations of the activating solution are taken into account as well. This chapter discussed the obtained results of the mechanical and durability properties such as compressive strength, wet compressive strength, water absorption and efflorescence. The characterization of materials and brick samples are investigated through the non- destructive techniques such as XRD, FTIR and Raman spectroscopy.

4.1 Compressive Strength of brine sludge based mortar cubical specimens-

Following sample preparation, samples were placed in an oven set at 70° C for 24 hours before being subjected to CTM testing. The curing ages of the brine sludge-based mortar cubical specimens are examined at 3 and 7 days. For each mix, a total of three specimens were cast, and the average of the three was used to determine the sample's compressive strength.

The Compressive Strength of a brine sludge-based mortar cubical specimen at 3 and 7 days is shown in Table 4.1.

- Mix – 1

Table 4.1: Compressive Strength of brine sludge based geopolymer mortar with different fine aggregates by weight proportion

Mixtures	No. of specimens	3 days (MPa)	7 days (MPa)
CW1	1	2.72	3.52
	2	2.64	2.8
	3	2.64	2.86
CW2	1	2.64	3.68
	2	2.72	3.8
	3	2.64	4.24
CW3	1	2.88	3.1
	2	2.8	3.2
	3	2.88	3.2
CW4	1	3.2	2.88
	2	2.88	2.8
	3	2.88	2.96

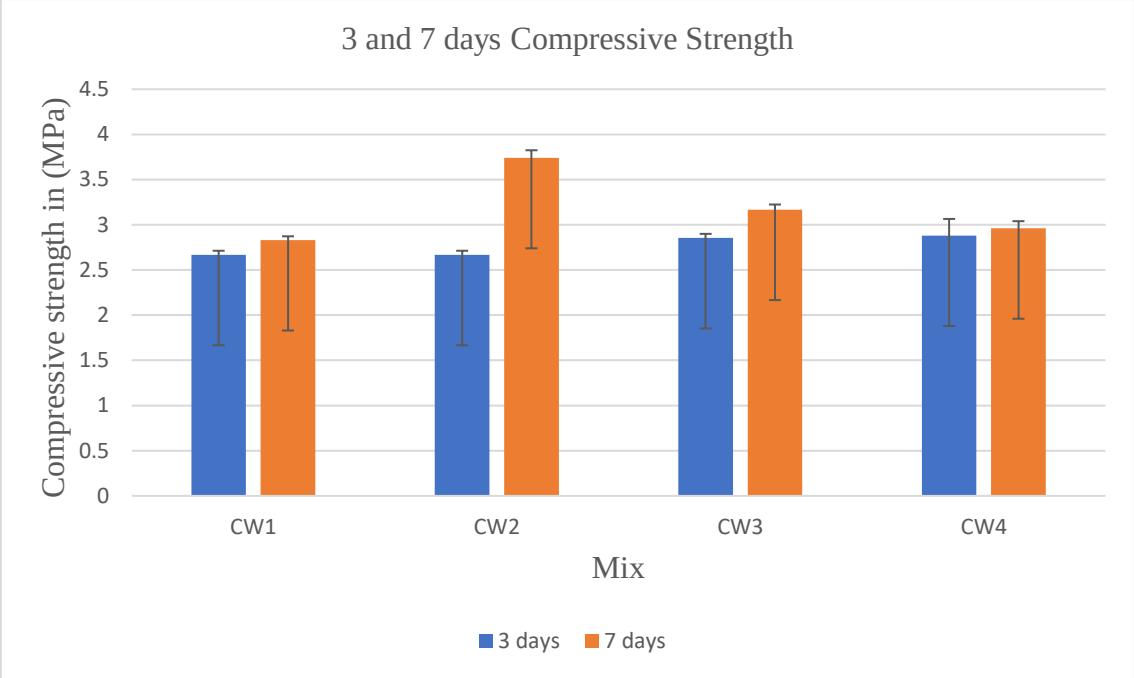

Figure 4.1: Average Compressive strength of mix - 1 at 3 and 7days

The average compressive strength of the weight based design mixes are shown in Fig 4.1 and their strength values were approximately equal.

- Mix - 2

There is no result for mix – 2 due to low percentage solution. As the cubical specimens were broken inside the moulds while demoulding.

- Mix - 3

Table 4.2: Compressive Strength of brine sludge based geopolymer mortar with different fine aggregates by volume proportion

Mixtures	No. of specimens	3 days (MPa)	7 days (MPa)
CV1	1	7.04	7.74
	2	6.24	7
	3	7.04	7
CV2	1	3.68	3.52
	2	3.4	3.62
	3	7.04	6.96
CV3	1	7.04	6.9
	2	3.44	3.52
	3	3.68	3.7
CV4	1	2.96	3.2
	2	3.44	3.5
	3	3.42	3.5

Because of the low % solution, in mix -3 there was increase in the % moisture as to obtain the compressive strength.

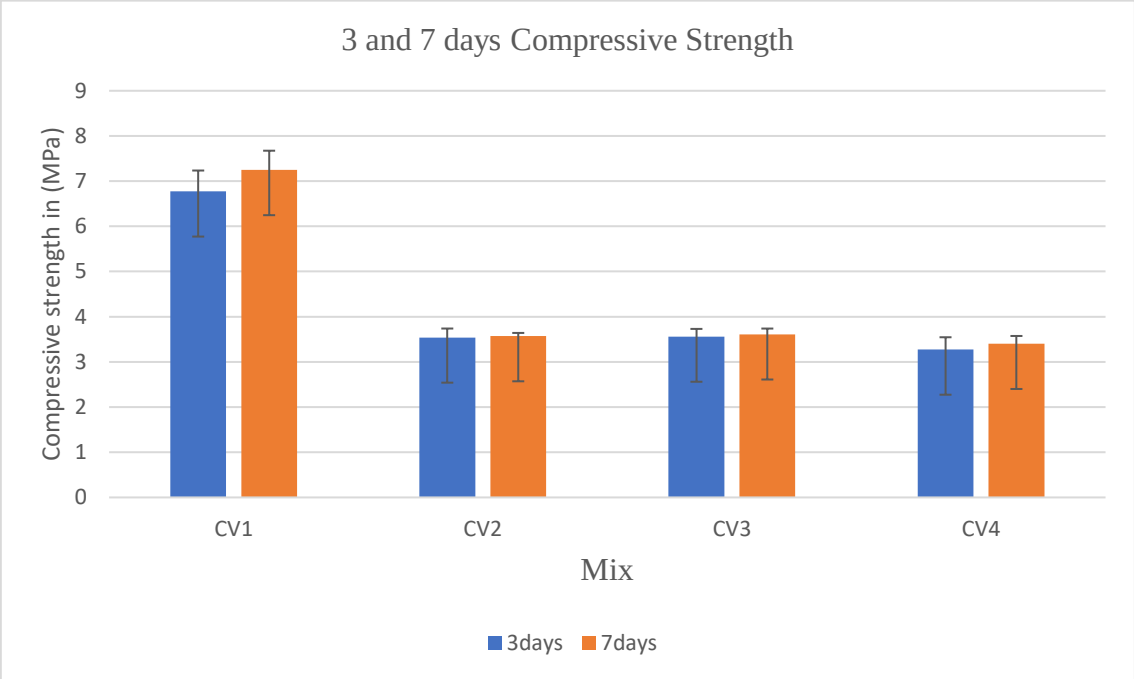

Figure 4.2: Average compressive strength of different mix - 3 at 3 and 7days

From Fig 4.2, there was sudden increase in the compressive strength of the fly ash mixture due to increase in the activating solution. But, the average compressive strength of the other mixtures remain constant.

- Mix – 4

Table 4.3: Compressive Strength of brine sludge based geopolymer mortar

Mixture	Molarity of NaOH	No. of specimens	7 days (MPa)
CV5	10M	1	8.2
		2	7
		3	7.4
CV6	10M	1	5.4
		2	6.28
		3	6.4

- Mix – 5

Mixtures	Molarity of NaOH	No. of specimens	3 days (MPa)	7 days (MPa)
CV7	10M	1	4.24	5.6
		2	4.16	5.6
		3	4.24	5.8
CV8	10M	1	-	4
		2	-	4.4
		3	-	4

- Mix – 6

Table 4.4: Compressive Strength of brine sludge based geopolymer mortar

Mixture	Molarity of NaOH	No. of specimens	7 days (MPa)
CV9	10M	1	5.2
		2	5.2
		3	5.6

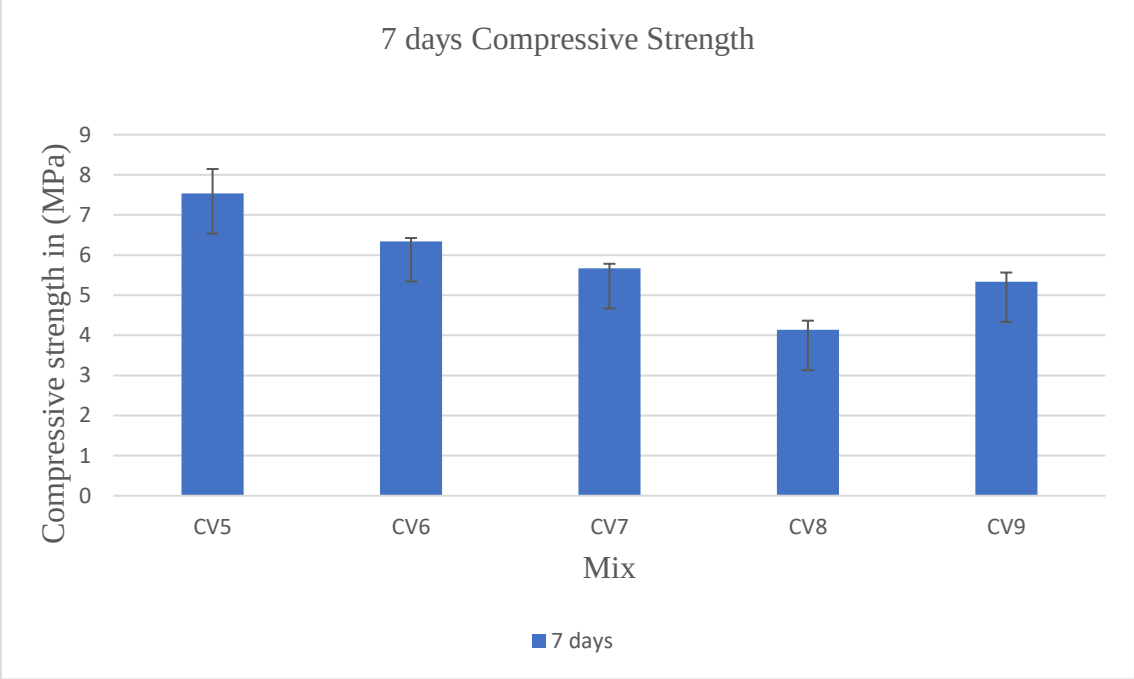

Figure 4.3: Average compressive strength of different mixes at 7days

(CV5 vs CV6 vs CV7 vs CV8 vs CV9)

The average compressive strength of the volume based design mixes were shown in the above graph. CV5 mix showed the highest compressive strength as compare to all the other design mix.

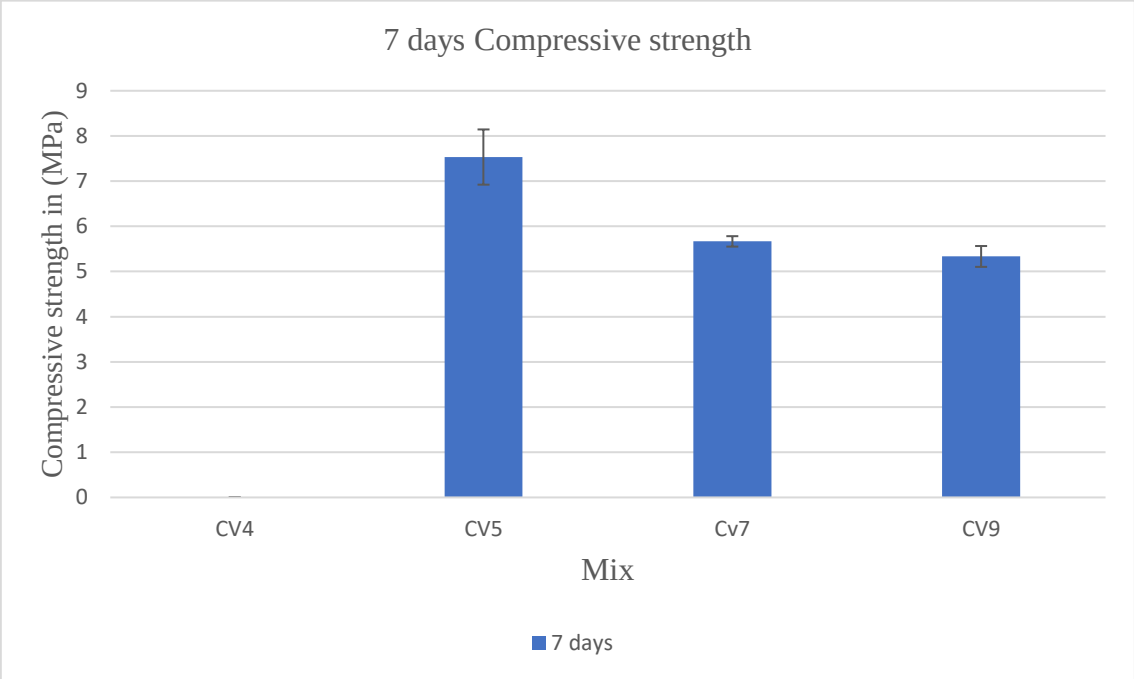

Figure 4.4: Average compressive strength of different mixes at 7days

(CV4 vs CV5 vs CV7 vs CV9)

The average compressive strength of the volume based design mixes were shown in Fig 4.4. CV4 showing zero strength due to the low % solution. CV5 mix showed the highest compressive strength as compare to all the other design mix.

4.2 Compressive Strength of brine sludge based mortar bricks-

Following sample preparation, samples were placed in an oven set at 70° C for 24 hours before being subjected to CTM testing. There are other bricks that have not been dried in an oven. The bricks made of mortar based on brine sludge are evaluated after 3, 7, 14, and 28 days of cure. For each mix, a total of three specimens were cast, and the average of the three was used to determine the sample's compressive strength.

The Compressive Strength of brine sludge-based mortar bricks at 3 and 7 days is shown in the following tables:-

Table 4.5: Compressive strength of the brine sludge based geopolymer 10M and 18M bricks at oven drying

Mixtures	Curing	Molarity	No. of specimens	7 days (MPa)
B1	Oven Drying at 70^{o} C	10M	1	7.16
			2	7.2
			3	7.26
B2	Oven Drying at 70^{o} C	18M	1	4.8
			2	5
			3	5.2

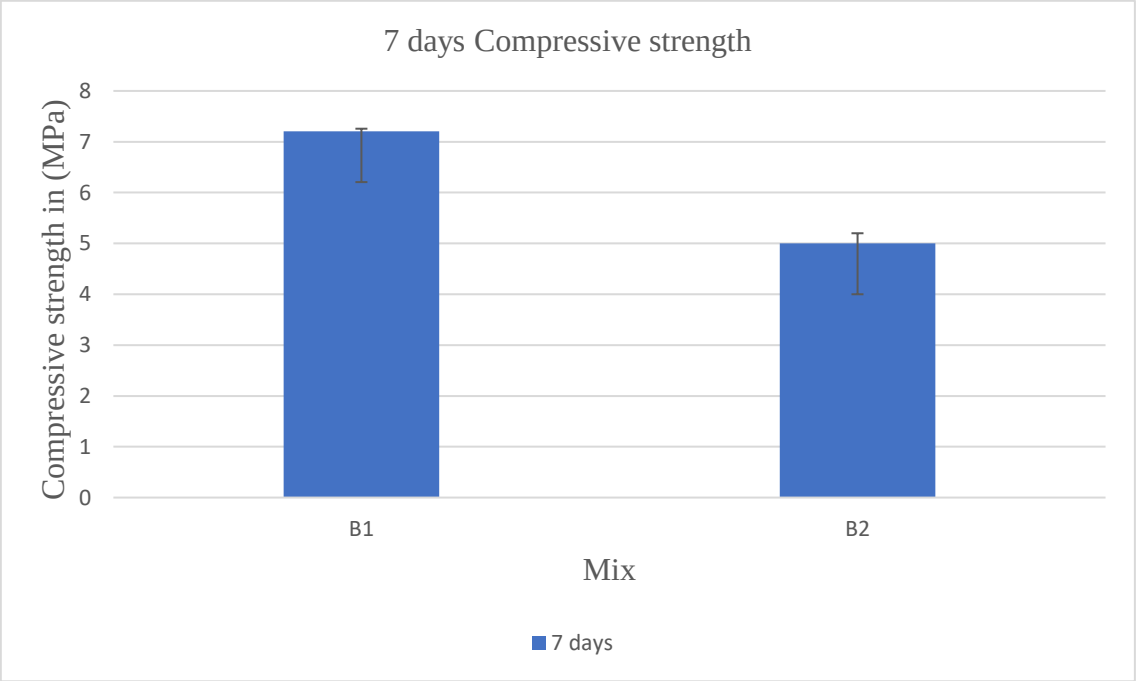

Figure 4.5: Average compressive strength at oven drying

Fig 4.5 showing the effect of different molarities in the volume based mixes when oven dried at 70^{o} C. B1 mix showed the higher compressive to B2 mix.

Table 4.6: Compressive strength of the brine sludge based geopolymer 10M bricks at different curing.

Mixtures	Curing	Molarity	No. of specimens	7 days (MPa)
B2	Oven Drying at 70^{o} C	10M	1	7.16
			2	7.2
			3	7.26
B3	Ambient Curing	10M	1	1.11
			2	1.00
			3	1.00

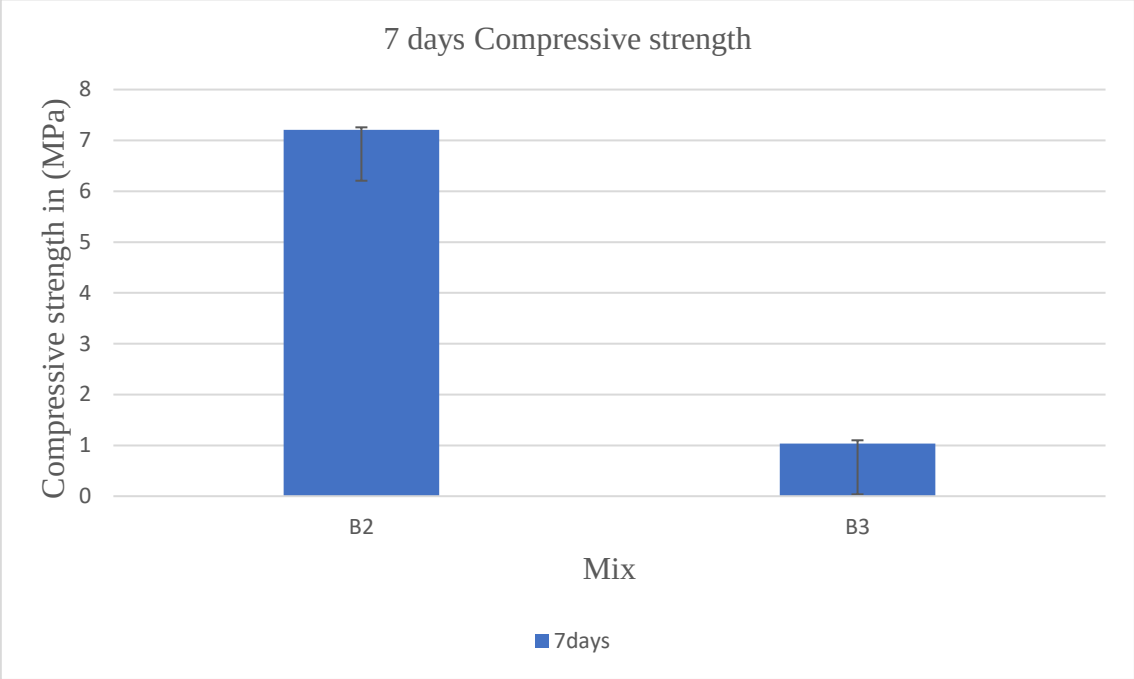

Figure 4.6: Average compressive strength at different curing

Fig 4.6 showing the effect of different curing in the volume based mixes. B2 mix showed the higher compressive to B3 mix.

Table 4.7: Compressive strength of the brine sludge based geopolymer 10M bricks at ambient curing with different internal blending ratio

Mixtures	Internal Blending Ratio of solution (NaOH : Na_2SiO_3)	Curing	No. of specimens	3 days (MPa)	7 days (MPa)
B4	1:1.5	Ambient Curing	1	0.54	0.85
			2	0.743	0.86
			3	0.74	0.93
B5	1:2	Ambient Curing	1	0.842	1.9
			2	0.743	1.80
			3	0.94	1.74
B6	1:2.5	Ambient Curing	1	0.41	0.55
			2	0.378	0.52
			3	0.447	0.6

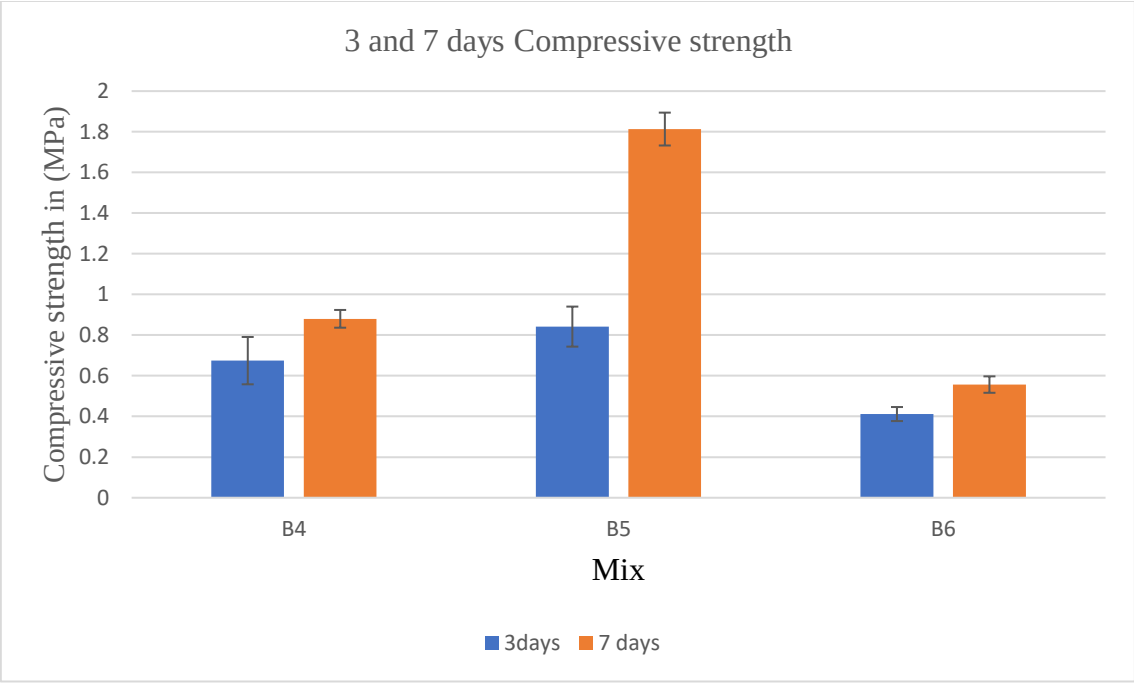

Figure 4.7: Average compressive strength at different blending ratio

Fig 4.7 showing the effect of the internal blending ratio of geopolymer solution in weight based mixes in ambient curing. B5 mix showed the higher compressive strength as compare to B4 and B6.

Table 4.8: Compressive strength of oven dried brine sludge based geopolymer 10M and 18M bricks

Mixtures	Curing	Molarity	No. of specimens	7 days (MPa)
B7	Oven Drying at 70° C	10M	1	4.93
			2	4.8
			3	4.76
B8		18M	1	16.8
			2	17.5
			3	17.2
B9		10M	1	10.4
			2	10
			3	9.8

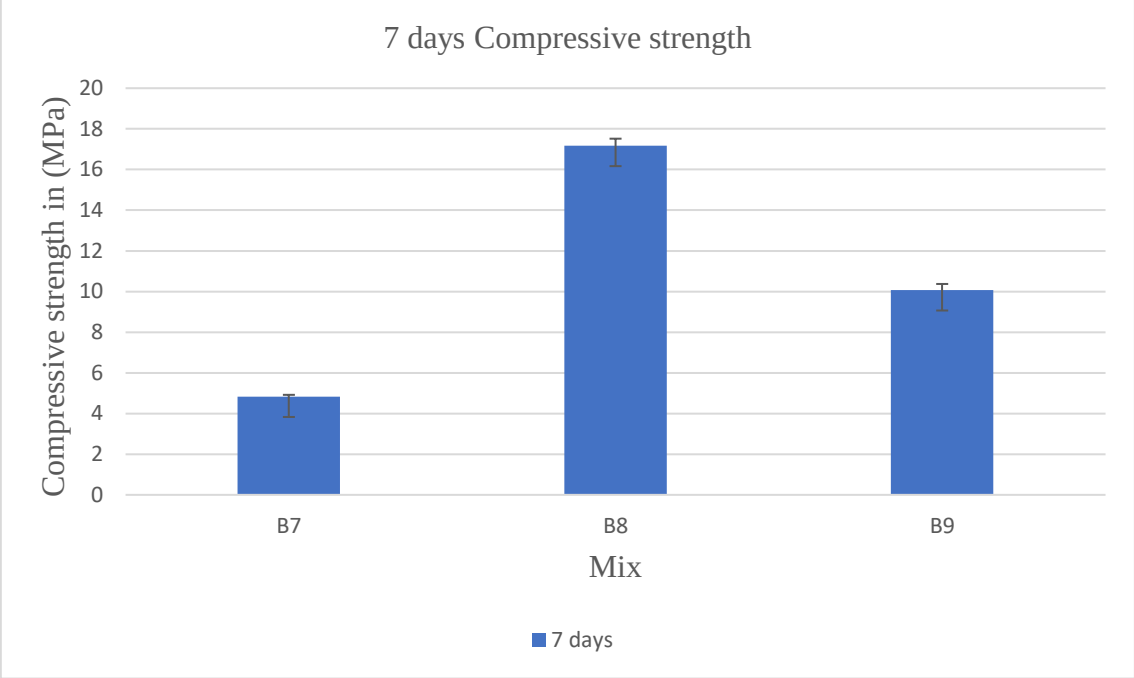

Figure 4.8: Average compressive strength of 10M and 18M bricks

Fig 4.8 showing the optimized weight based mixes for both the molarities and solution content in oven drying at 70° C. B8 and B9 mix showed the maximum compressive strength and superior to all other mixes.

Complete testing of the optimized mixes:-

The optimized mixes for 18M and 10M bricks were B8 and B9, picked for additional testing to ascertain the samples' dry compressive strength (both at 14 and 28 days), wet compressive strength (28 days), water absorption (28 days), efflorescence (28 days).

Table 4.9: Dry Compressive Strength of brine sludge based geopolymer mortar bricks

Mixtures	Designation of Brick	14 days (MPa)	Designation of Brick	28 days (MPa)
B8	S16	17.8	S1	18.8
	S17	18.2	S2	18.6
	S18	18	S3	18.4

Table 4.10: Dry Compressive Strength of brine sludge based geopolymer mortar bricks

Mixtures	Designation of Brick	14 days (MPa)	Designation of Brick	28 days (MPa)
B9	S16	10.8	S1	12.2
	S17	11	S2	11.6
	S18	10.6	S3	11.2

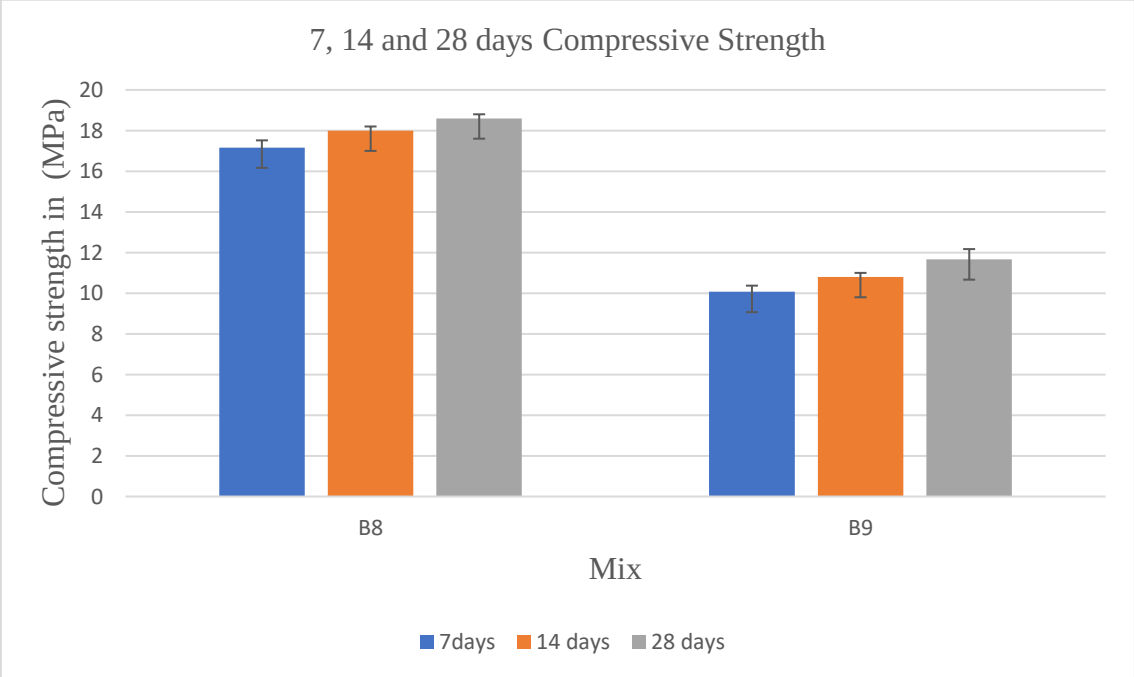

Figure 4.9: Average dry compressive strength of different mixes at 7, 14 and 28 days

4.3 Wet compressive strength of brine sludge based mortar bricks-

After 28 days, the wet compressive strength test was performed, the bricks were submerged in the water bucket for 24 hours. The sample frogs were then filled with cement paste after being removed from the water.

Table 4.11: Compressive Strength of brine sludge based geopolymer mortar bricks

Mixtures	Curing	No. of specimens	Molarity	28 days (MPa)
B8	Oven Drying at 70° C	S10	18M	15.30
		S11		15.32
		S12		15.11

Table 4.12: Compressive Strength of brine sludge based geopolymer mortar bricks

Mixtures	Curing	No. of specimens	Molarity	28 days (MPa)
B9	Oven Drying at 70° C	S11	10M	8
		S12		8.15
		S13		9.30

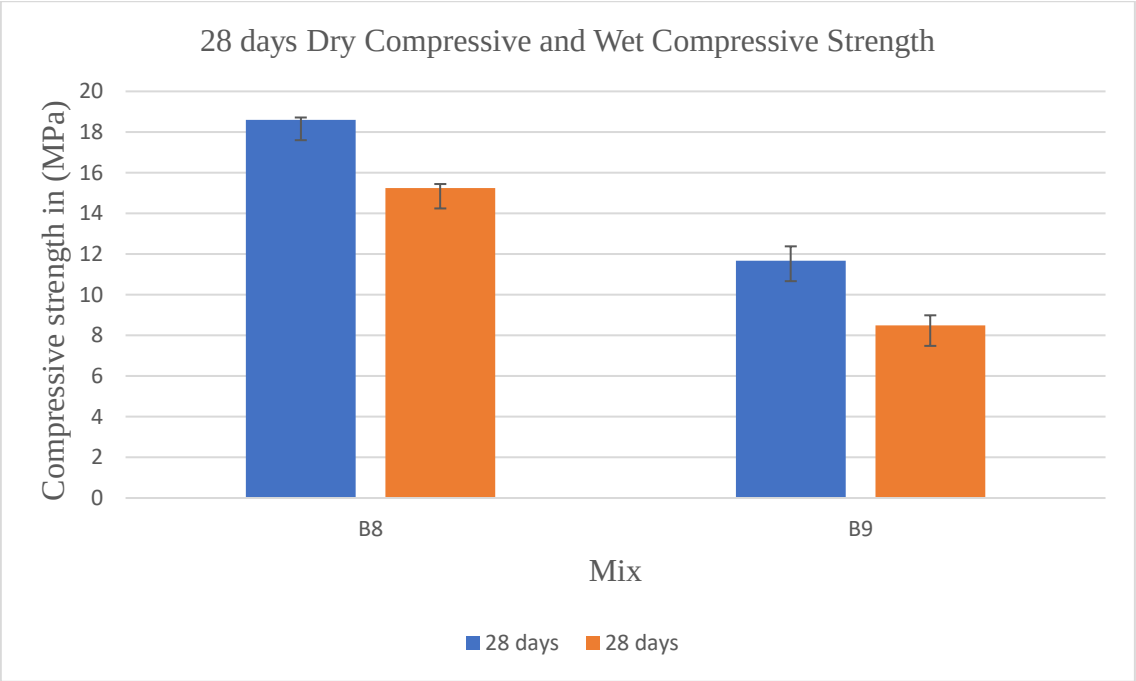

Figure 4.10: Average dry compressive vs wet compressive strength

As per IS 12894 (2002), brick mix (B8) achieved the strength not less than 15.0 are classified in class designation 15, where as brick mix (B9) achieved not less than 7.5 are classified in class designation 7.5. The average percentage decrease of wet compressive strength with respect to the dry compressive strength are 18.04 % and 27.73% for B8(18M) and B9(10M) mixes.

4.4 Water absorption of brine sludge based mortar bricks-

After 28 days, the water absorption test was performed.

a. Water Absorption (%) = $\frac{W2 - W1}{W2}$ x 100

b. Max. Water absorption (%) for first class brick = 15 %

c. Brick size = 230 mm x 100 mm x 75 mm

For 10M Geopolymer bricks:-

Table 4.13: Water absorption % (10M bricks)

Sr.no.	Sample no.	Initial Weight (W1) (kg)	Final Weight (W2) (kg)	Water Absorption (%)	Average Water Absorption (%)
1.	S4	3.286	3.680	10.7	10.63
2.	S5	3.294	3.678	10.4	
3.	S6	3.266	3.664	10.8	

For 18M Geopolymer bricks:-

Table 4.14: Water absorption % (18M bricks)

Sr.no.	Sample no.	Initial Weight (W1) (Kg)	Final Weight (W2) (kg)	Water Absorption (%)	Average Water Absorption (%)
1.	S4	3.598	3.742	3.8	4.13
2.	S5	3.600	3.744	3.8	
3.	S6	3.544	3.726	4.8	

As per IS 12894 (Beureau of Indian Standards, 2011), after submerged in the cold water for 24 hours, the bricks shall have the average water absorption not more than 20 percent by mass up to class 12.5 and 15 percent by mass for higher classes.

Brick mix (B8) shall have average water absorption 4.13 % by mass for designated class 15, where as brick mix (B9) 10.63% by mass for designated class 7.5. Both brick mixes satisfies the criteria of codal provision.

4.5 Efflorescence of brine sludge based mortar bricks-

The efflorescence test was conducted after 28 days. It is a powdery layer of salts formed on the surface of bricks. It is caused by numerous soluble salts, such as the calcium, sodium, potassium, and magnesium sulphate or carbonate compounds.

For 10M Geopolymer bricks:-

Figure 4.11 Formation of salts layer on front face

Figure 4.12: Marking of the layer

Figure 4.13: Dividing the layer into different areas

Table 4.15: Efflorescence showing the average exposed area % (10M) bricks

Sr. no.	**Designation**	**Total Area (mm^2)**	**Exposed Area (mm^2)**	**Exposed Area %**	**Average Exposed Area %**
1.	S7	95500	9220.5	9.65	9.90
2.	S8	95500	9503.2	9.95	
3.	S9	95500	9655.12	10.11	

Result:-

Percentage of the white patches on the bricks is 9.90% (light minerals). It means that these bricks are showing the slight deposit of the salts i.e. Good bricks.

For 18M Geopolymer bricks:-

(a) Front face

(b) Left face

(c) Back face

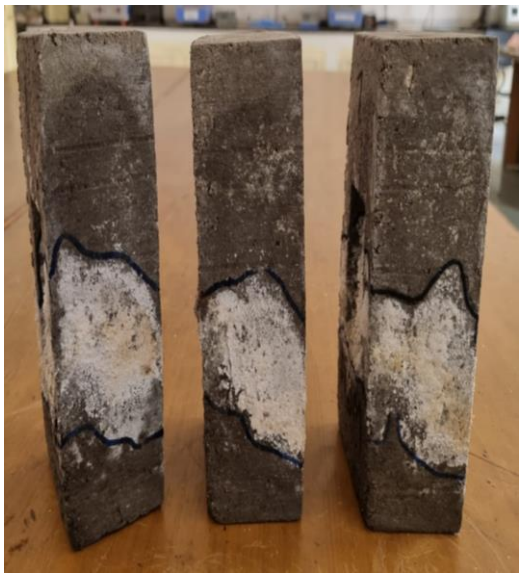

(d) Right face

Figure 4.14: Actual images after efflorescence test of geopolymer bricks having 18M solution

(a) Front face

(b) Left face

(c) Back face

(d) Right face

Figure 4.15: Actual images with grid lines after efflorescence test of geopolymer bricks having 18M solution

Table 4.16: Efflorescence showing the average exposed area % (18M) bricks

Sr. no.	**Designation**	**Total Area (mm^2)**	**Exposed Area (mm^2)**	**Exposed Area %**	**Average Exposed Area %**
1.	S7	95500	22062	23.10	22.53
2.	S8	95500	20029	20.9	
3.	S9	95500	22529	23.59	

Result:-

Percentage of the white patches on the bricks is 22.53% (moderate minerals). It means that these bricks are showing the moderate deposit of the salts.

Discussion:-

As per IS 12894, the bricks having class 12.5 or below can have the efflorescence up to moderate whereas for higher classes slight efflorescence is recommended. Although the brick mix B8 having 18M activating solution achieve the higher strength as compared to brick mix B9 having 10 M activating solution that has not qualified the criterion of efflorescence test as per IS 12894. Therefore, only brick mix B9 having the activating solution 10M satisfies the requirement of IS 12894.

4.6 XRD Analysis-

The mineralogy was analysed by X-ray diffraction technique. In the XRD arrangement, the angle 2θ varies between 5 and 75 degrees. The data obtained from XRD is analysed using X'pert HighScore Plus.

- Brine Sludge-

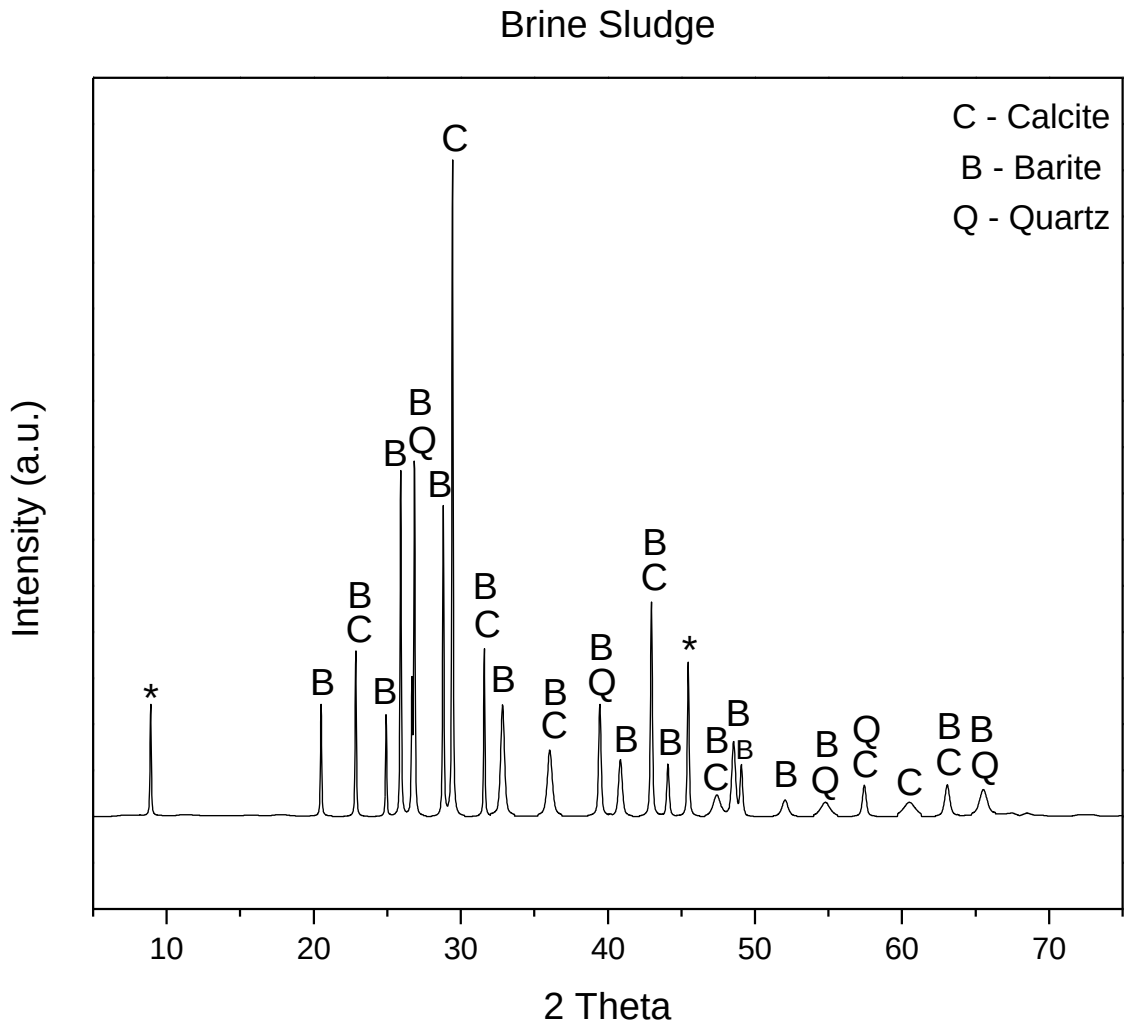

Figure 4.16: XRD of brine sludge sample

The X-ray diffraction spectra of the brine sludge sample were shown in Fig 4.18. The results indicated the major minerals of the sample such as Quartz (SiO_2), Calcite $Ca(CO_3)$ and Barite ($BaSO_4$) with reference code (01-085-0335), (01-083-0578) and (01-076-0213) respectively.

∗ denoted the unidentified peaks. These patterns contained numerous sharp peaks, proving that the sample primarily has a crystalline structure.

- Fly ash-

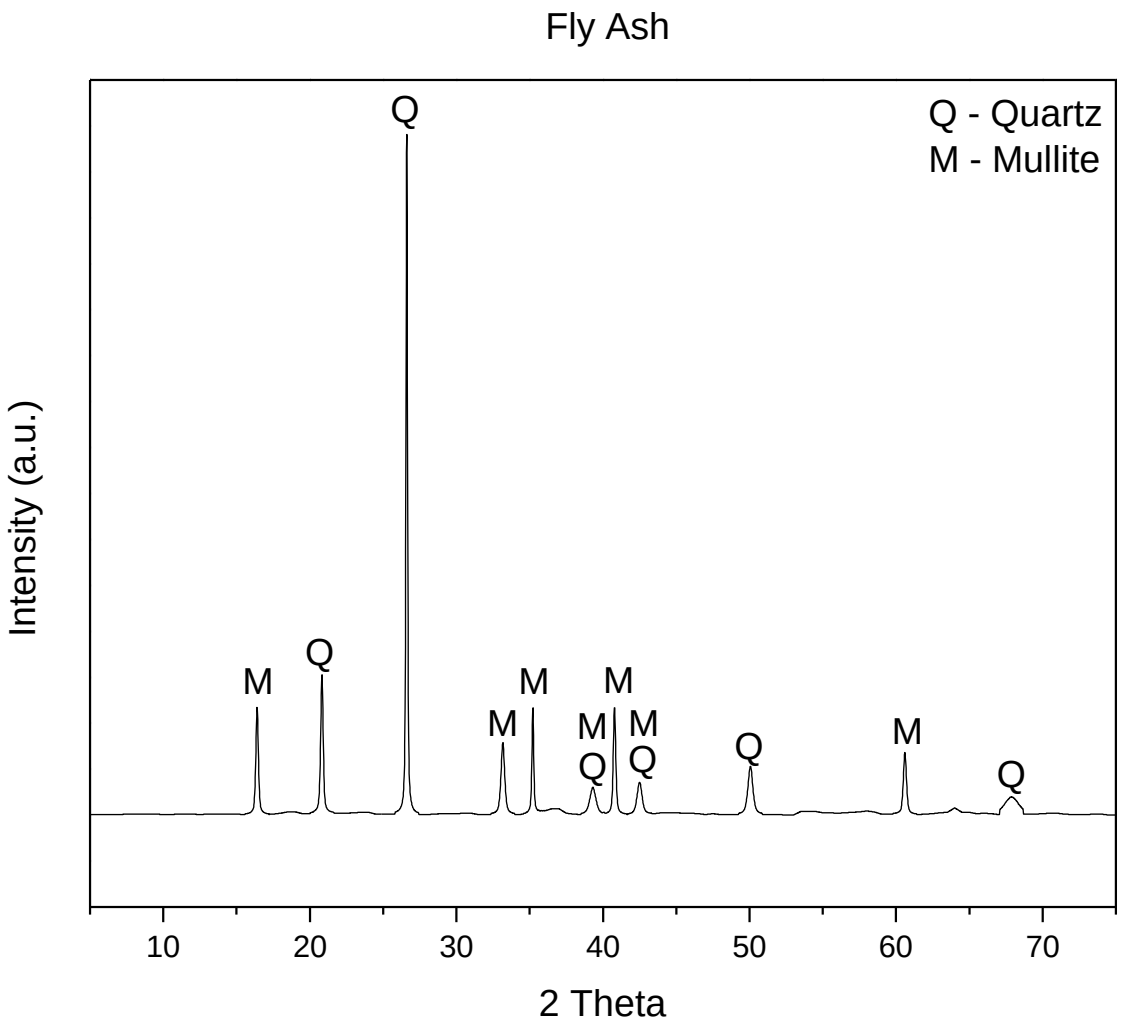

Figure 4.17: XRD of fly ash sample

The X-ray diffraction spectra of the fly ash sample were shown in Fig 4.19.The results indicated the major minerals of the sample such as Quartz (SiO_2) and mullite ($Al_{4.75}Si_{1.25}O_{9.63}$) with reference code (01-083-0539) and (01-079-1454) respectively. These patterns contained numerous sharp peaks, proving that the sample primarily has a crystalline structure.

- Stone Dust-

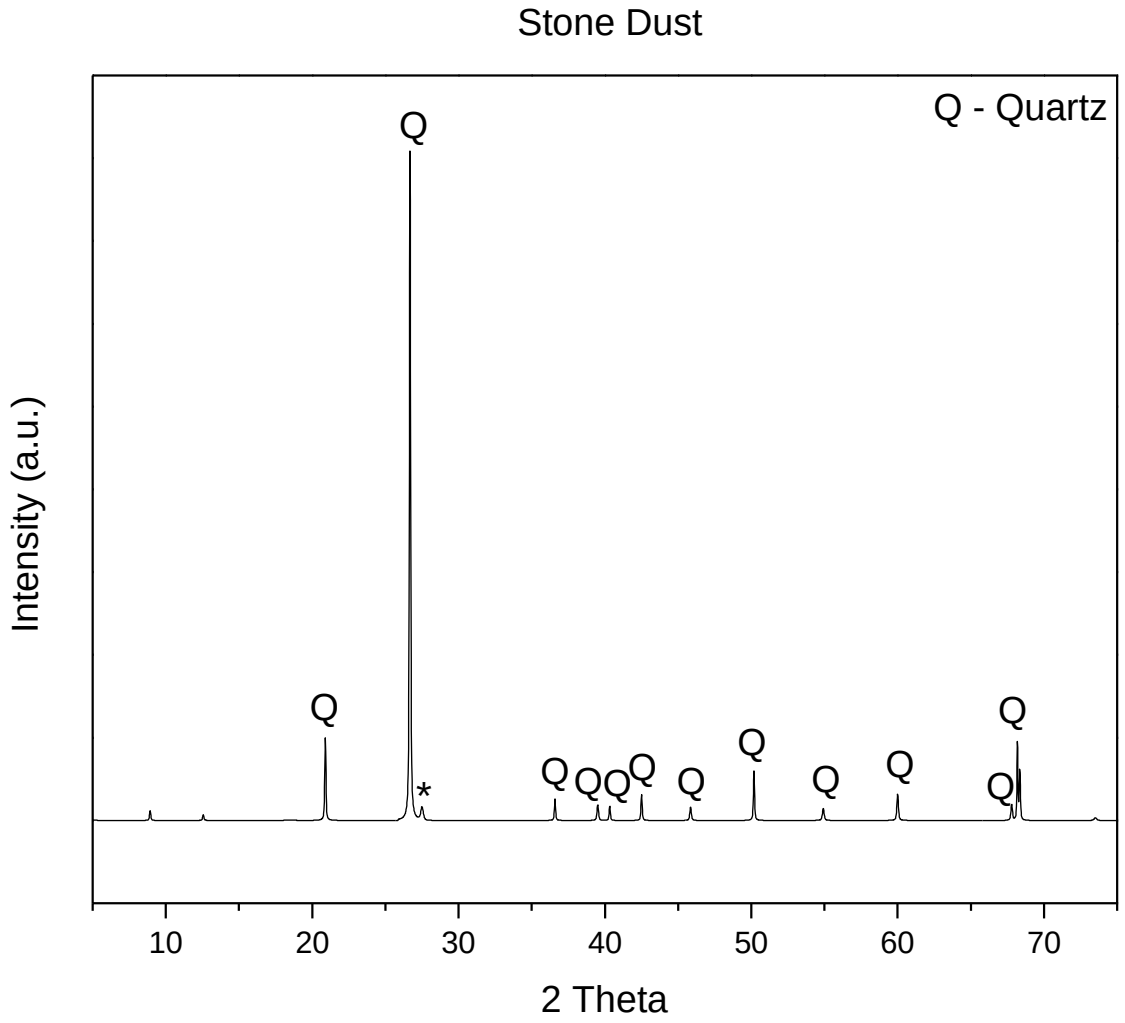

Figure 4.18: XRD of stone dust sample

The X-ray diffraction spectra of the stone dust sample were shown in Fig 4.20.The results indicated the main compounds of the sample was Quartz (SiO_2) with reference code (00-046-1045). * denoted the unidentified peaks, these patterns contained numerous sharp peaks, proving that the sample primarily has a crystalline structure.

- 10M Brick after 28 days-

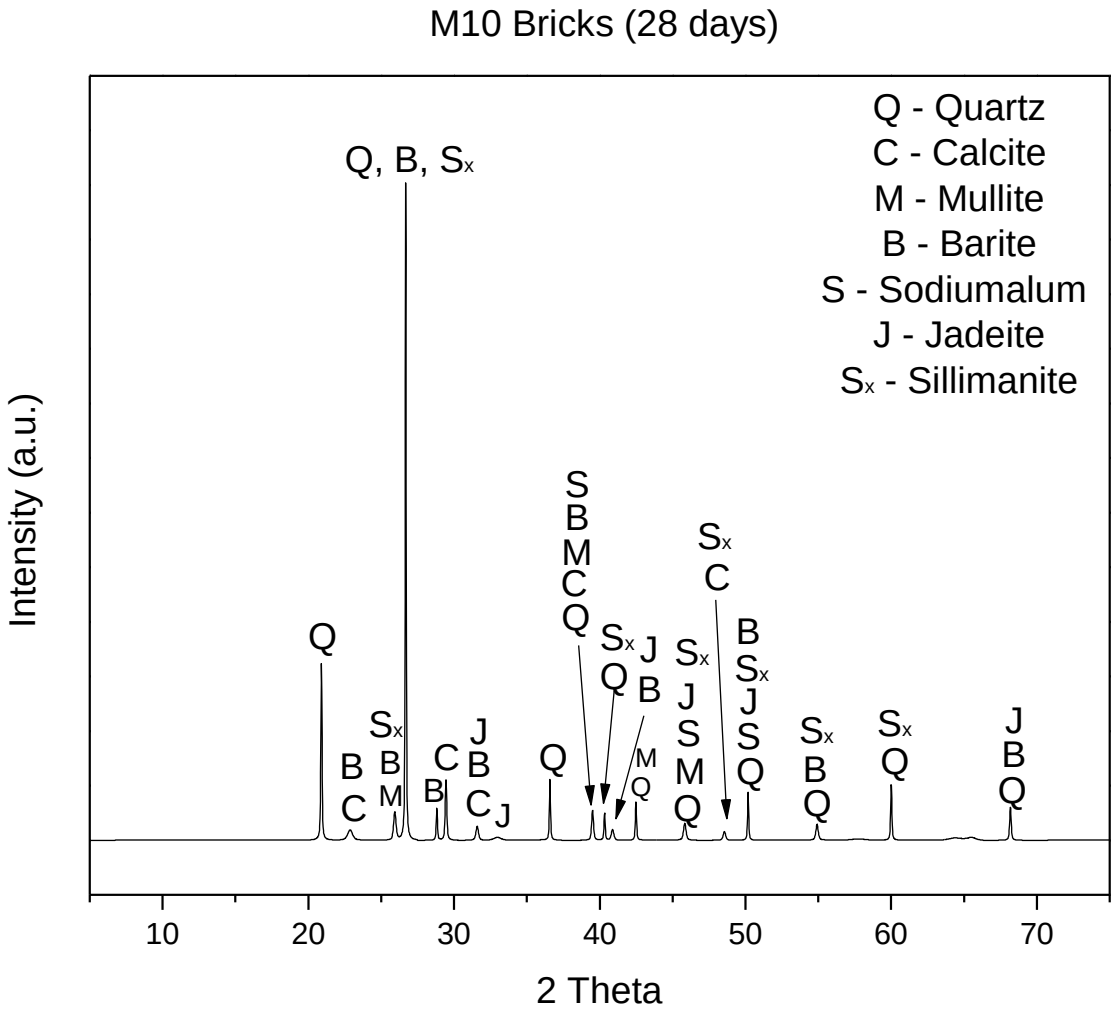

Figure 4.19: XRD of 10M brick sample

The X-ray diffraction spectra of the 10M brick sample were shown in Fig 4.21.The results indicated the major minerals of the sample such as Quartz (SiO_2), calcite ($CaCO_3$), Mullite ($Al_{4.52}Si_{1.48}O_{9.74}$), Barite ($BaSO_4$), Sodiumalum ($NaAl(SO_4)_2{\cdot}12H_2O$), Jadeite ($NaAlSi_2O_6$) and Sillimanite ($Al_2SiO_5$) with reference code (00-046-1045), (01-083-0578), (01-079-1457), (01-080-0512), (00-029-1167), (01-071-1505) and (01-083-1562) respectively. These patterns contained numerous sharp peaks, proving that the sample primarily has a crystalline structure.

- 18M Brick after 28 days-

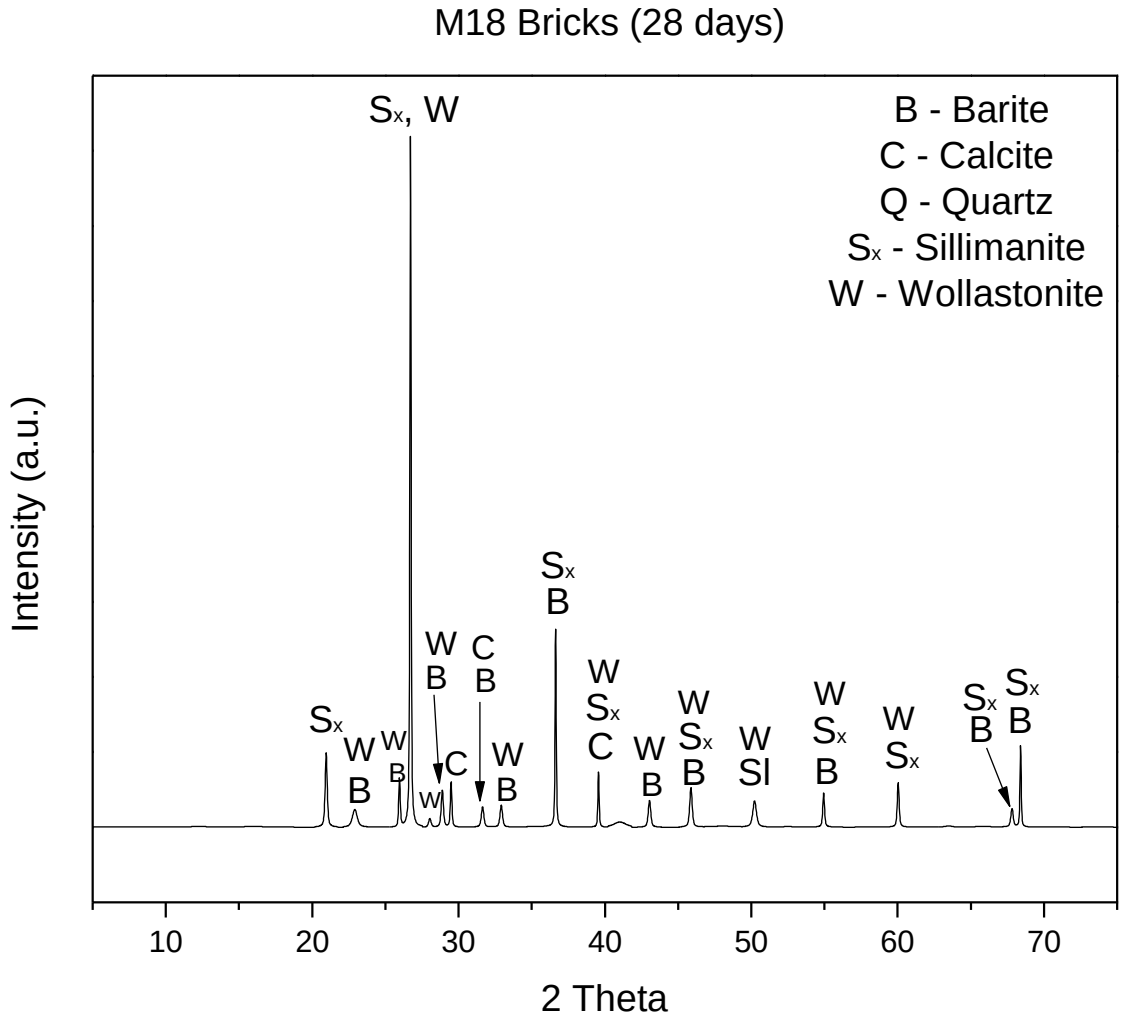

Figure 4.20: XRD of 18M brick sample

The X-ray diffraction spectra of the 18M brick sample were shown in Fig 4.22.The results indicated the major minerals of the sample such as Barite ($BaSO_4$), Calcite ($CaCO_3$), Quartz (SiO_2), Sillimanite (Al_2SiO_5) and Wollastonite ($CaSiO_3$) with reference code (01-076-0213), (01-072-1651), (01-086-1628), (01-079-1339) and (01-073-1110) respectively. These patterns contained numerous sharp peaks, proving that the sample primarily has a crystalline structure.

- Efflorescence-

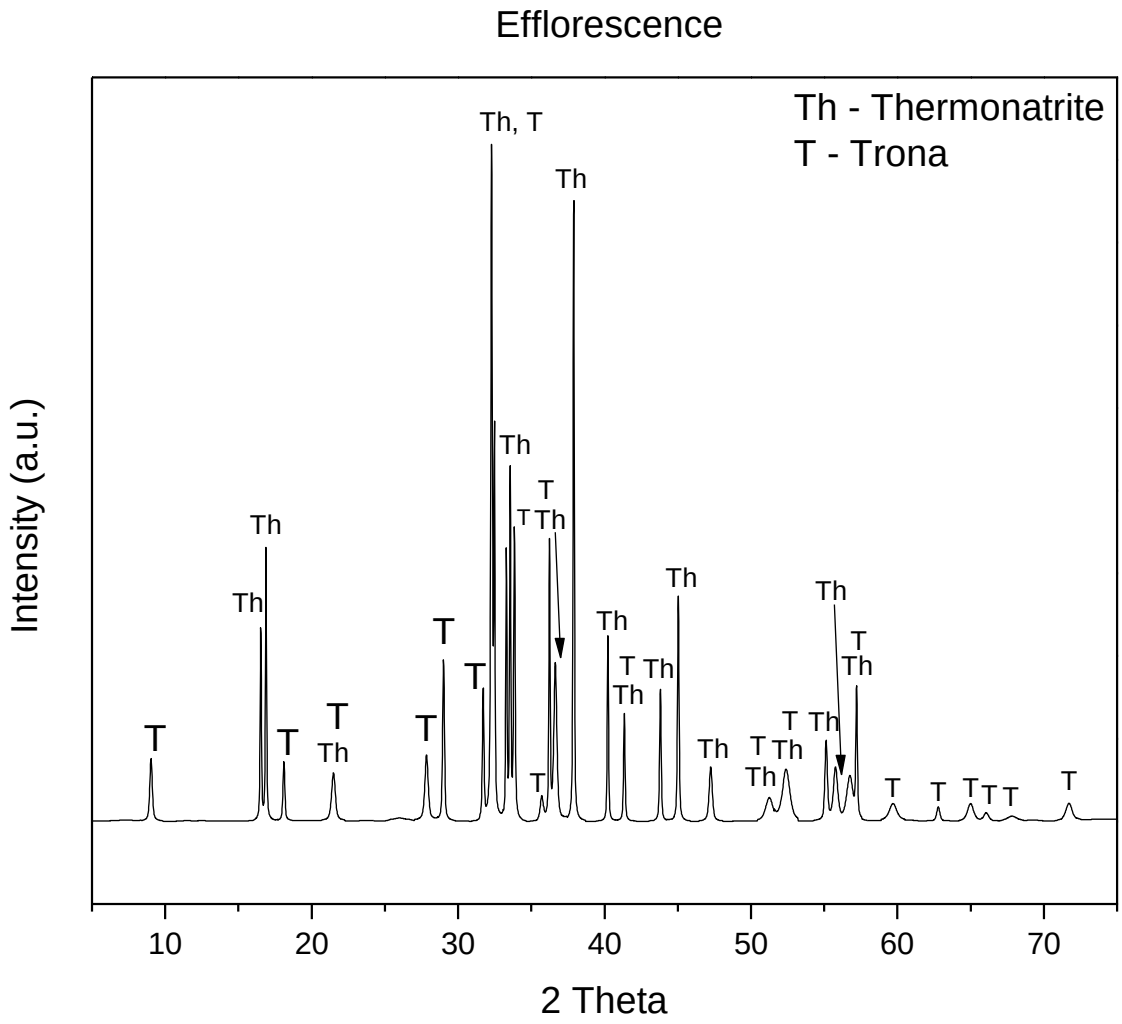

Figure 4.21: XRD of efflorescence sample

The X-ray diffraction spectra of the efflorescence sample were shown in Fig 4.23. The results indicated the major minerals of the sample such as Thermonatrite ($Na_2CO_3H_2O$) and Trona ($Na_3H(CO_3)_2(H_2O)_2$) with reference code (00-0008-0448) and (01-078-1064) respectively. The X –ray analysis of salt precipitates during the efflorescence test was done to interpret the possible chemistry behind the salt precipitation. The XRD analysis revealed the formation of Thermonatrite (Na_2CO_3 H_2O) and Trona ($Na_3H(CO_3)_2(H_2O)_2$) majorly the carbonate hydrate of sodium salt which shows the presence of un utilized concentration of sodium which might get converted and precipitated in the form of salts in the presence of CO_2 and capillary water. This suggest the need for future regarding optimization of sodium concentration in the geopolymeric solution. These patterns contained numerous sharp peaks, proving that the sample primarily has a crystalline structure.

4.7 FTIR Analysis-

In FTIR spectra, the important vibration bands of the different materials were identified in the 400 – 4000 cm^{-1} range.

- Brine Sludge-

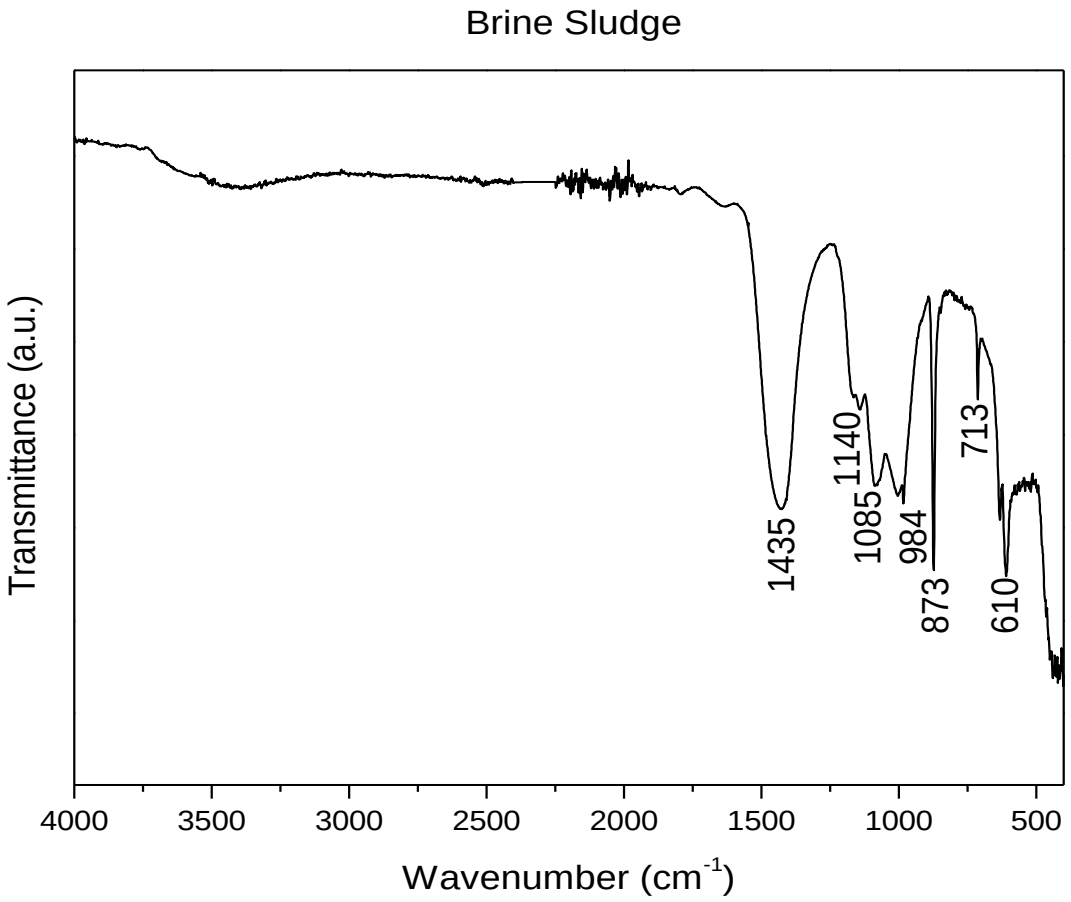

Figure 4.22: FT-IR spectra of brine sludge sample

The FT-IR spectra of the brine sludge sample were shown in Fig 4.24. The results indicated the allotropes of crystalline carbonate i.e.; calcite. Usually, calcite structure showed IR absorption frequencies for the carbonate ion at around 873 cm^{-1} (ν2), and 713 cm^{-1} (ν4). Barite structure showed IR absorption frequencies at 610 cm^{-1}, 984 cm^{-1} and 1140 cm^{-1}. Quartz structure showed IR absorption frequencies at 1085 cm^{-1}. The major minerals of the brine sludge sample identified in the X-ray diffraction (XRD) analysis were also detected in the Fourier-transform infrared (FTIR) spectroscopy analysis.

- Fly ash-

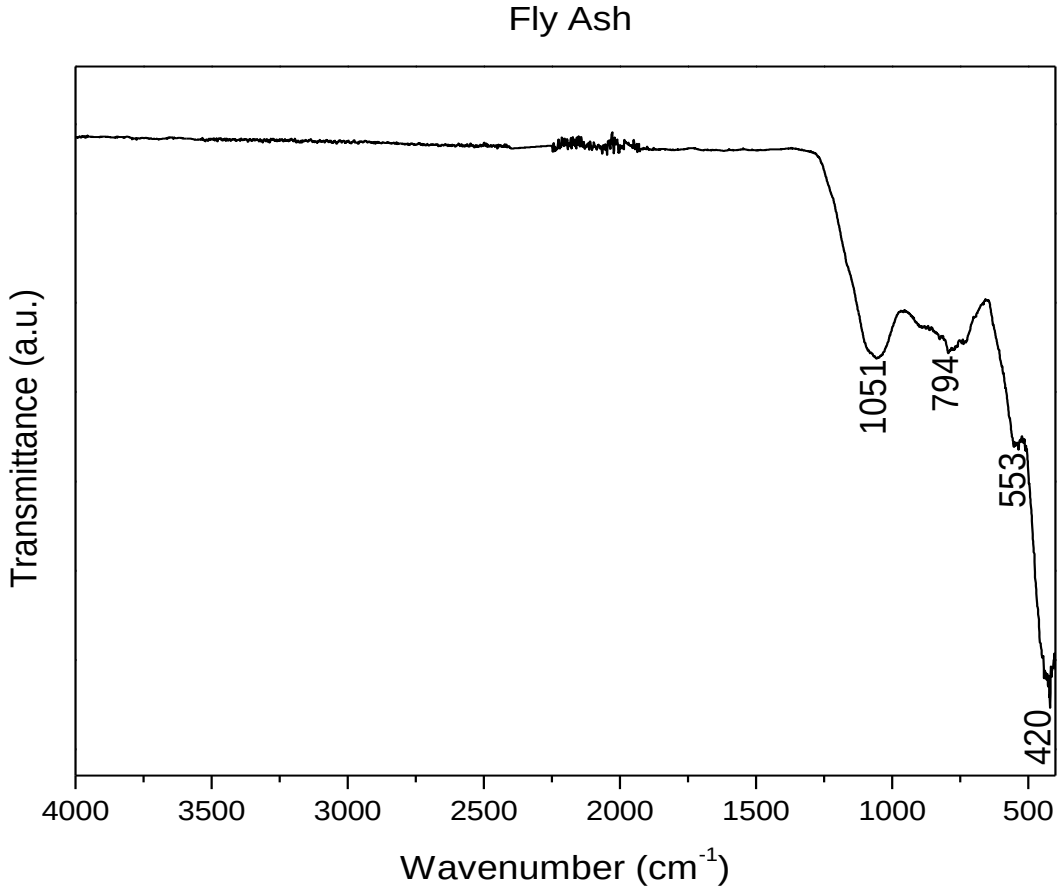

Figure 4.23: FT-IR spectra of fly ash sample

The FT-IR spectra of the fly ash sample were shown in Fig 4.25. Quartz structure showed IR absorption frequencies at 462 cm^{-1} showed asymmetric Si-O bending vibrations. The characteristic peak of quartz mineral at 1051 cm^{-1} showed the asymmetric and symmetrical Si-O stretching vibrations. Mullite structure showed IR absorption frequencies at 553 cm^{-1}. The major minerals of fly ash sample identified in the X-ray diffraction (XRD) analysis were also detected in the Fourier-transform infrared (FTIR) spectroscopy analysis.

- Stone Dust-

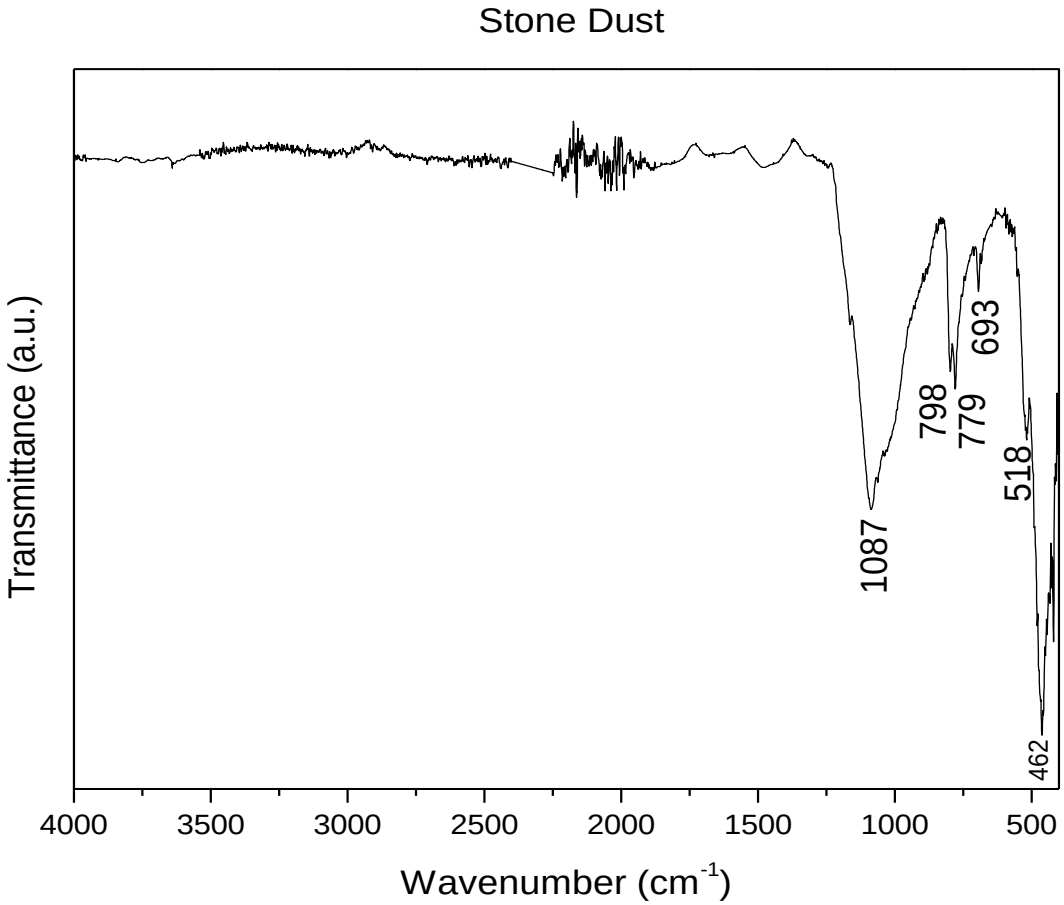

Figure 4.24: FT-IR spectra of stone dust sample

The FT-IR spectra of the stone dust sample were shown in Fig 4.26. The characteristic of infrared bands associated with quartz crystals are in the range of 1200-400 cm^{-1}. The characteristic peaks of pure quartz mineral at 1087 cm^{-1} and 779 cm^{-1} showed the asymmetric and symmetrical Si-O stretching vibrations, respectively and the peak at 462 cm^{-1} showed asymmetric Si-O bending vibrations. It is well known that in the infrared spectra of amorphous silica the symmetrical bending vibration of the Si-O group found at 693 cm^{-1}**.** The major minerals of stone dust identified in the X-ray diffraction (XRD) analysis were also detected in the Fourier-transform infrared (FTIR) spectroscopy analysis.

- 10M Brick after 28 days-

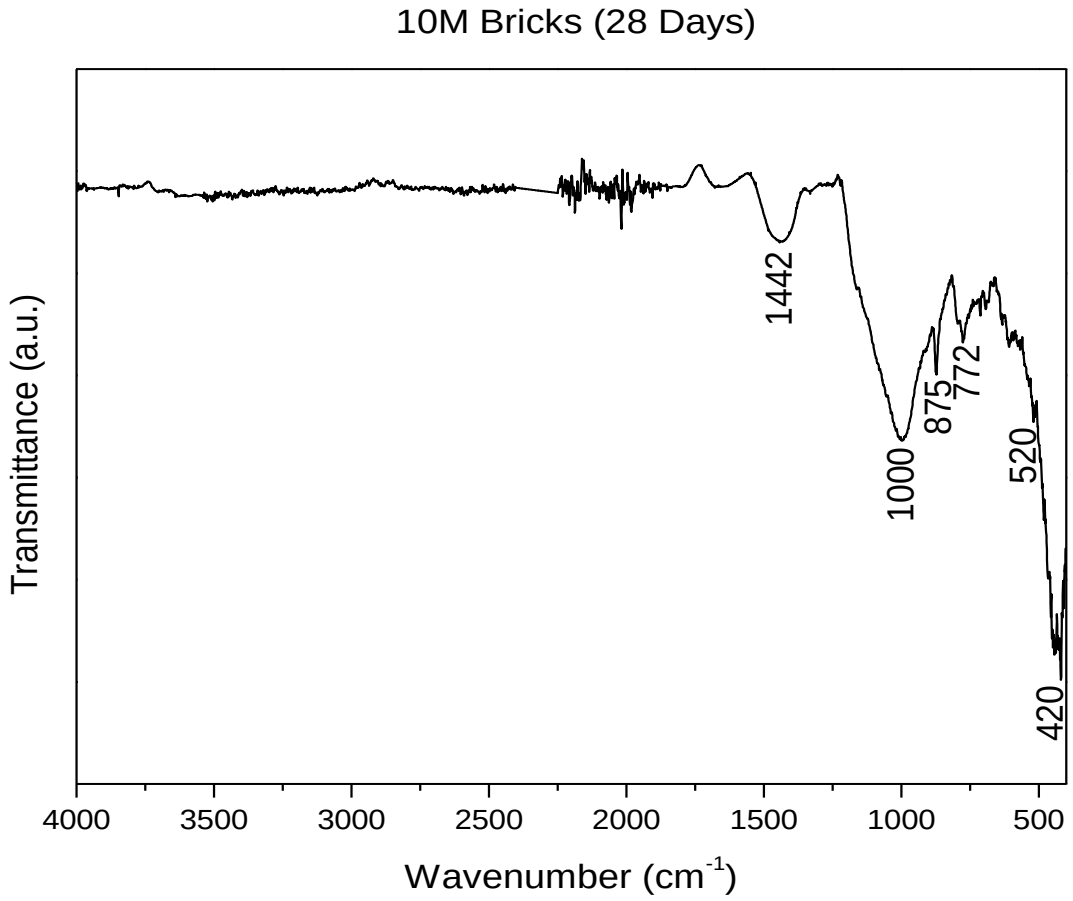

Figure 4.25: FT-IR spectra of 10M brick sample

The FT-IR spectra of the 10M brick sample were shown in Fig 4.27. The characteristic peaks of pure quartz mineral at 772 cm^{-1} showed the asymmetric and symmetrical Si-O stretching vibrations. Calcite structure showed IR absorption frequencies for the carbonate ion at around 873 cm^{-1} (ν2), Sodiumalum showed IR absorption frequencies at 1000 cm^{-1} and 1442 cm^{-1}. In the XRD (X-ray diffraction) analysis, all of the major minerals of the 10M brick sample identified were also confirmed by FTIR (Fourier-transform infrared) spectroscopy, with the exception of calcite, mullite, barite, jadeite, and sillimanite.

- 18M Brick after 28 days-

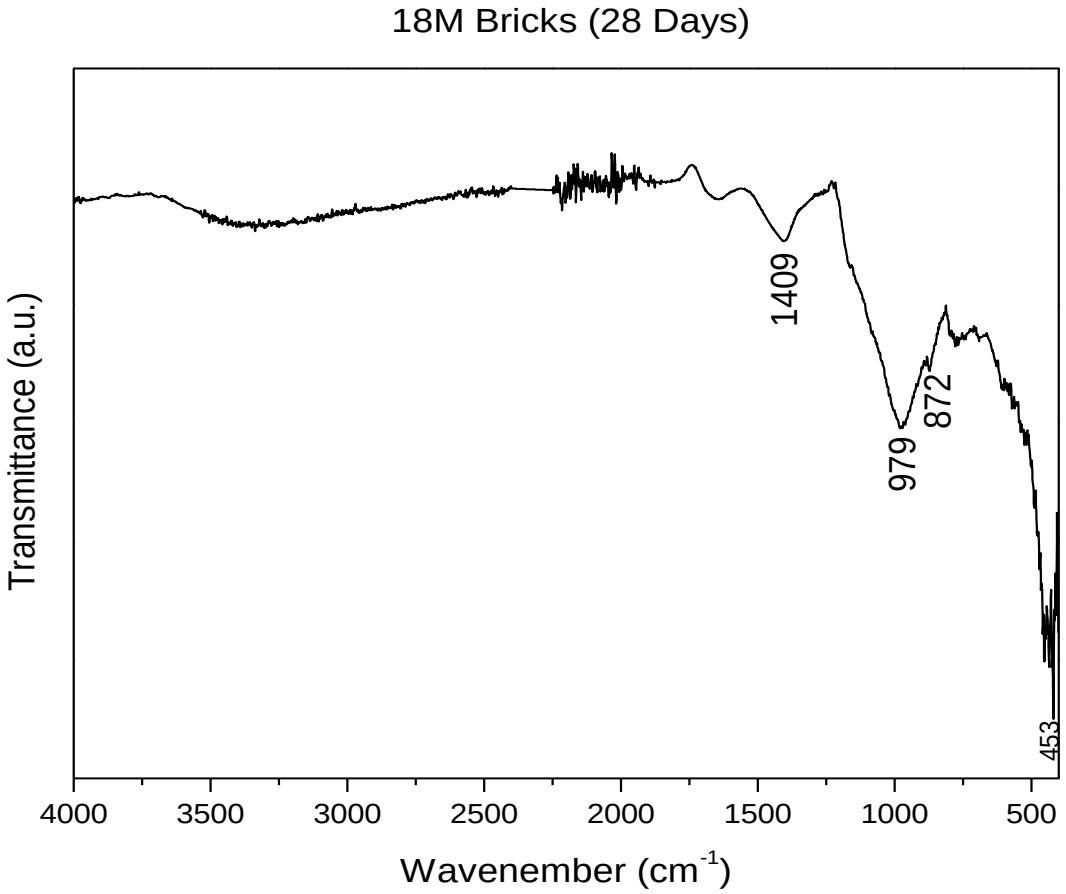

Figure 4.26: FT-IR spectra of 18M brick sample

The FT-IR spectra of the 18M brick sample were shown in Fig 4.28. Usually, calcite structure showed IR absorption frequencies for the carbonate ion at around 872 cm^{-1} and 1409 cm^{-1}. Barite structure showed IR absorption frequencies 979 cm^{-1}. Wollastonite at showed IR absorption frequencies 453 cm^{-1}. In the XRD (X-ray diffraction) analysis, all of the major minerals of the 18M brick sample identified were also confirmed by FTIR (Fourier-transform infrared) spectroscopy, with the exception of quartz and sillimanite.

- Efflorescence-

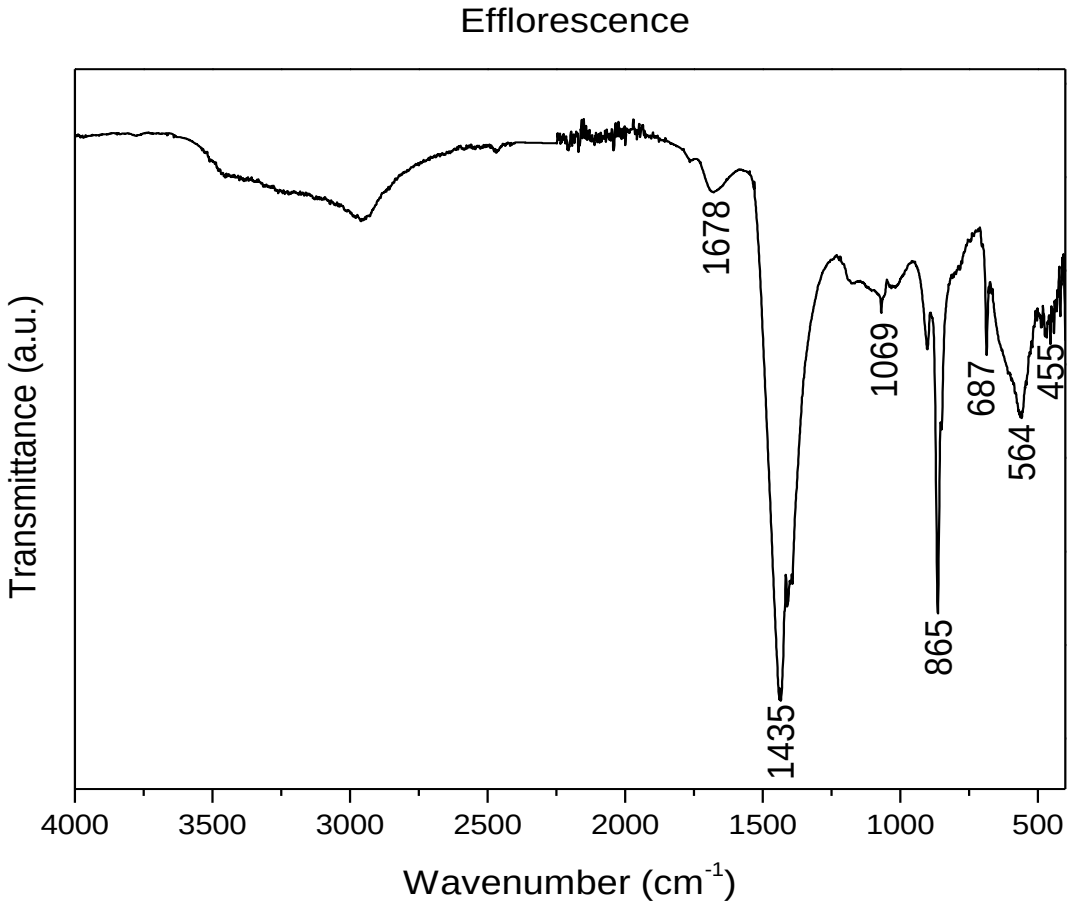

Figure 4.27: FT-IR spectra of efflorescence

The FTIR spectra of the efflorescence were shown in Fig 4.29. Trona showed IR absorption frequencies at 564 cm^{-1}, 865 cm^{-1}, 1069 cm^{-1}, 1435 cm^{-1} and 1678 cm^{-1}.The major minerals identified in the X-ray diffraction (XRD) analysis were also found in the Fourier-transform infrared spectroscopy (FTIR) analysis, with the exception of thermonatrite.

Table 4.17: Mineral phases confirmed using FT-IR spectra for raw materials and geopolymer bricks

Material	**Mineral Phase**	**Chemical Formula**	**Peaks observed in the present study**	**Peaks observed in the previous study**	**References**
Brine Sludge	Calcite	$CaCO_3$	713, 873, 1435	711, 876, 1402	Myszka et al. (2019)
	Barite	$BaSO_4$	610, 984, 1140,	608, 637, 982, 1072, 1118, 1192	Ramaswamy et al. (2010)
	Quartz	SiO_2	462, 1085,	456-462, 692-694, 776-778, 792-798, 1058, 1086-1102	Gupta et al. (2020)
Stone dust	Quartz	SiO_2	462, 693, 779, 798, 1087	456-462, 692-694, 776-778, 792-798, 1058, 1086-1102	Gupta et al. (2020)
	Unidentified		518	-	-
Fly ash	Quartz	SiO_2	794, 1051	456-462, 692-694, 776-778, 792-798, 1058, 1086-1102	Gupta et al. (2020)
	Mullite	$Al_{4.75}Si_{1.25}O_{9.63}$	553,	456, 567, 751, 882, 1137, 1152	Goren et al. (2012)
	Unidentified		420		
10M brick	Quartz	SiO_2	772,	456-462, 692-694, 776-778, 792-798, 1058, 1086-1102	Gupta et al. (2020)

	Calcite	$CaCO_3$	875,	711, 876, 1402	Myszka et al. (2019)
	Sodiumalum	$NaAl(SO_4)_2.12H_2O$	1000, 1442	454, 567, 681, 757, 942, 980, 1474	Abdelrahman et al. (2020)
	Unidentified		420, 520,	-	-
18M brick	Calcite	$CaCO_3$	872, 1409	711, 876, 1402	Myszka et al. (2019)
	Barite	$BaSO_4$	979,	608, 637, 982, 1072, 1118, 1192	Ramaswamy et al. (2010)
	Wollastonite	$CaSiO_3$	453		
Efflorescence	Trona	$(Na_3H(CO_3)_2(H_2O)_2)$	564, 865, 1069, 1435, 1678	578, 848, 1070, 1098 1455, 1681	rruff.info/ R050228
	Unidentified		455, 687		

4.8 Raman Spectroscopy-

In Raman spectra, the important vibration bands of the different materials were identified in the 200 – 2000 cm^{-1} range.

- Brine Sludge-

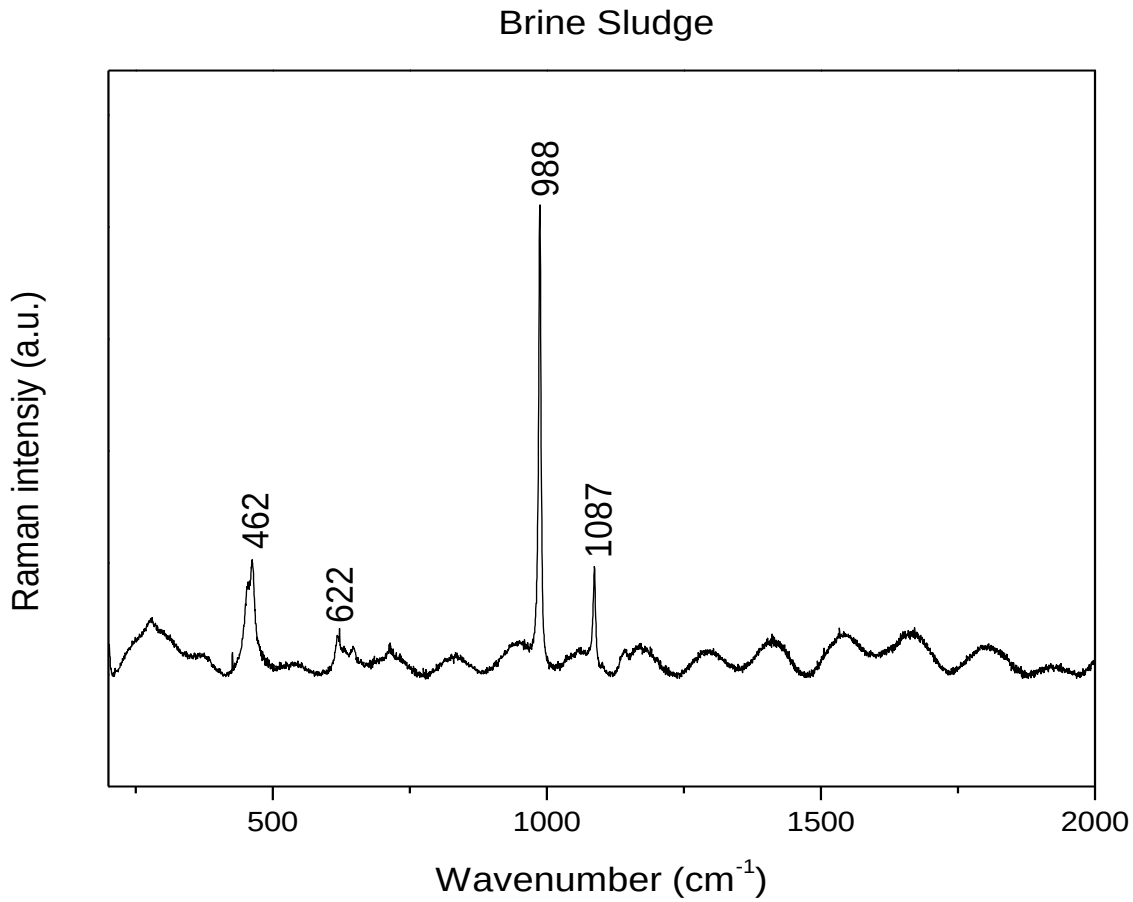

Figure 4.28 : Raman spectra of brine sludge sample

The Raman spectra of the brine sludge sample were shown in Fig 4.30. Raman spectra of barite consists of very clear and sharp bands that can be attributed to the fundamental vibrational modes of SO_4 tetrahedra. Therefore, the most intense line at 988 cm^{-1} is assigned to the ν1 symmetric stretching mode and the other band is found at 622 cm^{-1}. The calcite characteristic bands were found at 1087 cm^{-1} for the antisymmetric modes. The peak of pure quartz was found at 465cm^{-1}. The major minerals of the brine sludge sample identified in the X-ray diffraction (XRD) analysis were also detected in the Raman spectroscopy analysis.

- Fly ash-

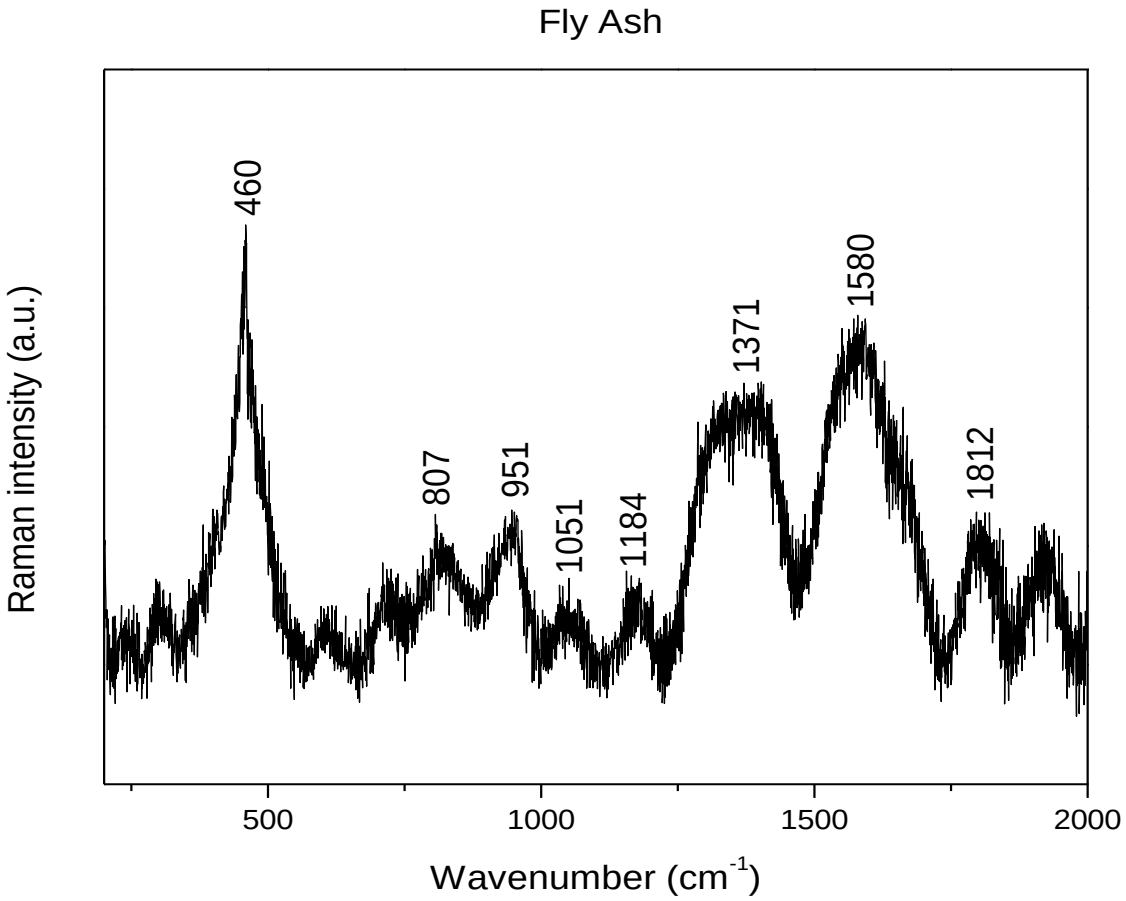

Figure 4.29: Raman spectra of fly ash sample

The Raman spectra of fly ash sample were shown in Fig 4.31. The peak of pure quartz was found at 460cm^{-1} and 708 cm^{-1}. The dehydrated (SiO_2) peak showed at 951 cm^{-1}and 1051 cm^{-1}.The D & G band of amorphous carbon found at 1341 cm^{-1} and 1580 cm^{-1}.The major minerals identified in the X-ray diffraction (XRD) analysis were also found in Raman analysis, with the exception of Mullite.

- Stone Dust-

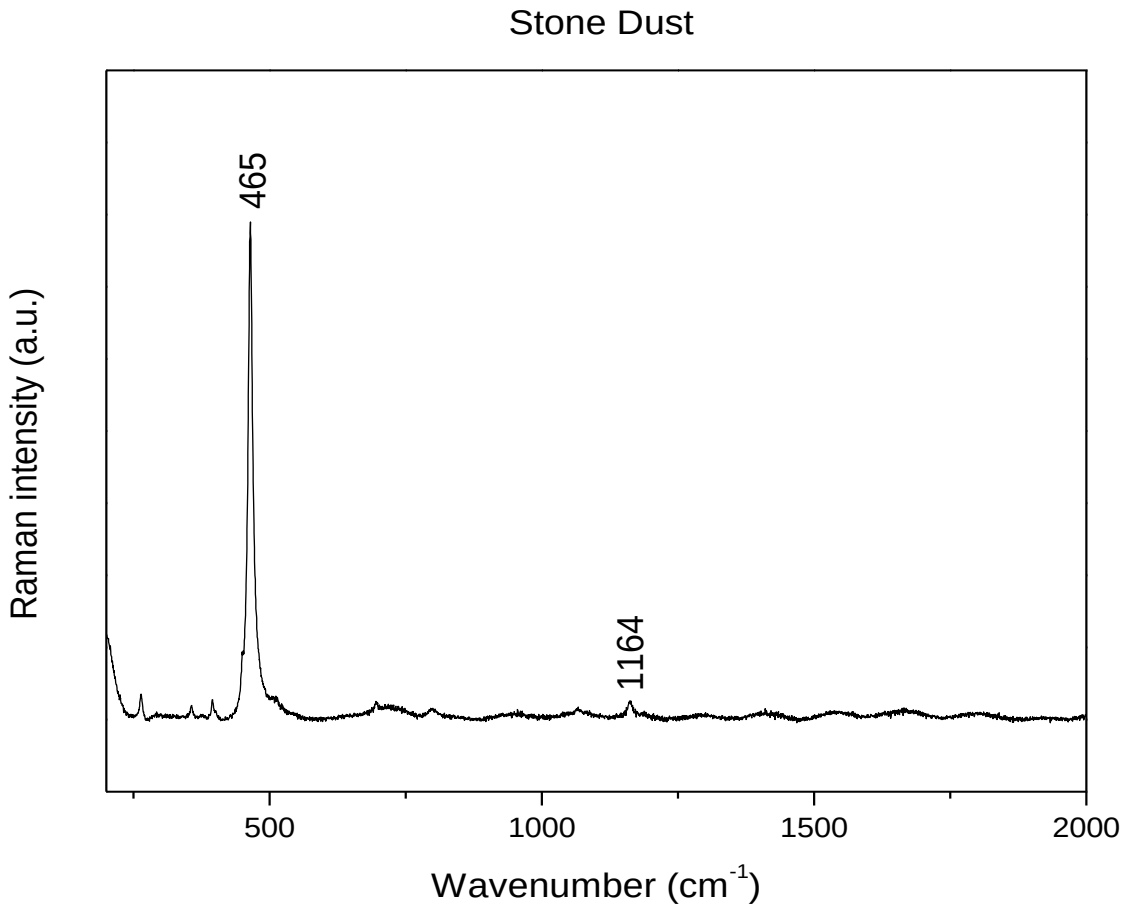

Figure 4.30: Raman spectra of stone dust sample

The Raman spectra of stone dust sample were shown in Fig 4.32. The peak of pure quartz was found at 465cm^{-1}. The major minerals identified in the X-ray diffraction (XRD) analysis were also found in Raman analysis.

- 10M Brick after 28 days-

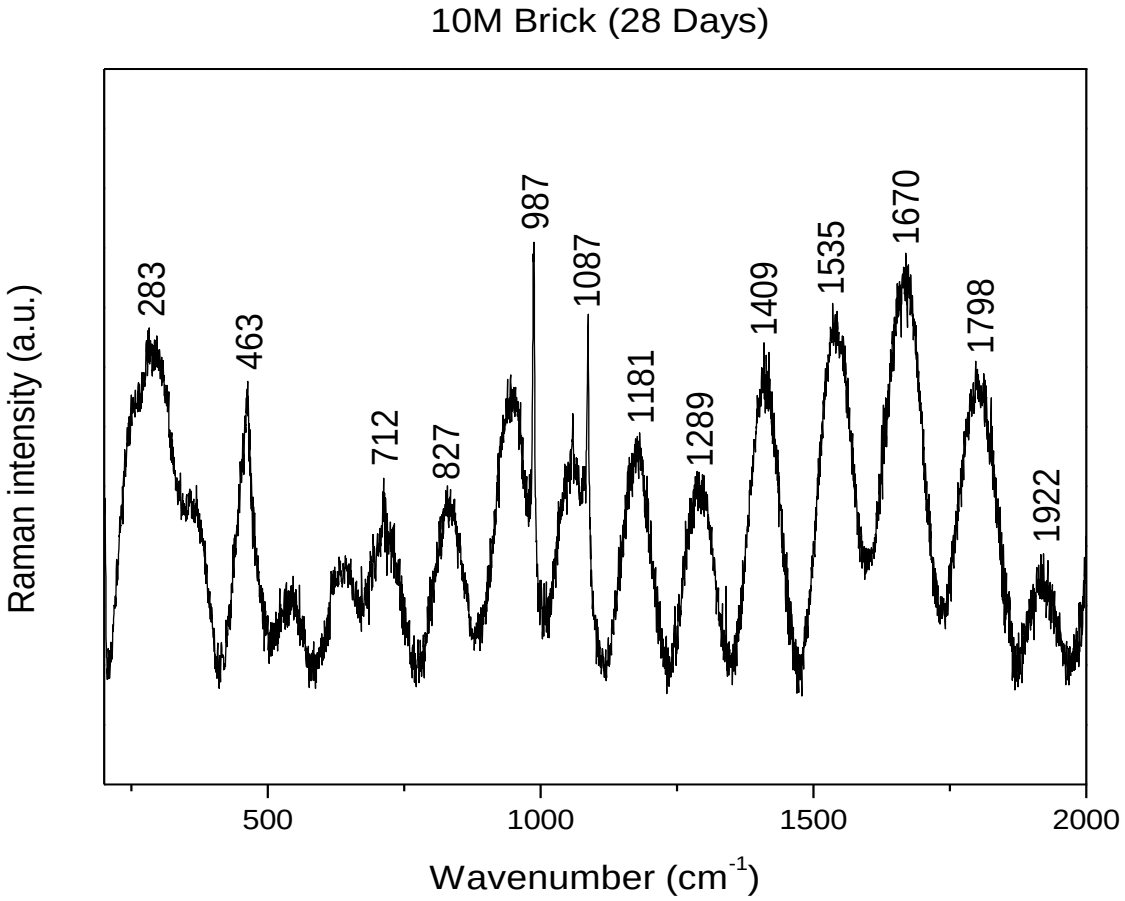

Figure 4.31: Raman spectra of 10M brick sample

The Raman spectra of 10M brick sample were shown in Fig 4.33. The peak of pure quartz was found at 463cm^{-1}. Therefore, the most intense line of barite at 987 cm^{-1} is assigned to the ν1 symmetric stretching mode. The calcite characteristic bands were found at (ν1) 283 cm $^{-1}$, (ν2) 712 cm $^{-1}$, (ν3) 1087 cm $^{-1}$ for the antisymmetric modes. The major minerals identified in the X-ray diffraction (XRD) analysis were also found in Raman analysis, with the exception of Mullite, Sodiumalum, Jadeite and Sillimanite.

- 18M Brick after 28 days-

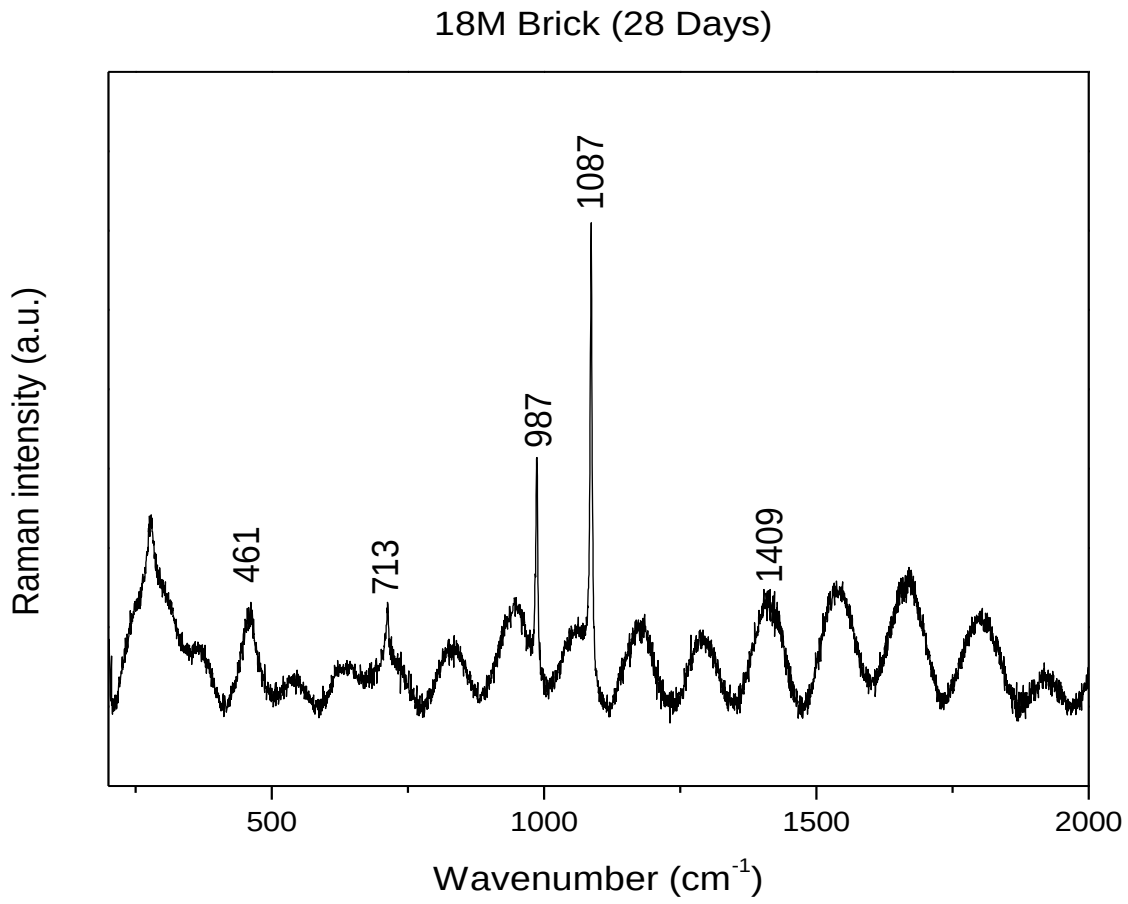

Figure 4.32: Raman spectra of 18M brick sample

The Raman spectra of 18M brick sample were shown in Fig 4.34. The peak of pure quartz was found at 463cm^{-1}. Therefore, the most intense line of barite at 987 cm^{-1} is assigned to the ν1 symmetric stretching mode. The calcite characteristic bands were found at (ν1) 283 cm $^{-1}$, (ν2) 712 cm $^{-1}$, (ν3) 1087 cm $^{-1}$ for the antisymmetric modes. The major minerals identified in the X-ray diffraction (XRD) analysis were also found in Raman analysis, with the exception of Sillimanite and Wollastonite.

- Efflorescence-

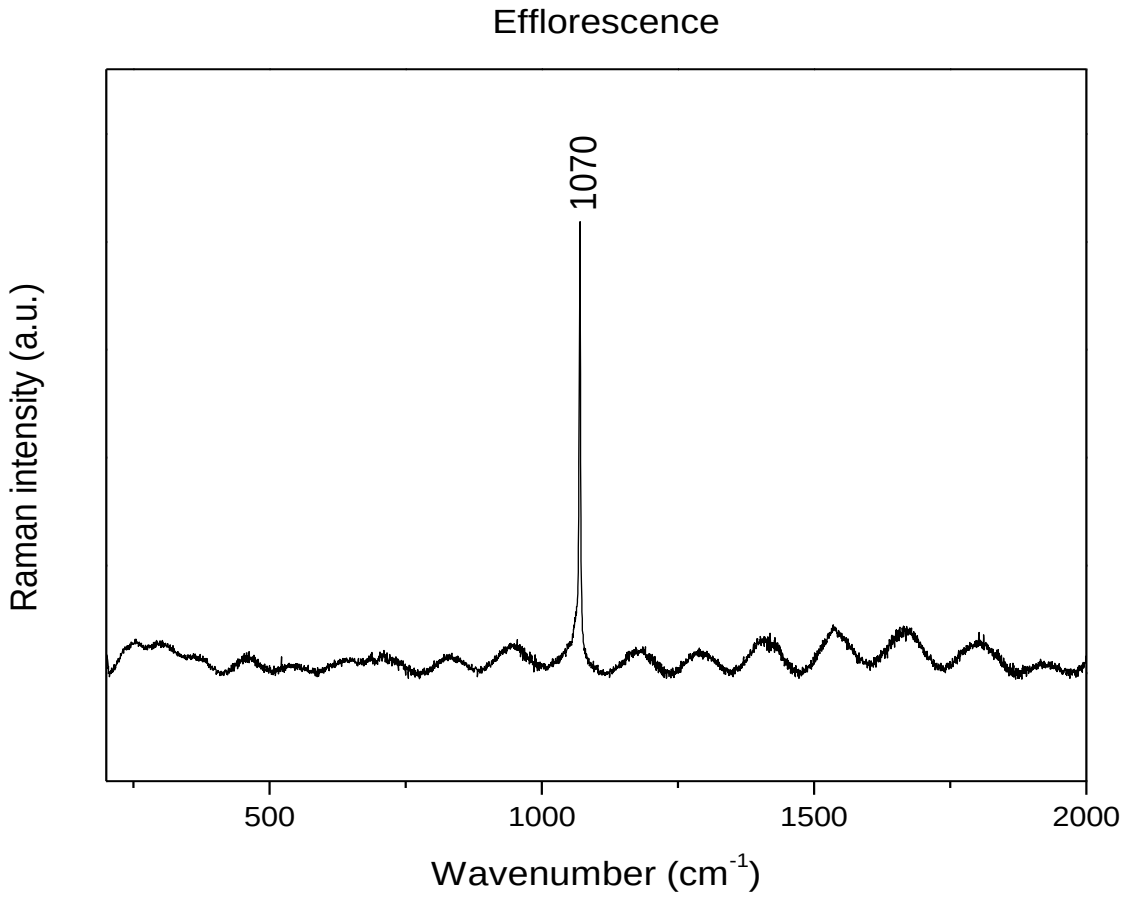

Figure 4.33: Raman spectra of efflorescence

The Raman spectra of efflorescence were shown in Fig 4.35. The most characteristics Raman peak of carbonate ion is the symmetric stretching mode ($\nu 1$), that is around 1070 cm^{-1}.

Table 4.18: Mineral phases confirmed using Raman spectra for raw materials and geopolymer bricks

Material	**Mineral Phase**	**Chemical Formula**	**Peaks observed in the present study**	**Peaks observed in the previous study**	**Ref.**
Brine Sludge	Calcite	$CaCO_3$	1087	158, 282, 711, 1087	Guedes et al. (2008)
	Barite	$BaSO_4$	622, 988,	461, 616, 628, 987, 1142,	Maftei et al. (2020)
	Quartz	SiO_2	462	202, 264-265, 402, 463-465, 698, 807	Guedes et al. (2008) & Palmeri et al. (2009)
Fly ash	Quartz	SiO_2	460, 807,	202, 264-265, 402, 461-465, 698, 807	Guedes et al. (2008), Palmeri et al. (2009) & Potgieter vermaak (2006)
	Dehydrated SiO_2		951, 1051,	950-970, 1030-1065, 1155	Lee & Wachs (2008)
	D & G band of amorphous Carbon		1341, 1580,	1353, 1603	Potgieter vermaak (2006)
	Unidentified		1184, 1812	-	-
Stone Dust	Quartz	SiO_2	465	202, 264-265, 402, 461-465, 698, 807	Guedes et al. (2008), Palmeri et al. (2009) & Potgieter vermaak (2006)
	Unidentified		1164	-	-
10 M Brick	Quartz	SiO_2	463,	202, 264-265, 402, 461-465, 698, 807	Guedes et al. (2008), Palmeri et al. (2009) & Potgieter vermaak (2006)
	Barite	$BaSO_4$	987,	461, 616, 628, 987, 1142,	Maftei et al. (2020)
	Calcite	$CaCO_3$	283, 712, 1087	158, 282, 711, 1087	Guedes et al. (2008)

	Unidentified		827, 1181, 1289, 1409, 1535, 1670, 1798, 1922	-	-
18 M brick	Quartz	SiO_2	461,	202, 264-265, 402, 461-465, 698, 807	Guedes et al. (2008), Palmeri et al. (2009) & Potgieter vermaak (2006)
	Calcite	$CaCO_3$	713, 1087,	158, 282, 711, 1087	Guedes et al. (2008)
	Barite	$BaSO_4$	987,	461, 616, 628, 987, 1142,	Maftei et al. (2020)
	Unidentified		1409	-	-
Efflorescence	Bending and stretching modes of carbonate	Carbonate ion	1070	1070	

4.9 Cost analysis of the bricks-

For 10M bricks:-

Table 4.19: Material cost of 10M bricks

Sr. No.	Items	Items Price in Rupee	For manufacturing of 1 Brick	Manufactured Price in Rupees
1.	NaOH	50 Rs/kg	0.400 kg	38 g × 50 = 1.9 Rs
2.	Sodium Trisilicate	22 Rs/kg		267 g × 22 = 5.87 Rs
3.	Brine Sludge	-	0.723 kg	-
4.	Stone Dust	44 Rs/ft	2.067 kg	2 Rs
5.	Fly Ash	1125 / ton Or 865 / ton	0.310 kg	0.35 Rs Or 0.27 Rs

Total Solution = 400 g

Water = 500 ml, NaOH (pallets) = 200g, Sodium trisilicate = 1400 g

NaOH = (0.4/21) × 2 = 0.038 kg

Silicate = (0.4/21) × 14 = 0.217 kg

Therefore, 1ft to m^3

= 0.0238 m^3 = 1680 x 0.0283 = 47.544 kg

44/47.544 = 0.9254 approx. = 1

Then, 1 ton = 1000 kg

= 1.125 × 0.310 = 0.35

= 0.865 × 0.310 = 0.27

The total cost of the 10M brick is Rs. 10.12 or 10.04.

For 18M bricks:-

Table 4.20: Material cost of 18M bricks

Sr. No.	Items	Items Price in Rupee	For manufacturing of 1 Brick	Manufactured Price in Rupees
1.	NaOH	50 Rs/kg	0.700 kg	97 g × 50 = 4.85 Rs
2.	Sodium Trisilicate	22 Rs/kg		480 g × 22 = 10.56 Rs
3.	Brine Sludge	-	0.723 kg	-
4.	Stone Dust	44 Rs/ft	2.067 kg	2 Rs
5.	Fly Ash	1125 / ton Or 865 / ton	0.310 kg	0.35 Rs Or 0.27 Rs

Total Solution = 700 g

Water = 500 ml, NaOH (pallets) = 360 g, Sodium trisilicate = 1720 g

NaOH = (0.7/25.8) × 3.6 = 0.097 kg

Silicate = (0.7/25.8) × 17.2 = 0.48 kg

Therefore, 1ft to m^3

= 0.0238 m^3 = 1680 x 0.0283 = 47.544 kg

44/47.544 = 0.9254 approx. = 1

Then, 1 ton = 1000kg

= 1.125 × 0.310 = 0.35

= 0.865 × 0.310 = 0.27

The total cost of the 18M brick is Rs. 17.76 or 17.68.

4.10 Comparison of Burnt clay and Geopolymer bricks-

A comparison of burnt clay and brine sludge based geopolymer bricks is presented in the Table 4.21 below which shows the mechanical, durable characteristics and cost comparison findings of burnt clay and geopolymer bricks. The result showed that the compressive strength 18M brick is comparatively high as compare to other bricks. The water absorption % of the geopolymer bricks is very less as compare to conventional bricks. The burnt clay shows no efflorescence as it is properly burnt and the soil composition contains very negligible composition of salts so the efflorescence is expected to be 'Nil' and 9.90% for 10M bricks, and 22.53% for 18M bricks. The total material cost of the 10M and 18M bricks is calculated as Rs. 10.12 and Rs. 17.76 respectively but the material cost of the conventional brick is less, but the total cost of first class burnt clay brick is Rs 9.5. The data of the burnt clay bricks has been collected from local vendors.

Table 4.21: Comparison of mechanical and durable properties of burnt clay and geopolymer bricks

Sr.no.	**Properties**	**Burnt Clay bricks**	**10M Bricks**	**18M Bricks**
1.	Compressive Strength	10 – 15 MPa	11.67 MPa	18.6 MPa
2.	Wet compressive strength	10 MPa	8.48 MPa	15.24 MPa
3.	Water Absorption	12 – 15 %	10.63 %	4.13 %
4.	Efflorescence	-	9.90 %	22.53 %

5. CONCLUSION

5.1 Introduction-

This research investigation is conducted for the utilization of the brine sludge in construction that can help in solving the negative impact of waste on the environment. The entire study is divided into two parts. In the first part, mechanical property of the brine sludge based mortar cubical specimens has been investigated with varying amount of the activating solution having constant molarity 10M. In the second part, assessment of the mechanical and durability properties of brine sludge based geopolymer bricks was done. The amount of the activating solution with two different molarities 10M and 18M has been varied and effect of different curing conditions such as oven drying condition and ambient condition has also been analysed.

5.2 Main conclusions of the study-

Based on the present study, the following conclusions can be drawn:-

- In flowable mortar for cubical specimen, the results obtained from the volume based design mix is far superior to the weight based design mix however, when it comes to low moist mortar for bricks all the trend was found reversed.
- Compressive strength of the brine sludge based mortar cubical specimens decreased with the increase in the concentration of activating solution. Compressive strength of the brine sludge based bricks decreases in the case of ambient curing as compared to oven dried curing done at 70°C.
- The mixes (B8) and (B9) for 18M and 10M bricks showed the maximum compressive strength at 28 days 18.6 MPa and 11.67 MPa among different brick mixes considered in the present study.
- Both wet and dry compressive strength has been studied for optimized brick mixes. The wet compressive strength has been found less 18.04 % and 27.73% for B8 (18M) and B9 (10M) mixes of the bricks as compared to their dry compressive strength results.
- The water absorption for the optimized mixes for 10M and 18M bricks are obtained as 10.63% and 4.13% respectively which are under the limits of the first class bricks.
- The efflorescence of the bricks has been found 9.90% for 10M bricks, i.e. slight efflorescence and 22.53% for 18M bricks, i.e. moderate efflorescence. Although the brick mix B8 having 18M activating solution achieve the higher strength as compared to brick

mix B9 having 10M activating solution that has not qualified the criterion of efflorescence test as per IS 12894. Therefore, only brick mix B9 having the activating solution 10M satisfies the requirement of IS 12894.

- The Mineralogy of raw materials and geopolymer bricks have been studied. XRD analysis of raw materials revealed the presence of quartz, mullite, calcite and barite. Further, new mineral phases i.e., sodiumalum, jadeite, sillimanite, wollastonite, thermonatrite and trona are identified in brine sludge based geopolymer bricks. Additionally, FTIR and Raman spectroscopy have been used to confirm the minerals identified in XRD patterns.
- The total material cost of the 10M and 18M bricks is calculated as Rs. 10.12 and Rs. 17.76 respectively.

5.3 Limitations and future scope of the study-

- The study can be extended to carry out the shrinkage test on the brine sludge-based geopolymer bricks in future.
- The TCLP test can be carried out on the geopolymeric bricks to ensure the environmental suitability of waste incorporated bricks.

References

A. Islam, U. J. Alengaram, M. Z. Jumaat, I. I. Bashar, The development of compressive strength of ground granulated blast furnace slag-palm oil fuel ash-fly ash based geopolymer mortar, Materials and Design 56 (2014) 833-841. DOI: https://doi.org/10.1016/j.matdes.2013.11.080

A.T. Lima, L. M. Ottosen, A. B. Ribeiro (2015), Assessing fly ash treatment: Remediation and stabilization of heavy metals, Journal of Environmental Management 95, S110 - S115, DOI: https://doi.org/10.1016/j.jenvman.2010.11.009.

Alam, M. Shahria, Geopolymer cement Compositions and method of making and using same, International Application Published under the Patent Cooperation Treaty WO 2015/149176 A1

ASTM C-109:2002, Compressive Strength of Hydraulic Cement Mortars (50-mm Cube Specimens), West Conshohocken, United States.

Bureau of Indian Standards, 2002, IS 2386 - 3: 1963, Methods of test for aggregates for concrete – Part 3: Specific Gravity, Density, Voids, Absorption and bulking, Bureau of Indian Standards, New Delhi, India.

Bureau of Indian Standards, 2002, IS 3495 - 1: 1992, Methods of tests of Burnt Clay Building Bricks – Part 1: Determination of Compressive Strength, Bureau of Indian Standards, New Delhi, India.

Bureau of Indian Standards, 2002, IS 3495 - 2: 1992, Methods of tests of Burnt Clay Building Bricks – Part 2: Determination of Water Absorption, Bureau of Indian Standards New Delhi, India.

Bureau of Indian Standards, 2002, IS 3495 - 3: 1992, Methods of tests of Burnt Clay Building Bricks – Part 3: Determination of Efflorescence, Bureau of Indian Standards, New Delhi, India.

Bureau of Indian Standards, 2008, IS 650 - 1991, Standard sand for testing cement – specification, Bureau of Indian Standards, New Delhi, India

Bureau of Indian Standards, 2011, IS 12894:2002, Pulverized Fuel Ash-lime Bricks – Specification, Bureau of Indian Standards, New Delhi, India.

Bureau of Indian Standards, IS 383 - 2016, Specification for coarse aggregates from natural sources for concrete, Bureau of Indian Standards, New Delhi, India.

C. C. Alcaina, J. L. S. Cabezas, A. Bes-Pia, M. C. V. Vela, J. A. Mendoza-Roca, L. Pastor-Alcañiz and S. Álvarez-Blanco (2020), Integrated Membrane Process for the Treatment and Reuse of Residual Table Olive Fermentation Brine and Anaerobically Digested Sludge Centrate, Membranes, 10, 253; DOI:10.3390/membranes10100253.

D. Ariono, M. Purwasasmita, G. Wenten (2016), Brine Effluents: Characteristics, Environmental Impacts, and Their Handling, July 2016, Journal of Engineering and Technological Sciences 48(4):367-387, DOI:10.5614/j.eng.technol.sci.2016.48.4.1

E. Masilela, L. Lerotholi, T. Seodigeng and H. Rutto (2018), The dissolution kinetics of industrial brine sludge wastes from a chlor-alkali industry as a sorbent for wet flue gas desulfurization (FGD), Journal of the Air & Waste Management Association, 68:2, 93-99, DOI: https://doi.org/10.1080/10962247.2017.1280097.

H. Biricik, M. S. Kırgız, A. G. de S. Galdino,S. Kenai, J. Mirza, J. Kinuthia, A. Ashteyat, A. Khitab, J. Khatib, Activation of slag through a combination of NaOH/NaS alkali for transforming it into geopolymer slag binder mortar eassessment the effects of two different Blaine fines and three different curing conditions, Journal of Materials Research and Technology 2021; 14: 1569-1584

H. Biricik, M. S. Kırgız, A. G. de S. Galdino,S. Kenai, J. Mirza, J. Kinuthia, A. Ashteyat, A. Khitab, J. Khatib, Activation of slag through a combination of NaOH/NaS alkali for transforming it into geopolymer slag binder mortar eassessment the effects of two different Blaine fines and three different curing conditions, Journal of Materials Research and Technology 2021; 14: 1569-1584

I. Hager, M. Sitarz, K.Mroz, Fly-ash based geopolymer mortar for high-temperature application – Effect of slag addition, Journal of Cleaner Production 316 (2021) 128168. DOI: https://doi.org/10.1016/j.jclepro.2021.128168

J. C. Izidoro, D. A. Fungaro, L. C. Viviani and, R. C Silva (2021), Brine sludge waste from a Chlor-alkali industry: characterization and its application for non-structural and structural construction materials, Journal of Applied Materials and Technology, DOI: https://doi.org/10.31258/Jamt.3.1.1-7.

M. Garg and A. Pundir (2014), Utilization of Brine Sludge in Non-structural Building Components: A Sustainable Approach, Journal of Hindawi Publishing Corporation, Article ID 389316, 7 pages, DOI: https://doi.org/10.1155/2014/389316

M. U. Kankia, L. Baloo, B. S. Mohammed, S. B. Hassan, S. Haruna, N. Danlami, E. A. Ishak, W. N. Samahani, Effects of petroleum sludge ash in fly ash-based geopolymer mortar, Construction and Building Materials 272 (2021) 121939, DOI : https://doi.org/10.1016/j.conbuildmat.2020.121939.

M.M. Ahmed, K.A.M. El-Naggar, D. Tarek , A. Ragab , H. Sameh, A. M. Zeyad, B. A. Tayeh, I. M. Maafa, A. Yousef, Fabrication of thermal insulation geopolymer bricks using Ferrosilicon slag and alumina waste, Case studies in Construction Materials 15 (2021) e00737. DOI: https://doi.org/10.1016/j.cscm.2021.e00737

N. Masilela, L. Lerotholi, T. Seodigeng & H. Rutto (2017), the dissolution kinetics of industrial brine sludge wastes from a chlor-alkali industry as a sorbent for wet flue gas desulphurisation (FGD), Journal of the Air & Waste Management Association, DOI: 10.1080/10962247.2017.1280097.

O.A. Hodhod, S.E. Alharthy, S.M. Bakr, Physical and mechanical properties for metakaolin geopolymer bricks, Construction and Building Materials 265 (2020) 120217. DOI: https://doi.org/10.1016/j.conbuildmat.2020.120217

P. Chokkalingam, H. El-Hassan, A. El-Dieb, A. El-Mir, Development and characterization of ceramic waste powder-slag blended geopolymer concrete designed using Taguchi method, Construction and Building Materials 349 (2022) 128744. DOI: https://doi.org/10.1016/j.conbuildmat.2022.128744.

P. Mwenge, H. rutto and C. Enweremadu (2021), Production of Biodiesel using Calcined Brine Sludge Waste from Chlor-Alkali Industry as a Heterogeneous Catalyst, Environmental and Climate Technologies 2021, vol. 25, no. 1, pp. 621–630. DOI: https://doi.org/10.2478/rtuect-2021-0046.

P. R. Yadav, V. Bhaskar, A. Shukla, S.K. Pattanaye (2017), Separation of Salts from Brine Sludge (Chlor-Alkali Process), DOI:10.13140/RG.2.2.31418.54721

P. Shukla (2015), Recovery of Barium Sulphate from Brine Sludge, Indian Journal of Environmental Protection, DOI: https://www.researchgate.net/publication/280444351.

R. Narasimhan, P.E., Narasimhan Consulting Services, Inc., disposal of brines, sludges and resins from radium and uranium removal processes.

S. Ahmari and L. Zhang, Durability and leaching behavior of mine tailings-based geopolymer bricks, Construction and Building Materials 44 (2013) 743-450. DOI: https://doi.org/10.1016/j.conbuildmat.2013.03.075

S. J. Chen, C. S. Chen, J. Y. Jhan and R. F. Chen (2019), Utilization of Brine Sludge in Controlled Low Strength Materials (CLSM), Trans Tech Publications Ltd, SSN: 1662-9795, Vol. 801, pp 436-441, DOI:10.4028/www.scientific.net/KEM.801.436.

S. Singh, M. A. Khan, V. K. Yadav, A. S. Yadav and U. Sharan (2020), Utilization of Brine Sludge in Manufacturing of Fly Ash Bricks, International Journal of Engineering Development and Research ISSN: 2321-9939, DOI: (www.ijedr.org).

S. Verma, S. S. Amritphale, M. A. Khan (2018), Utilization of Brine Sludge and Fly Ash Waste as Complementary Resources, for Making Non-toxic, Geopolymeric (Cement-Free) Materials, Iranian Journal of Science and Technology, Transactions of Civil Engineering, DOI: https://doi.org/10.1007/s40996-018-0191-3

S. Verma, S. S. Amritphale, Mohd. Akram Khan, A. Anshul and S. Das (2016), Development of Advanced Geopolymerized Brine Sludge Based Composites, DOI: 10.1007/s10924-016-0877.

Salt Brine Tank Sludge (2021), Minnesota Department of Transportation 395 John Ireland Blvd, St. Paul, MN 55155-1800.

Sh. K. Amin, S.A. El–Sherbiny, A.A.M. Abo El–Magd, A. Belal, M.F. Abadir (2017), Fabrication of geopolymer bricks using ceramic dust waste, Construction and Building Materials 157, 610-620. DOI: https://doi.org/10.1016/j.conbuildmat.2017.09.052.

V. Pingle and S. Saraswat (2018), Experimental Study of Use of Brine Sludge in Cement Concrete, International Journal for Scientific Research & Development.

Z. Liu, M. Haddad, S. Sauve and B. Barbeau (2021): Alleviating the burden of ion exchange brine in water treatment: From operational strategies to brine management, DOI: 10.1016/j.watres.2021.117728.